A THREE MONTH STREAM FLOW FORECAST
FOR WATER MANAGEMENT
IN THE UPPER OLIFANTS CATCHMENT

by

Mmotong Obed Phahlane

In partial fulfilment of the requirements
for a degree of
Masters of Science in Agriculture
in Agrometeorology

Faculty of Natural and Agricultural Sciences
Department of Soil, Crop and Climate Sciences
Agrometeorology Division
University of the Free State

Promoter: Prof S. Walker
External Promoter: Dr A.L. Du Pisani

November 2007

TABLE OF CONTENTS

CHAPTER 1: Introduction

CHAPTER 2: Literature Review

ABSTRACT

A THREE MONTH STREAM FLOW FORECAST FOR WATER MANAGEMENT IN THE UPPER OLIFANTS CATCHMENT

Mmotong Obed Phahlane

(M.Sc. Agric. in Agrometeorology, University of the Free State, 2007)

A Climate Predictability Tool was used to evaluate the relationship between sea-surface temperatures and stream flow at different lead-times in the upper Olifants catchment in Mpumalanga, South Africa. Four stream flow stations were selected from each of the sub-catchments of the upper Olifants, namely the Groot Olifants on the eastern side and the Wilger on the western side of the catchment.

Canonical correlation analyses were used to make three month stream flow forecasts for October-November-December (OND) and January-February-March (JFM) seasons. Monthly global-scale SSTs were used to evaluate the effect of lead-times on correlations between global Sea-Surface Temperatures (SSTs) and stream flow. Then the lead-times with Pearson's correlation values greater than 0.50 were selected to be used for evaluating possible origins of stream flow forecasting skill in the Equatorial Atlantic, Southern Atlantic, Equatorial Indian and Pacific Oceans.

Although local climatic and hydrological characteristics were not considered in this study good hit score skill from the Southern Atlantic Ocean was found at a short lead-time of two months for both OND and JFM seasons. The equatorial Atlantic Ocean gave a good hit skill score at longer lead-times of seven and eight months. The equatorial Indian Ocean gave a higher Heidke score at a short lead-time of two months during OND and JFM seasons in the Groot Olifants sub-catchment. The oceanic domains adjacent to the southern African subcontinent gave a good Heidke score at a shorter lead-time as compared to the equatorial Pacific Ocean. These forecasts could be used for planning water storage and releases in dams that are down stream of these stream flow monitoring points.

Keywords: Stream flow, Olifants River, Sea-Surface Temperature, Climate Predictability Tool

OPSOMMING
'n DRIE MAAND STROOMVLOEI VOORSPELLING VIR WATERBESTUUR IN DIE BO-OLIFANTS OPVANGGEBIED
Mmotong Obed Phahlane

(M.Sc. Agric. in Landbouweerkunde, Universiteit van die Vrystaat, 2007)

'n Klimaatvoorspellingshulpmiddel is gebruik om die verwantskap te evalueer tussen see-oppervlaktemperature en stroomvloei by verskillende aanlooptye in die bo-Olifants opvanggebied in Mpumalanga, Suid-Afrika. Vier stroomvloeistasies is gekies vir elk van die sub-opvanggebiede van die bo-Olifants, nl. die Groot-Olifants aan die oostekant en die Wilger aan die westekant van die opvanggebied.

Kanoniese korrelasie analise is gebruik om 'n drie maande stroomvloei voorspelling vir die Oktober-November-Desember (OND) en Januarie-Februarie-Maart (JFM) seisoene te genereer. Maandelikse globale-skaal see-oppervlaktemperature is ingespan om die uitwerking van voorgeetye op korrelasies tussen globale see-oppervlaktemperature en stroomvloei te bestudeer. Die aanlooptye met Pearson se korrelasiewaardes van meer as 0.50 is dan gekies om die moontlike oorspronge van stroomvloei voorspellingsvaardigheid in die Ekwatoriale en Suidelike Atlantiese, Ekwatoriale Indiese en Ekwatoriale Stille Oseane vas te pen.

Alhoewel die plaaslike klimaat en hidrologiese eienskappe nie oorweeg is in hierdie studie nie, is 'n goeie treftelling waargeneem vir die Suidelike Atlantiese Oseaan vir 'n kort aanlooptyd van twee maande vir beide OND en JFM seisoene. Die Ekwatoriale Atlantiese Oseaan het 'n goeie treftelling gebied by langer aanlooptye van sewe en agt maande. Die Ekwatoriale Indiese Oseaan het 'n hoër Heidke treftelling verskaf by die kort voorgeetyd van twee maande gedurende OND en JFM seisoene in die Groot-Olifants sub-opvanggebied. Die oseaanstreke aangrensend aan die Suider-Afrikaanse subkontinent het 'n goeie Heidke treftelling vir korter aanlooptye gebied as dié van die Ekwatoriale Stille Oseaan. Hierdie voorspellings kan gebruik word om waterstoring en–vrylating in damme te beplan wat stroomaf van hierdie stroomvloeimoniteringspunte geleë is.

DECLARATION

I hereby declare that this dissertation is my own work except where acknowledged and to the best of my knowledge contains no work submitted previously as a dissertation or thesis for any degree at any other university. I furthermore cede copyright of the dissertation in favour of the University of the Free State.

Signed: _____

ACKNOWLEDGMENTS

Firstly, I would like to thank God for giving me the endurance and courage to complete this task, despite many setbacks that provided opportunity to grow.

My promoter Prof. S. Walker, for her continued guidance, support throughout this study, unlimited belief in me for without her knowledge, I would have never completed this task. Dr A.L. Du Pisani my external promoter was positive with all my work I thank you for the advice. Mr. Stephan Steyn for your willingness to help especially with the explanation of the local climatic factors of South Africa also Ronelle Etzebeth and Linda de Wet. Prof. W.A. Landman and Mrs. Mary-Jane Kgatuke for your availability to help me with the explanation of data set-up for the Climate Predictability Tool.

Ms. Nditsheni Heidi Mabannda I am gratified by your guidance and the all-important facilitating role that you played throughout the writing and correcting of this dissertation.

Ms. Mamatime Kholofelo Thobejane, thank for your kindness, continuous help throughout the past years in Bloemfontein.

I am forever indebted to my family for their endless patience and encouragement when it was most required my parents, Mr. Letsepe and Mrs. Mmapheko Phahlane and siblings: Lekgale, Mmadikgoane, Thumetse, Matibe, Tselaborwa and Ngoaleakopa. I am deeply grateful to you all. It would have been impossible to have come this far without you.

I am indebted to my many colleagues at ARC-ISCW and to my officemate Mokhele Edmond Moeletsi for providing a stimulating and fun environment in which to learn and grow. I am also thankful for the funding from the ARC during the Professional Development Programme.

I would like to thank Mr Olubokolwa Oyewumi, my family in Christ Embassy Bloemfontein and Pretoria: for being a source of spiritual encouragement that spurred me to go on during trying times.

LIST OF TABLES

LIST OF FIGURES

LIST OF APPENDICES

LIST OF ABBREVIATIONS

AOH	Atlantic Ocean High Pressure
ARC-ISCW	Agricultural Research Council Institute for Soil, Climate and Water
CAB	Congo Air Boundary
CCA	Canonical Correlation Analysis
COADS	Comprehensive Ocean-Atmosphere Data Set
CPT	Climate Predictability Tool
CSIRO	Commonwealth Scientific and Industrial Research Organization'
DARLAM	Division of Atmospheric Research Limited-Area Model
DWAF	Department of Water Affairs and Forestry
ENSO	El Niño Southern Oscillation
EOF	Empirical Orthogonal Function
ERSSTv2	Extended Reconstructed Sea-Surface Temperature dataset Version 2
Eq Atl JFM	Equatorial Atlantic Ocean JFM Season
Eq Atl OND	Equatorial Atlantic Ocean OND Season
Eq Ind JFM	Equatorial Indian Ocean JFM Season
Eq Ind OND	Equatorial Indian Ocean OND Season
Eq Pac JFM	Equatorial Pacific Ocean JFM Season
Eq Pac OND	Equatorial Pacific Ocean OND Season
GCM	Global Circulation Model
GDP	Gross Domestic Products
IOCZ	Inter-Ocean Convergence Zone
IOH	Indian Ocean High
IRI	International Research Institute for Climate and Society
ITCZ	Inter-Tropical Convergence Zone
JFM	January-February-March
MAP	Mean Annual Precipitation
NCDC	National Climate Data Centre
NOAA	National Oceanic and Atmospheric Administration
OND	October-November-December
PCR	Principal Components Regression
RCM	Regional Circulation Models
S Atl JFM	Southern Atlantic Ocean JFM Season
S Atl OND	Southern Atlantic Ocean OND Season
SAWS	South African Weather Service
SO	Southern Oscillation
SST	Sea-Surface Temperature
SWC	South Western Cape

CHAPTER 1

General Introduction

1.1 Background

South Africa is an arid country with average rainfall of less than 500 mm per annum (Lévite and Sally, 2002; Viljoen and Booysen, 2006). This situation is made more complex by the fact that the rainfall in South Africa is unevenly distributed both geographically and through time. Uneven rainfall distribution results in about 60% of the river flow coming up from 20% of the net South African area (DWAF, 1997). The net result of this is that it has been estimated at current rates of growth, water use by 2025 is expected to increase by 20 to 50%. Evidence of this is already being seen at a local level with some catchments experiencing substantial stress in terms of meeting water demands (Cosgrove and Rijsberman, 2000).

Rainfall is the most important atmospheric variable in water resource management and agriculture (Ropelewiski and Halpert, 1997). Jury (2002) indicated that South African summer rainfall depends mainly on the global and regional circulation patterns. One of the most important global circulations is the Walker circulation, which is a series of zonally directed cells that respond to sea-surface temperatures (SSTs) over the Pacific Ocean (Preston-Whyte and Tyson, 1988). On a global scale, SST anomalies are analysed to better understand the factors which may be responsible for anomalously drier or wetter rainfall seasons in various regions (Rautenbach and Smith, 2001).

The expected future increase in demand for water emphasises the need to manage our scarce water resources as effectively and efficiently as possible (Cosgrove and Rijsberman, 2000). To achieve these new goals in water management, systematic monitoring and evaluation of information have become critical. The tools used for achieving efficient water use and catchment protection are no longer simple engineering methods. The application of law, economics, and natural resource management approaches reinforced with the skills of communication have become more important (RSA, 1997). Natural climate variability has a direct and fundamental bearing on water

resources and water management. Some of this variability is thought to be forced remotely via El Niño Southern Oscillation (ENSO) teleconnections (Nicholson and Kim, 1997; Reason, Allan, Lindesay and Ansell, 2000).

The complex atmospheric connection called teleconnection between oceans and the regional climate can play a major role in stream flow and rainfall prediction. Attempts have been made to improve the understanding of the relationship between global SSTs and climate after the 1982/1983 El Niño event. Ropelewski and Halpert (1987) demonstrated that a significant contributor to the inter-annual rainfall variability throughout much of the global tropics is caused by the ENSO events, which evolve in the equatorial Pacific Ocean region (Rautenbach and Smith, 2001). Kruger (2004a) and Jury (2002) state that seasonal forecasts of rainfall and stream flow can be made if SSTs and their relationship with climate are known. The oceans are a source of energy and the atmospheric systems depend on the ocean for kinetic and potential energy.

The hydrological and geological fundamental parameters also play a major role in river stream flow. Even though these two aspects play a major role, according to Jury (2002) South African water resources depend on how summer rainfall respond to global and regional circulation patterns. It was also shown by Jury (2002) that global and regional circulation patterns can be used to predict 50% of the variance for hydrological targets. Statistical models which are based on global predictors using stepwise multivariate linear regression have demonstrated a reasonable ability to capture regional and remote climate signals (Landman, 1997).

1.2 Statement of the Problem

The poor communities and those with the least capacity to cope with the impacts of climate variability and water resources are the most vulnerable. Actions that directly deal with the more immediate water management problems while preparing for the consequences of longer term climate changes will usually be the best approach to minimize the vulnerability. An increasing frequency and magnitude of climate variability across the entire globe has focused the need for research onto the predictability of stream flow in South Africa. Therefore more research is needed to improve on the understanding

of the relationship between climate variability and water resources, particularly the processes of the hydrological cycle in relation to the changing atmosphere and biosphere conditions. Probabilistic stream flow projections might be of significant value for hydrological planning and catchment water resource management. However in this project only a deterministic model was used as that is what is available.

1.3 Assumptions

It is assumed that the stream flow would have a positive relationship with the rainfall and sea-surface temperatures at different lead-times. Therefore the connection between rainfall and sea-surface temperatures can be used to predict the stream flow at different lead-times.

1.4 Objectives of the Study

The main objective of this study is to evaluate the effects of SSTs on stream flow and then to develop a three month stream flow forecast for water management in the upper Olifants catchment. This project will look at the two main sub-catchments in the upper Olifants catchment namely: the Wilger and Groot Olifants according to the Department of Water Affairs and Forestry (DWAF) catchment description. The following sub-objectives will guide us in order to reach the main objective:-

1. To learn how to use the Climate Predictability Tool (CPT);
2. To analyse the relationship between rainfall and stream flow;
3. To select the best method between Principal Components Regression (PCR) and Canonical Correlation Analysis (CCA), which will then be used for further analysis;
4. To evaluate the effects of different lead times and global SST on stream flow;
5. To evaluate the effect of different lead times and different SSTs domains on stream flow;
6. To validate the stream flow forecast from 1998-2005 using the best correlation values at different lead-times and from different oceanic domains.

1.5 Significance of the Study

The practice of water management in Southern Africa has moved in step with the societal needs of the region over the past several decades. The needs have passed through phases

which placed most emphasis on getting more water and then using it more efficiently. The need for a stream flow forecast as a guide for the coming season has become necessary. The improvement of methodologies to forecast climatic conditions and stream flow at seasonal to inter-annual timescale will improve water management techniques and planning in South Africa. This study is an attempt to improve such forecasting methodologies.

1.6 Organisation of the Study

The thesis is organised in seven chapters. The outline of the contents of each chapter is as follows:

Chapter 1. Introduction: This chapter presents the introduction, objectives and problem statement of the study.

Chapter 2. Literature Review: Literature on the state of South African water management, including Seasonal forecasts, statistical verification in climatology, ENSO events and teleconnections between sea-surface temperatures and stream flow.

Chapter 3. Description of the Upper Olifants Catchment: This chapter provides a description of the catchment area, highlighting location, municipal districts as well as rainfall stations and DWAF stream flow stations within the study area.

Chapter 4. Materials and Methods: The primary purpose of this chapter is to provide an overview of different phases of the research including model set-up, model inputs and output, analysis and verification of results.

Chapter 5. Stream Flow Forecast Equation for OND and JFM Seasons: Evaluation of the selected oceanic domains influence on stream flow in the upper Olifants catchment.

Chapter 6. Evaluation of Oceanic Domains for Forecasting Skill: Evaluation of the skill of the model at selected lead-times using different oceanic SST

Chapter 7. Stream Flow Hindcasting in the Upper Olifants Catchment: This final chapter highlights the conclusions and recommendations arising from the development of seasonal hindcast for the upper Olifants catchment.

CHAPTER 2

Literature Review

2.1 Introduction

El Niño is a natural feature of the global climate system. Originally it was the name given to the periodic development of unusually warm ocean waters along the tropical South American coast and out along the equator to the dateline. Now it is more generally used to describe the whole ENSO phenomenon, the major systematic global climate fluctuation that occurs at the time of an ocean warming event. On a seasonal time-scale, the ENSO phenomenon (Zhang, Wallace and Battisti, 1997) affects the atmospheric circulation outside the tropics (Philander, 1990) and southern Africa tends to experience dry conditions during warm ENSO events (Ropelewiski and Halpert, 1987). The dominant inter-annual mode over the tropical Southern Hemisphere is ENSO and is known to project strongly over southern Africa and the South Atlantic (Lindesay, 1988; Venegas, Mysak and Straub, 1997; Reason, *et al.,*, 2000).

Kruger (2004a) suggests that seasonal predictions of rainfall and temperature can be made if SSTs and their relationship with climate are well understood. ENSO has the most profound impact on climate variability; generally speaking, changing SST implies also changing the humidity content and stability characteristics of the overlying air mass. This will influence the intensity of convective activity and hence the release of latent heat in upper air layers. In addition, it can be reasoned that changing SST can influence the mean temperature and density profile in the overlying air mass. Taken together, these changes may very well reverberate as changes in the intensity and orientation of the synoptic scale pressure patterns and could, in some cases, even lead to a reversal of the large scale circulation patterns (Glantz, Katz and Nicholls, 1991).

Rainfall and stream flow variability in Australia and southern Africa are reportedly the highest in the world (Chiew, Piechota, Dracup and McMahon, 1998). Rainfall is the fundamental driving force and pulsar input behind most hydrological processes. However

it is the most variable hydrological element (Hamlin, 1983), an accurate estimate of areal rainfall is a basic input into catchment rainfall-runoff models. Hall and Barclay (1975) and Corradini (1985) found that stream flow was very sensitive to variations in precipitation during their study in the Upper Maquoketa River Watershed. Because of the sensitivity of stream flow to rainfall, the minimum rainfall record length for hydrological modelling has to be considered very carefully. The variability of rainfall is generally higher in areas of low rainfall (Schulze, 1983) and the use of short-term records can bias estimates of mean annual precipitation significantly. Semi-arid areas are likely to require a longer record for hydrological risk analysis than wetter areas. Lynch and Dent (1990) found that a minimum rainfall sequence of between 15 to 35 years is sufficient to use in the generation of spatial mean annual precipitation information set for southern Africa (WMO, 1966). However, WMO (1966) requires at least 30 years continuous data for a good analysis.

2.2 Oceanic Areas Affecting Rainfall and Stream Flow in South Africa

The appearance of unusually warm surface waters in the eastern tropical Pacific Ocean is one of the most prominent aspects of El Niño. Sea-surface temperature is the most important feature of El Niño because it is the only oceanic parameter that significantly affects the atmosphere. The heat flux across the ocean surface, advection, upwelling and mixing processes all influence sea-surface temperatures in the tropical oceans. A change in the balance between these processes causes sea-surface temperature variations. According to Philander (1990) the tropical Pacific and Atlantic oceans have similarities because both are forced by the trade winds; they have differences because the wind fluctuations are not identical and because the dimensions and geometries of the two basins are vastly different. The dimensions of the Atlantic and Indian oceans are approximately the same but the monsoons over the Indian Ocean have little in common with the trade winds (Philander, 1990).

2.2.1   The equatorial Pacific Ocean

The interaction of the atmosphere and ocean is an essential part of El Niño (La Nina) events which are characterized by warmer (cooler) than average sea-surface temperatures in the tropical Pacific; they are also associated with changes in wind, pressure, and

rainfall patterns. During an El Niño, the sea level pressure tends to be lower in the eastern Pacific and higher in the western Pacific while the opposite tends to occur during a La Nina. This see-saw in atmospheric pressure between the eastern and western tropical Pacific is called the Southern Oscillation (SO). During the low phase of the SO (an El Niño event characterised by anomalously high SSTs) the easterly trade winds weaken and become light westerly at times while low-level convergence sets in along the central and eastern equatorial Pacific which results in enhanced convection and rain. This brings about a reversed vertical circulation cell over the tropical Pacific Ocean. The larger-scale meridional circulation, as portrayed by the Walker Circulation (Fig. 2.1) is subsequently also reversed. This implies that the shifting of tropical rainfall patterns during El Niño and La Nina not only affects the tropical Pacific region but areas away from the tropical Pacific as well. This includes many tropical locations as well as some regions outside the tropics like the summer rainfall region of South Africa (Ropelewiski and Halpert, 1987; Nicolson and Entekhabi, 1986; Kruger, 2004a).

2.2.2   The equatorial Indian Ocean

The changing SST over the tropical Indian Ocean will change the moisture and stability profile within the atmosphere and subsequently the amount of moisture advected around the periphery of the mid-level anticyclone to the central and eastern interior of South Africa.
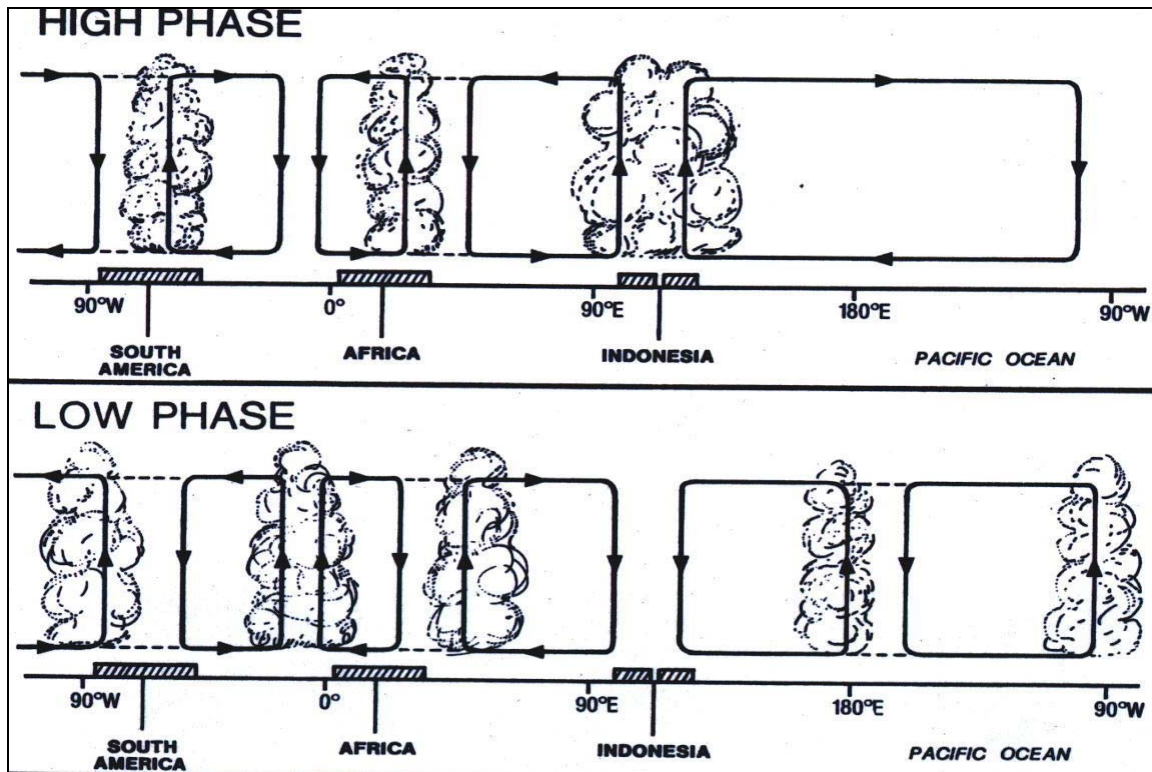
Fig. 2.1 The Walker Circulation during high and low phases of the Southern Oscillation (Lindesay, 1988, after Tyson, 1986)

Changes in the stability profile may change the orientation and intensity of the middle- and upper-air anticyclone depicted in Fig 2.2, which in turn may affect the intensity of convection as well as the amount of high energy tropical air that reaches the north-eastern interior. In their discussion of the Quasi-Biennial Oscillation, Pathak Jury Shillington and Courtney (1993) indicated that during wet conditions over South Africa the air mostly ascends over the subcontinent and sinks east of Madagascar with easterlies predominating at low levels between the Indian Ocean and South Africa, while westerlies predominate aloft.

During dry conditions over the subcontinent, the mean vertical circulation reverses (Fig. 2.3). An increase in the frequency and intensity of the tropical cyclones in the Indian Ocean is influenced by the above normal temperature in the Indian Ocean which is associated with dry conditions over South Africa. The corresponding SST anomalies

north and east of Madagascar (i.e. in the tropical Indian Ocean) are then negative for wet conditions and positive for dry conditions (Mason, 1995; Jury, 1996 and Kruger, 2004a).
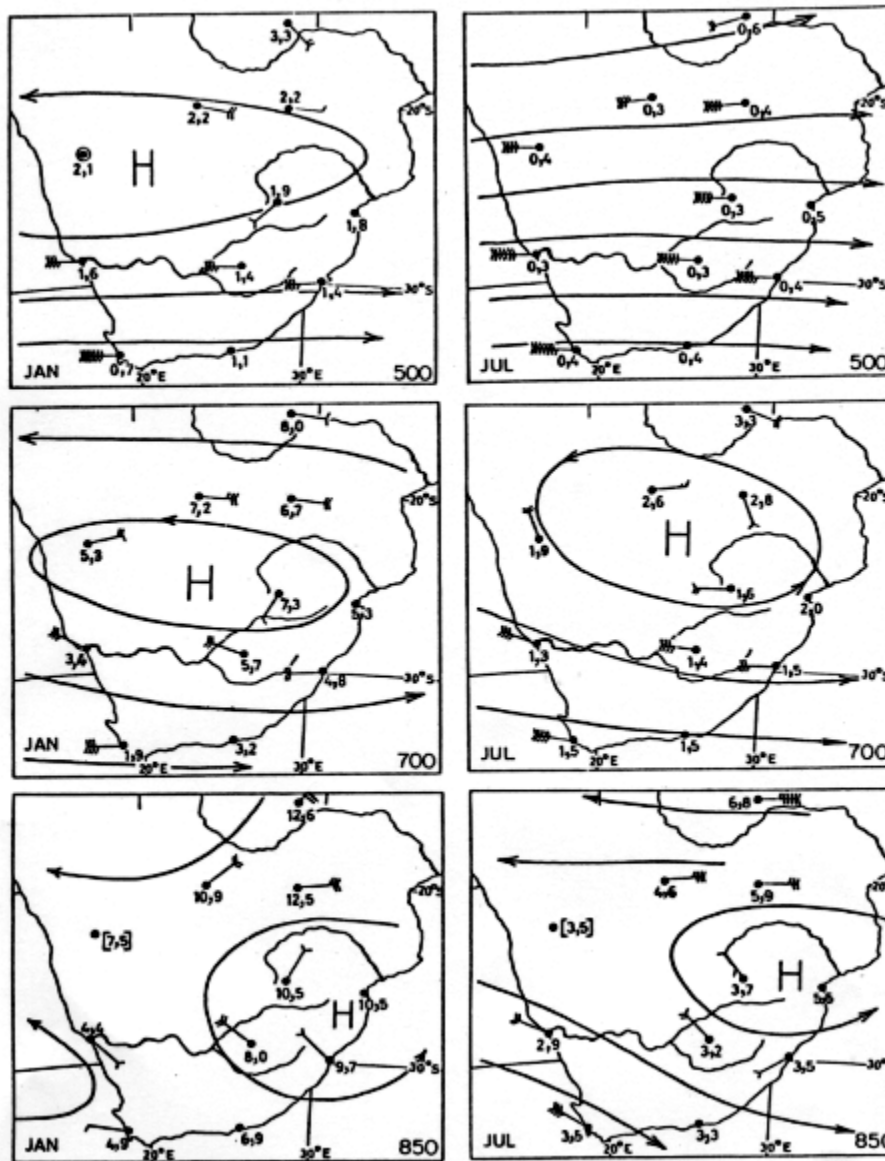
Fig. 2.2 Humidity mixing ratios (g/kg^{-1}), mean winds (one feather equals 1 ms^{-1}) and pressure patterns at 850, 700, 500 hPa in January and July (Taljaard, 1970)

According to Taljaard (1996), it is also logical to visualize that periodically reversing vertical circulation cells such as the Walker Circulation encompassing the vast Equatorial and sub-Equatorial Pacific Ocean, should also affect the circulations over the tropical Indian Ocean.
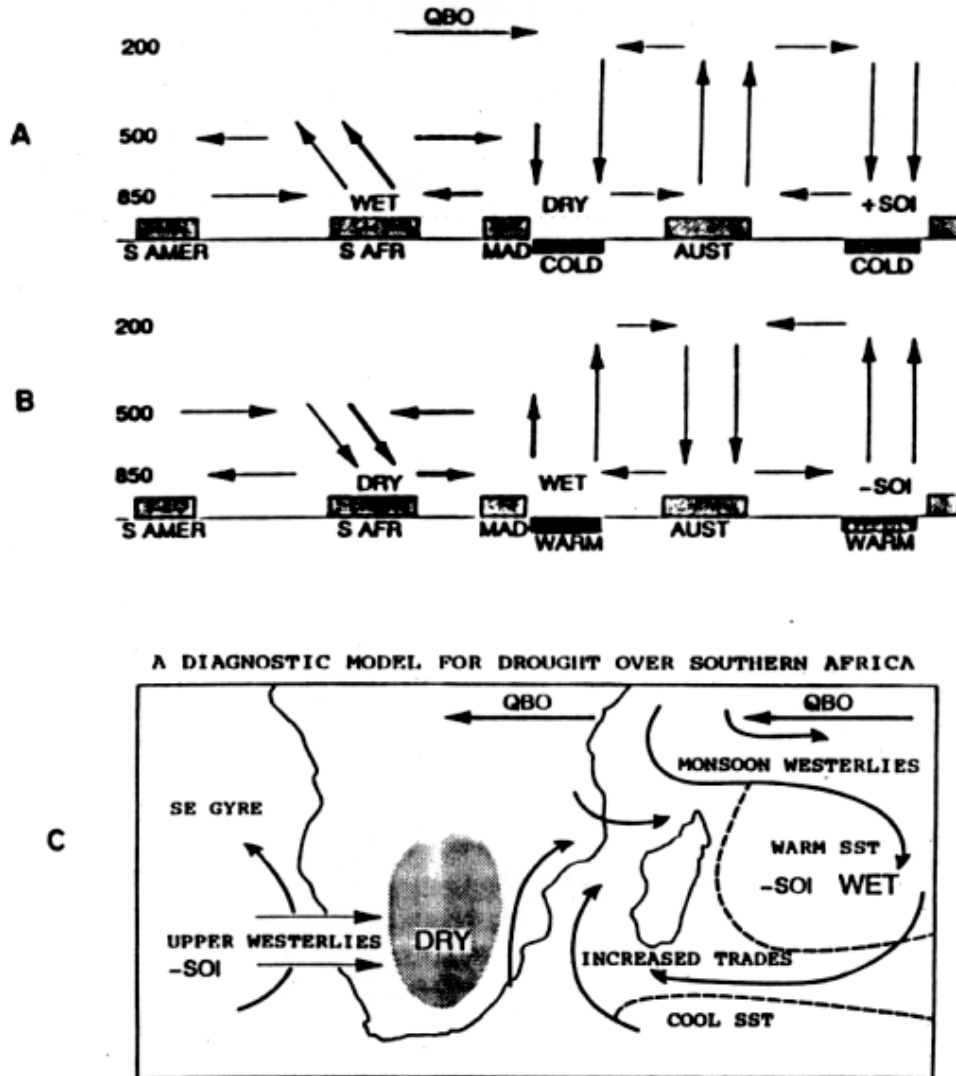
Fig. 2.3 Vertical and horizontal anomalous wind components along a section from the South Atlantic Ocean across southern Africa to the Indian Ocean during A, wet conditions and B, dry conditions over the subcontinent in conjunction with above and below normal SSTs in the Indian and Pacific Ocean (After Pathak *et al.,* 1993)

2.2.3   The equatorial Atlantic Ocean

The effects from the Atlantic region occur mainly via the Rossby wave propagation in the Pacific South America pattern (Mo and Paegle, 2001; Colberg, Reason and Rodgers, 2004). Modern modelling work on rainfall impacts of a particular event over southern Africa are facilitated by the way the Angola low and the neighbouring SST are forced to change during the ENSO season (Reason and Jagadheesha, 2005). Along with the obvious changes in atmospheric moisture content, changing SSTs over the equatorial

Atlantic Ocean influence the strength of the easterly trades and particularly that of the south-westerly monsoon during the austral summer (Fig. 2.4a). This will have a direct impact on the intensity of the convergence along the Inter-Tropical Convergence Zone (ITCZ) and Congo Air Boundary (CAB) over Africa, which in turn will impact on the frequency of the development of tropical-temperate troughs which has a large impact on South Africa's summer rainfall (Hirst and Hastenrath, 1983; Kruger, 2004a; Philander, 1990).

2.2.4   The southern Atlantic Ocean

According to Hirst and Hastenrath (1983) and Lough (1986), not much work has been done on Atlantic influences on southern African climate. Changing SST anomalies over the southern Atlantic Ocean have an effect on the steepness of the temperature gradient to the southwest of the subcontinent which may impact on cyclogenesis and the intensity and subsequent movement of westerly troughs and cut-off lows. A lack of awareness of the complexities of the atmosphere-ocean coupling in the associated tropical extratropical interactions and the southern African region has lead to little development of Atlantic influences on southern African climate (Reason, Landman and Tennant, 2006a).

Taljaard and Steyn (1991) found that sea-level pressure and isobaric heights are anomalously high/low south of the subcontinent during most wet/dry spells in summer. This is related to the thicknesses between the isobaric surfaces, which is closely associated with the mean air-column temperatures and through the thermal wind component also to the upper-air wind speeds and directions. Again, Taljaard (1996) found that the wind assumes an increasingly northerly component during wet spells as compared to dry conditions and at Gough Island the wind veers to north-west during rainy spells over Southern Africa.
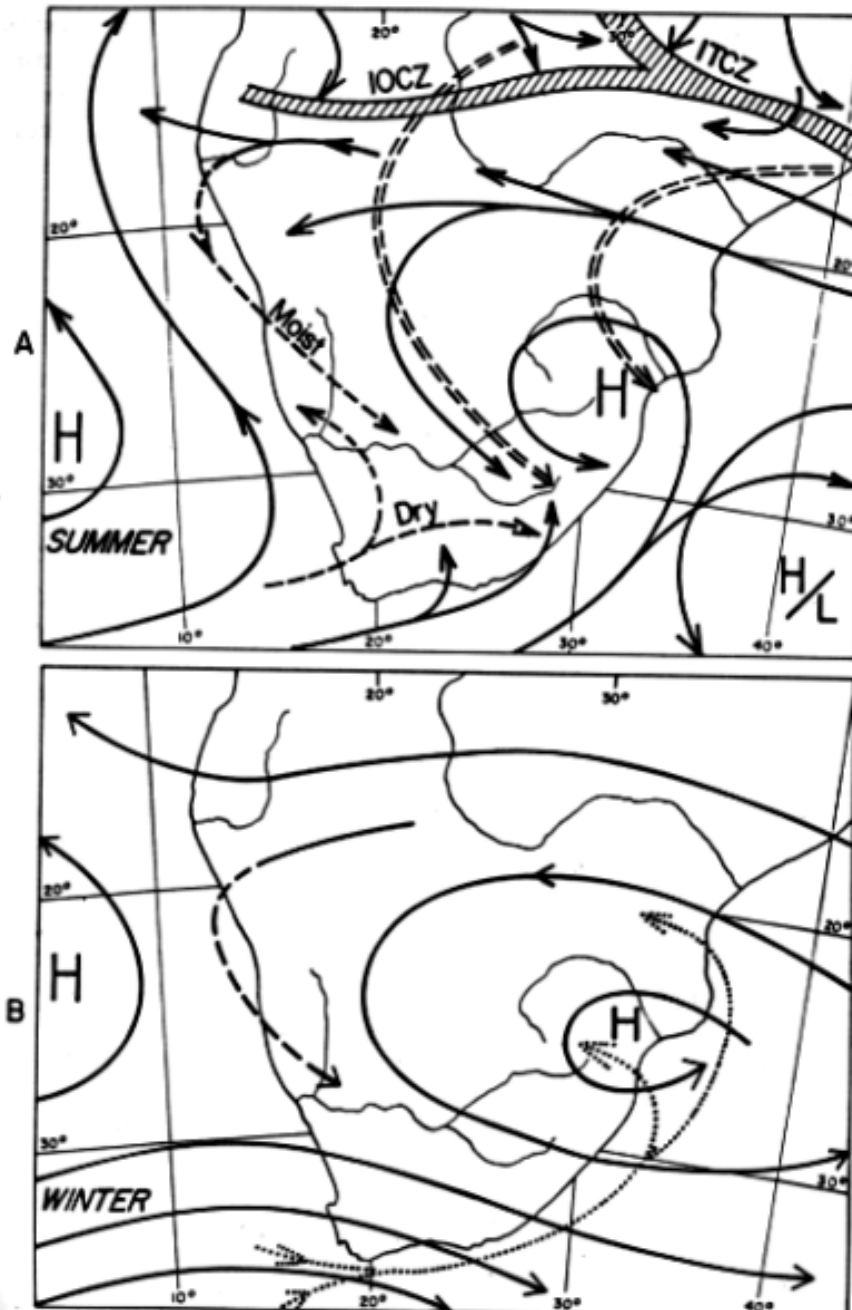
Fig. 2.4 Predominant flow patterns in the lowest few km above the surface in summer (above, A) and winter (below, B) the broken line over Namibia indicates frequent flow of relatively moist warm air at plateau level (not sea level) and higher. The broken lines over Cape Town indicate a highly frequent flow of dry air. The broken double line over Zimbabwe, Zambia, Botswana and Limpopo basin indicate occasional southward flow of very humid tropical air when the IOCZ and ITCZ troughs are ruptured or indistinct (Taljaard, 1996)

2.3 Lead-Times in Seasonal Forecasting

The forecast is only a small part of a management process. It does not really matter how a forecast was obtained but it should be generated taking important decisions like lead-time into account and being incorporated into the forecast model. Lead-times can be defined as the number of months between the predictor data and the first predictand season. A short lead-time is the shortest practical time between the predictor data and the predicted time. The longer range predictions help one to plan for major peaks or valleys over several seasons. With different lead-times predictability of the seasonal rainfall can be improved significantly (Brown, 1964; Landman and Mason, 1999; Box and Jenkins, 1976).

The use of three-month seasonal mean (e.g. OND or JFM) has the capability to capture evolving long-term phenomenon like the cooling or warming of oceanic features (Barston, Thiao and Kumar, 1996; Landman and Mason, 1999). Advantages of using evolving features like early winter and warm western equatorial Pacific in late austral autumn would then be indicating the development of an El Niño. Expected rainfall for the coming season would be different depending on the occurrence of the two mentioned scenarios (Glantz *et al.,* 1991; Landman and Mason, 1999).

When there is error in the observed data, the error gets amplified by an increasing lead-time. Therefore it is very important to make the lead-time as short as possible in order to reduce the error effect. Another way of solving the error effect is by acquiring data with small error (Brown, 1964).

2.4 Water Management in South Africa

Water management needs have passed through different phases from any emphasis on being able to store and supply more water then to focusing on using water more efficiently. However, the era of allocating water and equitably has begun (Turton and Lichtentaler, 1999) and this is now the dominant focus. The need to broaden participation and thereby democratise the process of water allocation is fundamental to economically viable and equitable progress in southern Africa. This need is important and urgent in a region mostly affected by conflict and inequalities, which worsen the already complex situation concerning the sustainable development of scarce water resources. To meet

these challenges, more research on stream flow and water management is required (Dent, 2000).

2.5 Application of Statistical Forecasting Models in Water Management

Several statistical methods are used for statistical climatological forecasting (Zhaobo, 1994), including regression analysis (Barnston, 1994; Singh, Bhadram and Mandal, 1995), discriminant analysis (Mason, 1998), cluster analysis, analogue methods (Drosdowsky, 1994), time series analysis and period analysis (Landman and Mason 1999). Cross validation is a model evaluation method that is better than residuals. The problem with residual evaluations is that they do not give an indication of how well the learner model will do when it is asked to make new predictions for data it has not already seen. One way to overcome this problem is to not use the entire data set when training a learner model. Some of the data is removed before training begins. Then when training is done, the data that was removed can be used to test the performance of the learned model on an independent data set (Brown, 1964).

The prediction technique selected for this study is called canonical correlation analysis (CCA) (Anderson, 1984; Wilks, 2006; Barnston and Smith, 1996). Barnett and Preisendorfer (1987); Chu and He, 1994; Jackson (1991) and Johnston (1992) discussed the theory of CCA in detail. Barnett and Preisendorfer (1987) and Landman and Mason (1999) mentioned and showed that CCA theory is above other statistical methods and sits highest in a regression modelling hierarchy. CCA has the ability to seek relationships between two sets of variables which vary in both time and space by identifying the optimum linear combination between the two sets with maximum correlation being produced. That is, CCA extracts relationships between pairs of data vector **x** and **y** that are contained in a joint covariance matrix (Wilks, 2006).

As Mason (1976) has pointed out, the growth of the world population, together with rising expectations and standards of living, is greatly increasing the pressure on natural resources of food and energy. The balance between supply and demand may be seriously affected by small changes in climate. It is well accepted that the climatic change does not

always take place uniformly over the globe, and that the global jigsaw of changes can only be fully understood once the regional pieces have been fitted together.

Some of the important atmospheric circulation anomalies associated with ENSO was discussed in a review by Mason and Jury (1997) then at the University of the Witwatersrand. Tyson, Dyer and Mametse (1975) discussed some of the important atmospheric circulation anomalies associated with ENSO effects over the region and the existence of the strongest interdecadal signals of a roughly 18-year cycle and inter-annual to interdecadal signals in summer rainfall. Most severe droughts over subtropical southern Africa seem to either be due to regional anomalies over the southeast Atlantic (Mulenga, Roualt and Reason, 2003; Tennant and Reason, 2005) or to strong El Niño events (Lindesay, 1988; Reason *et al.,* 2000).

A better understanding of the catchment scale influences and their potential predictability should lead to improvements in prediction efforts for southern Africa. In this section, prediction efforts that are currently operating are discussed (Reason, Engelbrecht, Landman, Lutjeharms, Piketh, Rautenbach, and Hewitson, 2006b). The drought experienced in southern Africa which was associated with the 1982-1983 ENSO event caused damages estimated to US $1 billion (Moura, Bengtsson, Buizer, Busalacchi, Cane, Lagos, Leetmaa, Matsumo, Mooney, Morel, Sarachik, Shukla, Sumi and Patterson, 1992; Landman, Mason, Tyson and Tennant, 2001). The previous years of drought over most of the region made the impact of this event worse.

Various mechanisms have been proposed including regional SST forcing modulations of the Southern Hemisphere circulation (Mason and Jury, 1997), and the projection of ENSO like decadal modes onto the region, which could also explain interdecadal variability observed in the south western Cape winter rainfall region (Reason and Rouault, 2002). These modes have a significant expression in SST over the South Atlantic (Allan, 2000); however, their rainfall impact over southern Africa arises via changes to the regional atmospheric circulation rather than directly from the South Atlantic sea-surface temperature.

The South African Weather Service (SAWS) is the only national meteorological service within the 15 southern African Meteorological services which continually performs dynamical model-based forecasting (Landman and Mason, 1999; Reason *et al.,* 2006a). Goddard and Mason (2002); Reason, Jagadeesha and Tadross (2003) indicated that when Global Circulation Models (GCMs) are forced in hindcast mode with SSTs GCMs may represent the regional climate and its variability reasonably well. Important biases exist, such as the tendency of the models to get the magnitude of the South westerlies incorrect, or to adequately represent the recurring of the northeast monsoonal flow north of Madagascar during austral summer (Tennant, 2003).

A software package like CPT has been used in several countries in Africa. It is a software package developed by Simon Mason from the International Research Institute for Climate and Society (IRI) and used to develop seasonal climate forecast equations. CPT is a Windows-based package that can be used by resource managers and decision makers to develop seasonal climate forecasts and to do validation. The software is specifically modified to perform CCA or PCR on two data sets. For example, the global SST forecast which is produced and stored at the IRI and local meteorological station historical data can be used. The CPT can help improve local capacity to manage climate by the provision of probabilistic climate forecasts (Mason, 1999).

Significant growth in the capacity to implement and use climate models for assessing the regional climate systems were achieved by the University of Pretoria and the University of Cape Town. The present and future mid-summer and mid-winter climate over southern Africa was simulated for two 10-year periods with the Commonwealth Scientific and Industrial Research Organisation's (CSIRO) Division of Atmospheric Research Limited-Area Model (DARLAM) at University of Pretoria. Engelbrecht (2005) found that there is general rise in temperature over South Africa with an increase in rainfall over the western and central interior of the country was projected. Some of these kinds of projections would increase the statistical model skills if they are to be incorporated in statistical models.

The empirical approaches and Regional Circulation Models (RCMs) have been developed largely under the support of the South African Water Research Commission (WRC) projects to improve regional climate change information. The skills base within South Africa has begun to be established to meet the needs of policy and resource management for climate change information through such projects (Reason *et al.,* 2006a). Tadross, Jack and Hewitson (2005) indicated that from a broad range of GCMs, characterizing to some degree the envelope of future change has lead to the development of daily projections of precipitation across South Africa. Most notable in these projections is the convergence of projected change between the different driving GCMs (Rautenbach and Mphepy, 2005).

2.6 Forecast Verification
The use of a time series to forecast the value at some future time can provide the basis for economic growth, control planning and optimization of natural resources (Box and Jenkins, 1976). In order to derive the best forecast, it is very important to specify the accuracy of the forecast, so that the risk associated with the decision based on the forecast can be minimized (Brown, 1964; Staski, Wilson and Burrows, 1989).

According to Jolliffe and Stephenson (2003) a scoring rule is a function of the forecast and observed values that is used to assess the quality of the forecasts. Verification measures and assesses the accuracy of the forecast against observations. Accuracy is a measure of the correspondence between individual pairs of forecasts and observations. The accuracy of a forecast may be expressed by calculating probability limits. The probability limits are used in such a way that the values of a forecast are within the stated limits.

There is an increasing concern about the socio-economic impacts of climate variability, therefore this emphasises the need for rapid model development and an increased urgency for climate prediction at the local and global scale (Beven and Hornberger, 1982). Two approaches are currently used to determine the future behaviour of the ocean-atmosphere system; namely a purely empirical statistical and a dynamical one. The advantages of the

classical statistical forecasting models over the dynamical ones involve their capacity to convert uncertainty values into probilistic terms (Wilks, 2006 and Brown, 1964).

Reitsma, Zigurs, Lewis, Sloane and Wilson (1996) reported on the effect of the subjective nature of the model for a specific time period. Sharing of models and information among interest groups assumes the acceptance by all parties of those models and data. Reitsma *et al.* (1996) states that at first this may seem straightforward and non-problematic since models are intended to represent the objective properties of the natural resource. Since models are the product of human thought and are, in essence, a sequence of assumptions they typically are influenced by the cultural background where they were developed. In addition, they are often developed within groups or organisations that also participate in the negotiation process, either as parties or as external areal experts. Reitsma *et al.* (1996) conclude with a strong statement that a careful study of the role of simulation models in water resource negotiation also requires an analysis of a number of strategic, tactical and managerial aspects of model use.

The importance of reliable methods for long range rainfall prediction is increasing because of the increasing demand for fresh water and the increasing population. The issue of seasonal forecasts started in South Africa in the early 1990s at a number of institutions. The primary predictors used as the main predictors at a global scale were cloud depth, upper-zonal winds and SSTs (Landman and Mason, 1999).

Systematic biases have created the need to downscale or recalibrate GCM simulations to a regional level. There are semi-empirical relationships between rainfall and observed large-scale circulation, if these relationships are valid during future climatic conditions then GCMs correlation variability, prediction of local precipitation can be well simulated from large scale correlation using equations (Landman and Mason, 2001). Landman *et al.* (2001) mentioned that forecasts with a high level of accuracy can be made when using the GCM-derived forecast of atmospheric fields over southern Africa. To downscale these forecasts to categorized stream flow will improve on the regional water

management efficiency. In this study the effects oceanic domains at different lead-times are used to assess the predictability of stream flow in the upper Olifants catchment.

2.7 Pearson's Correlation

The most common measure of correlation is the Pearson Product Moment Correlation (called Pearson's correlation in short). The correlation between two variables reflects the degree which the variables are related to one another. When measured in a population the Pearson's correlation is designated by the Greek letter rho "ρ" and when computed in a sample it is designated by the letter "r". The Pearson's correlation reflects the degree of linear relationship between two variables. It ranges from +1 to -1. Where a correlation of +1 means that there is a perfect positive linear relationship between variables. A -1 correlation means that there is a perfect negative linear relationship between variables. A Pearson's correlation of zero means that there is no linear relationship between variables (Box and Jenkins, 1976).

CHAPTER 3

Description of the Upper Olifants Catchment

3.1 Location and Background

Mpumalanga is one of the nine provinces of the Republic of South Africa. The name means 'Place where the sun rises', and it is bordered by Mozambique and Swaziland in the east, Gauteng in the west, and by KwaZulu-Natal to the south and Limpopo to the north. This is a summer rainfall area divided by the Escarpment into the Highveld region with cold frosty winters and the Lowveld region with mild winters and a sub-tropical climate. The area of study, South Western Mpumalanga, is located between latitudes 25˚-26˚ S and 31˚-33˚ E. Encompassing about 25% of Mpumalanga, with favourable conditions for agricultural activities (Fig. 3.1). The upper Olifants catchment area falls within the Olifants water management area. The major rivers in the Olifants water management area include the Olifants, Elands, Wilger and Steelpoort Rivers. The Olifants River in the upper Olifants catchment has two main tributaries which are the Wilger River and the Groot Olifants River. Fig. 3.1 shows the Groot Olifants sub-catchment which is labelled B1 and the Wilger sub-catchment which is labelled B2. The main features of this area are coal mining, power generation, agriculture, industrial development and large residential areas.

3.2 Economic Activities

Mpumalanga produces about 80% of the country's coal and remains the largest production region for forestry and agriculture. Mining, manufacturing and electricity contribute about 65% of the province's Gross Domestic Product (GDP), while the remainder comes from government services, agriculture, forestry and related industries. Mpumalanga is the fourth biggest contributor to the country's GDP. Mpumalanga's official unemployment rate is 25% (Stats SA, 2003). Even though it is one of the smaller provinces (79 490 km^2 in surface area), Mpumalanga has a population of more than 3.2 million people (Stats. SA, 2003). According to the 2001 Census results, some 27.5% of those aged 20 years or older have not undergone any schooling, while the population growth rate is higher than the national average.
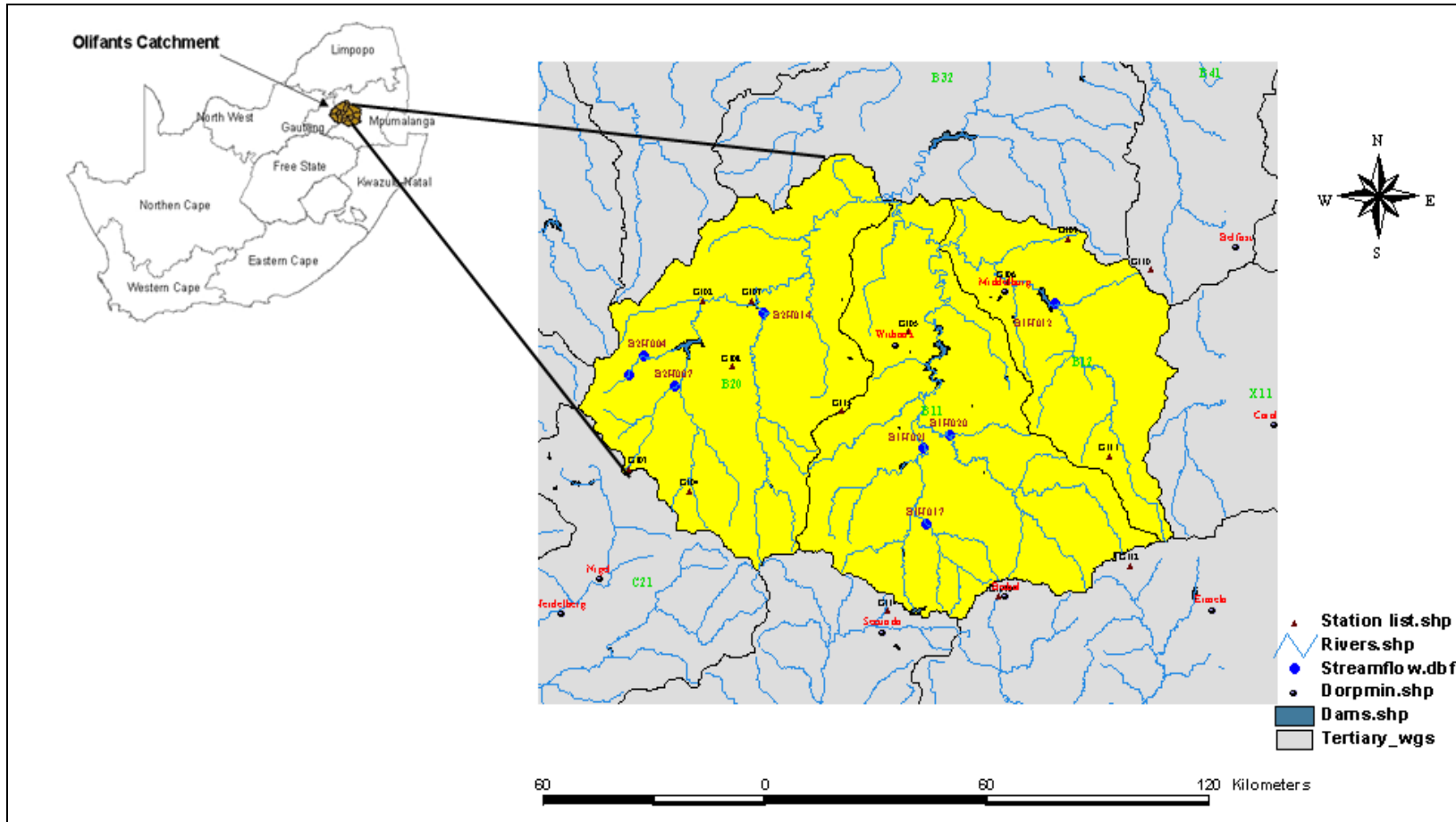
Fig. 3.1 Location of the upper Olifants catchment (ARC-ISCW Gislib, 2004)

3.3 Towns and Municipalities in the Upper Olifants Catchment

The catchment falls within two district municipalities namely Nkangala district municipality and Motsweding district municipality. The district municipalities are made up of local municipalities, as listed on Table 3.1. The Groot Olifants sub-catchment falls mainly within the Nkangala district municipality and the Wilger sub-catchment falls mainly within the Motsweding district municipality.

Carolina-Bethal-Ermelo is a sheep production area with potatoes, sunflower seed, maize and groundnuts also being produced in this region. One of the country's largest paper mills is situated in the Groot Olifants sub-catchment close to its timber source. Middleburg produces steel and vanadium, while Witbank is the biggest coal producer in Africa (http://www.demarcation.org.za/municprofileonline).

Table 3.1 Description of municipalities and major towns within the upper Olifants catchment

District Municipalities	Nkangala			Motsweding
Local Municipalities	Highland	Steve Tshwete	Emalahleni	Kangweni
Major Towns	Stoffberg	Middelburg	Witbank	Bronkhortspruit
	Belfast	Hendrina	Ermelo	
	Carolina	Bethal		

Source: http://www.demarcation.org.za/municprofileonline

3.4 Vegetation Description within the Catchment

The province falls mainly within the Grassland Biome. The Escarpment and the Highveld form a transitional zone between this grassland area and the savana biome (Low and Rebelo, 1996). The dominat grass species are Redgrass (*Themeda trianda),* Tough Love Grass *(Eragrostis plana),* Bushveld Turpentinegrass *(Cymbopogon plurinodis)* and Broom Needlegrass *(Triraphis andropogonoides)*. The Karoo bushes in the area are Bitterkaroo *(Pentzia globosa)* and Oldwood *(Leucosidea sericea)*. During summer most of the land is used for maize production (Kruger, 2004b).

3.5 Soil Description within the Catchment

The Groot Olifants sub-catchment area has shales and sandstones of the Vryheid and Volksrust Formations (Karoo Sequence) dominated by the underlying rock types giving rise to deep, red to yellow sandy soils. The Wilger sub-catchment soils are formed by shale, ridges and plains of quartzite. A very large area of the upper Olifants interior is occupied by Plantic catena which in its perfect form is represented by Hutton, Bansvlei, Avalon and Longlands soil forms (Fitzpatrick, Hahne, Kristen and Hawker, 1986; Hahne and Fitzpatrick, 1985). Glenrosa or Mispha soil forms are found in the south western parts of Witbank in the Groot Olifants sub-catchment. These soil forms accommodate soil forms of pedologically young landscapes that are not predominantly rock and not predominantly alluvial or Aeolian. The dominant soil forming processes have been rock weathering, the formation of orthic topsoil horizon and commonly, clay illuviation, giving rise typically to lithocutanic horizons (Fitzpatrick *et al.,* 1986; Hahne and Fitzpatrick, 1985). The soil characteristics are given in details in Appendix 1.

3.6 Stream Flow Stations

Stream flow data was obtained from eight stream flow stations within the upper Olifants catchment. In order to avoid the effect of dams, the stream flow stations that are located above the dams on the stream were selected for this study. The selected stations are located between 25.81˚ and 26.31˚ S and 28.55˚ and 29.59˚ E. The stream flow data was downloaded from the Department of Water Affairs and Forestry website (http://www.dwaf.gov.za/hydrology/cgi-bin/his/cgihis.exe/station). The stream flow data downloading procedure will be discussed in detail in chapter four.

3.7 Rainfall Analysis for the Upper Olifants Catchment

The problem associated with the spatial variation in rainfall and errors in calculating areal averages and their effect on stream flow have been considered when selecting the rainfall measuring points within the upper Olifants catchment. Beven and Hornberger (1982) have indicated that the use of a non-representative set of rain gauges can also result in poor stream flow predictions. Dawdy and Bergman (1969) indicated that the use of a

single rainfall record as lumped input can best predict peak discharge of a catchment within a standard error of the order of 20%. There were 15 rainfall stations selected for this study influenced largely by long term data availability. There are six rainfall stations in the Wilger sub-catchment and nine rainfall stations in the Groot Olifants sub-catchment. More about the rainfall pattern will be discussed in chapter four.

The upper Olifants catchment falls within the highveld region according to Köppen classification (Schulze, 1997). The yearly average rainfall in this region is from 650 mm to 900 mm (Kruger, 2004a). The dominating rainfall type is convective precipitation in this region, mainly with showers and thunderstorms receiving an average of about 75 thunderstorms annually. The duration of rainfall during the summer season in this region is from October to March. The maximum rainfall or heavy rainfall can easily reach 125mm to 150 mm per day in January. The thunderstorms in the upper Olifants catchment are violent with severe lightning and strong westerly winds and can bring hail the size of golf balls. Tornadoes also occur in this region and often cause huge damage if they strike a highly populated area (Schulze, 1994).

Jury and Pathack (1991); Nicholson and Entekhabi (1987); Mason Lindesay and Tyson (1994); Mason (1995); Rocha and Simmonds (1997); Landman and Mason (1999); Walker (1990) mentioned that, South African rainfall has a strong relation between SST anomalies of the equatorial Pacific Ocean and other two Oceans bordering southern African coast line. Furthermore Walker and Lindesay (1989) mentioned that predictions of both the severe and rain producing synoptic weather events will be improved by incorporating the SSTs datasets from the oceanic domains surrounding the South Africa coastline.

Fig. 3.2 shows the three-month rainfall average for JFM and OND from 1950 to 2002 as a mean value across the 15 selected rainfall stations within the upper Olifants catchment. The average JFM rainfall is higher than the average OND rainfall. This simply means that there is more precipitation towards the second half or end of the summer season as compared to the beginning of the season. The JFM season also has a high variability

across the years with some extreme events near 500 mm. The stream flow data used in this study starts from the year 1990 and ends in the year 2005 but the rainfall data in Fig. 3.2 starts from 1990 and ends on 2002. The highest three-month sum of rainfall on the JFM graph is during 1995, at a value of 565.73 mm and the lowest three month rainfall value is during the year 2002, at a value of 144 mm. The highest rainfall on the OND graph is during the year 1953, at a value of 228 mm and the lowest rainfall value is during the year 1962, at a value of 51.3 mm. In water resource management this kind of information is very important but it is not sufficient for decision making purposes. Therefore a relationship between stream flow and rainfall would be useful. The water resource managers can use relationships between stream flow and rainfall to plan for the seasonal water allocation if a seasonal stream flow forecast is issued. The main objective of this study is to develop a three month stream flow forecast.
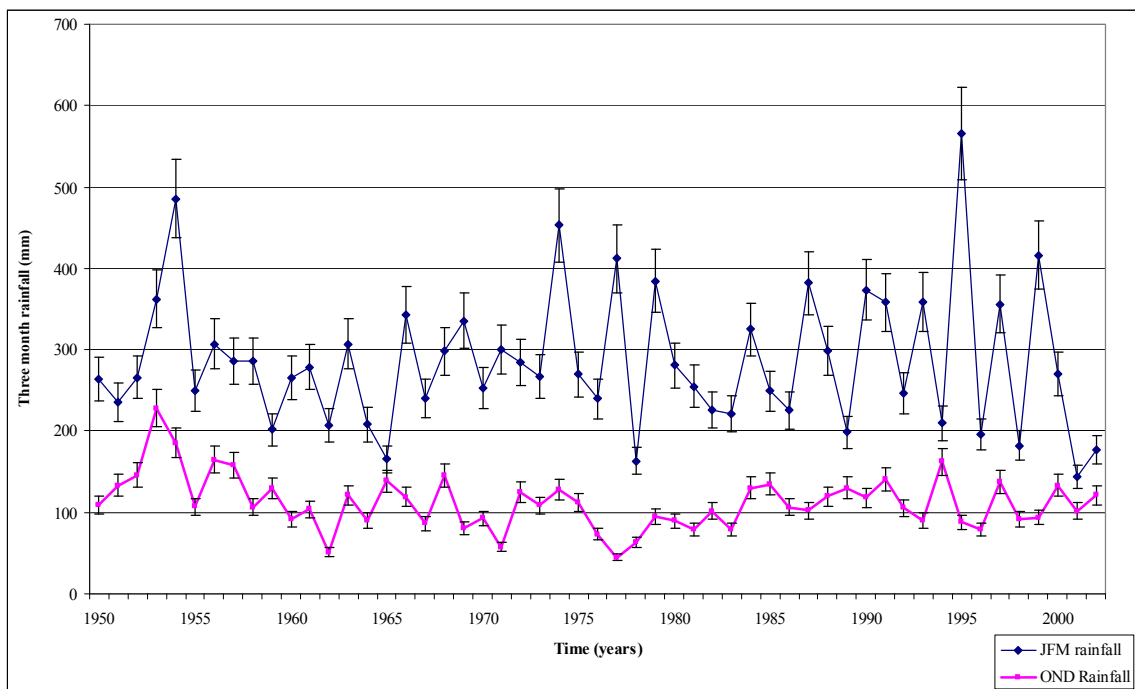
Fig. 3.2 JFM and OND average rainfall from 1950 to 2002 in the upper Olifants catchment

The complexity of summer rainfall at mid-latitudes and its multifaceted nature makes it difficult to be represented by Global Circulation Models (GCM). Therefore GCMs tend to overestimate local rainfall over southern Africa (Mason and Joubert, 1997; Rouault, Florenchie, Fauchereau and Reason, 2003; Cook, Reason and Hewitson, 2004). Time and

again rainfall at mid-latitudes is not well estimated because of its complexity (Landman *et al.,* 2001; Goddard and Mason, 2002). The rainfall and SSTs variability are rather high during the summer season over South Africa. When using only the SSTs to predict the October month, Pathack *et al.* (1993) and Landman and Mason (1999) have found that regional rainfall is not well predicted during the summer months, however February and March are well predicted using the central equatorial Indian Ocean.

The type of rainfall plays a very important role in the hydrological cycle. There are also other factors that have a major effect on stream flow. Attempting to determine variables that can be used to construct a stream flow forecast, a simple regression analysis is shown using three month rainfall and the three month stream flow (Fig 3.3 and 3.4). Both the OND and JFM curves show a R^2 of less than 0.5. Landman and Mason (1999) illustrated the difficulties of predicting the stream flow using only rainfall; with similar findings as shown in Fig. 3.3 and 3.4. The low regression coefficient emphasizes the effect of other factors like vegetation cover, soil characteristics topography and the type of rainfall on stream flow forecasting. During the OND season, more than 50 % of rainfall between 90 and 170 mm did not result in more than 10 million m^3 s^{-1} of stream flow. This can be related to factors other than rainfall intensity only. As it was mentioned earlier, the rainfall pattern of the area is of a convective type.

During JFM, there are also more than 50 % of rainfall years between 120 and 360 mm that did not result in more than 10 million m^3 s^{-1} of stream flow (Fig. 3.4). This means that there is a high amount of precipitation that results to smaller amounts of stream flow. During this season (JFM), there is a better relationship between total amount of rainfall and the total amount of runoff. However, there are also some years which do not lie near to the straight line (e.g. when 190 mm of rain resulted in nearly 30 million m^3 s^{-1}). This was obviously a rainy season when a large amount of rain was received in a short time period. In contrast, there are two years which received about 360 mm of rain but had low flow (4.77 and 6.64 m^3 s^{-1}).
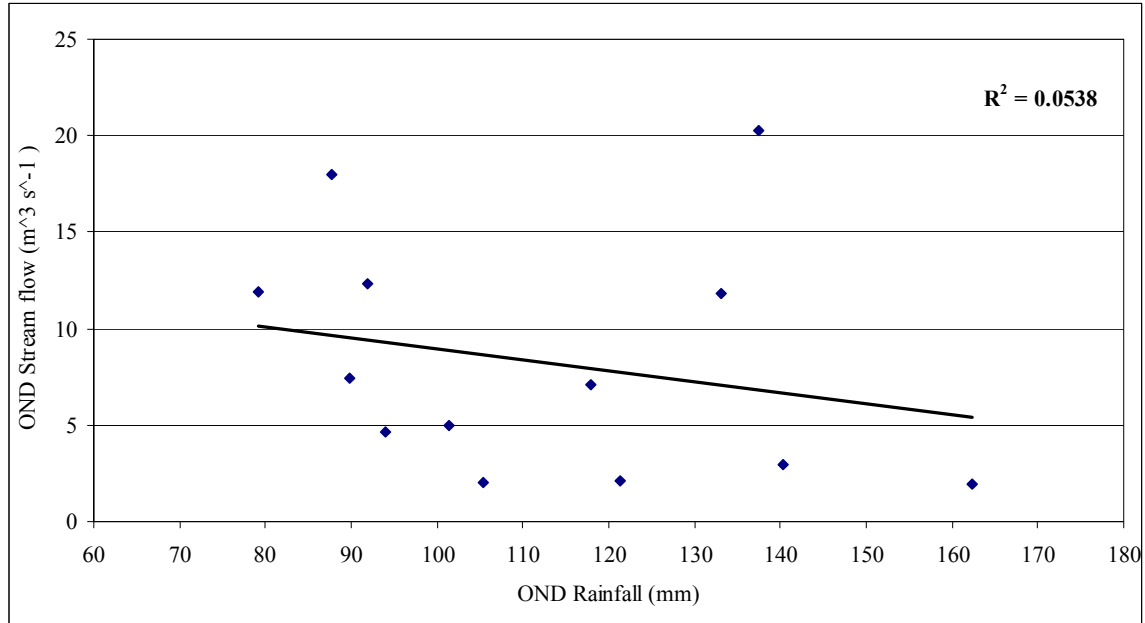
Fig. 3.3 OND stream flow vs. OND rainfall from 1990 to 2002 in the upper Olifants catchment

These years probably had more even distribution of small rain storms at regular intervals). The graphs show the complexity of the relationship between stream flow and rainfall as there are many other factors that have an effect to the stream flow. Schulze (1983) mentioned the importance of including the hydrological factors in stream flow simulation. The high variability of rainfall also makes the stream flow prediction very difficult, although probably time period of three months is not sourceful for this type of relationship.

The spatial and temporal variations of rainfall are very high therefore for a significant rainfall analysis these two factors have to be included in the rainfall analysis. Lynch and Dent (1990) found that a longer rainfall period can be used to generate spatial mean annual precipitation. Since that study focused on monthly stream flow but annual values would not be so easy. Rainfall will not be further analysed in this study.
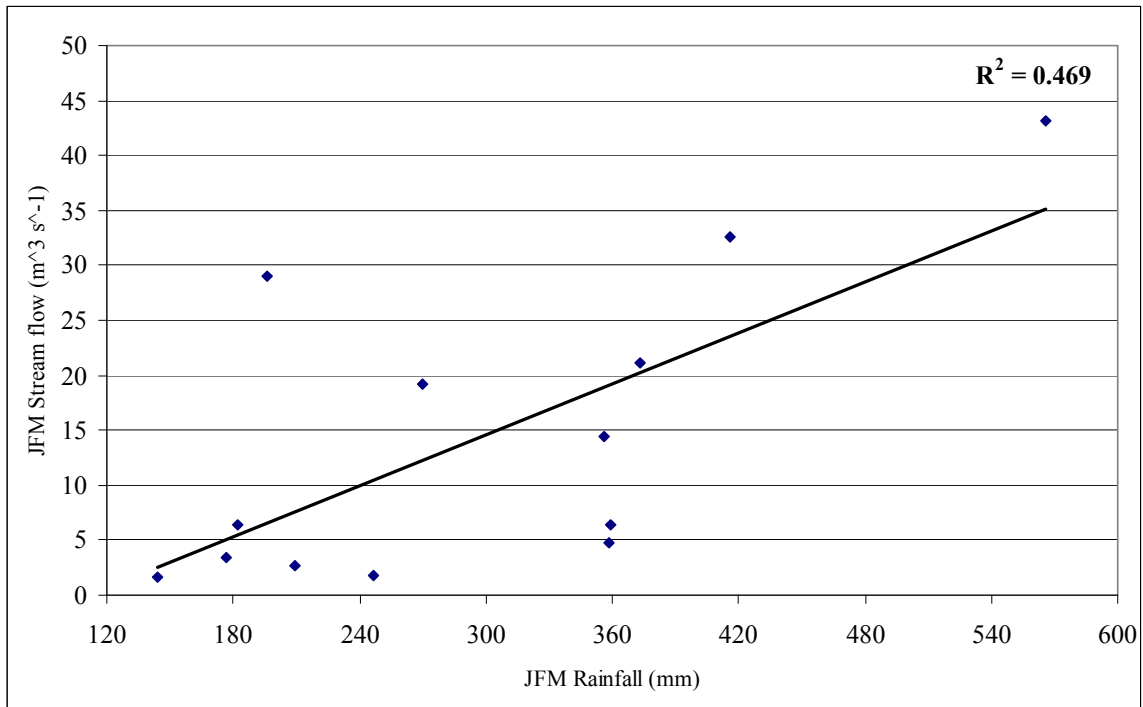
Fig. 3.4 Average JFM Stream flow vs. average JFM rainfall from 1990 to 2002 in the upper Olifants catchment

CHAPTER 4

Materials and Methods

The IRI Climate Predictability Tool (CPT) has been selected as a forecasting tool for this study. This chapter describes the version of the forecasting model used, how the model and the necessary data were obtained and prepared for use in the CPT model. CPT was then used to analyse data in the two upper Olifants sub-catchments and the upper Olifants catchment as a unit.

4.1 Climate Predictability Tool

The CPT model was downloaded from http://iri.columbia.edu/outreach/software/ and installed on a computer. After starting the software, the 'Introductory Window' will be opened, indicating the title of the software, and showing the IRI banner. There are three menu items on the introductory window namely: "File", "View" and "Help", the most important of which is the View icon. From the introductory window select "View", which will give the user an option to choose the "CCA" or "PCR" Input Window. Select CCA. Then an Input Window should be opened once an analysis method has been selected. There should be six menu items: "File"; "Edit"; "Actions"; "Options"; "View" and "Help" on the input window. The Input Window requests information relating to the data to be used to construct the model. Two datasets are required by CPT: the first dataset contains the X variables and the second dataset contains the Y variables. Data acquisition and data formatting for the model is explained in paragraph 4.2.1 to 4.2.3.

Figure 4.1 illustrates the type of data required to be entered on the input window, for example at zero months lead-time using December SSTs to predicate JFM stream flow. The X input file where the predictor data is, is then selected. After the input file has been successfully selected, the number of grid points, first year of data in the file would be visible in the columns below respectively. The user can then adjust the first year of the training period. In this study the first year for the training period is 1990 (Fig. 4.1). The predictant data is selected as the Y input file.

Canonical Correlation Analysis					
Project Name					
Explanatory (X) Variables			**Response (Y) Variables**		
Training Data File			**Training Data File**		
X Input File	Dec 1990-07.tsv	**Browse**	**Y Input File**	JFMStreamFlow.txt	**Browse**
Number of Grid points	7740		Number of stations	8	
First years of data in file	1990		First years of data in file	1990	
First year of training period	1990		First year of training period	1990	
EOF Modes			**EOF Modes**		
Minimum number of modes	1		Minimum number of modes	1	
Maximum number of modes	4		Maximum number of modes	4	
Training data			**CCA modes**		
			Minimum number of modes	1	
Length of training period	8		Maximum number of modes	3	
Length of cross-validation window	8				

Fig. 4.1 Canonical correlation analysis input window illustrating data requirements for explanatory (X) and response (Y) variables

The explanatory variable which is the sea-surface temperature datasets in this study was specified by selecting the browse button next to X input file. Input files are stored in a sub-directory file called DATA, but files can be read from any directory. The response variable (Y) which is the stream flow datasets in this study was specified by selecting the browse button next to Y input file.

The optimal Empirical Orthogonal Function (EOF) and CCA modes were selected by trial and error. The EOF modes were set to one at minimum and four at maximum for both explanatory (X) variable and response (Y) variable. It is very important to specify the length of the training period, as this defines the total number of years available to construct the forecasting model. In this study the length of training period was set to be eight years since the stream flow data is from 1990 to 2006. The first half of the data was used for the training period and the second half of the data was used for validation. The length of the cross-validation window defines how many years to leave out when

performing cross-validation, either, for calculating performance statistics or in calculating the optimum number of modes. In this study, the cross-validation window was set to five years for calculating performance statistics. In addition to specifying the numbers of EOF modes for the X and Y variables when performing CCA, it is also very important to define the numbers of CCA modes. The CCA mode fields work in an identical way to the EOF mode fields, the minimum number of CCA modes were set to one and the maximum was set to three.

After all the fields have been defined correctly in the input window, then the user can run the model to perform the CCA. Select the action menu item, and then the cross-validated forecast item. The cross-validated calculation option fits a CCA model, and then produces cross-validated forecasts for all years in the training period. These cross-validated forecasts are made available for output to a file and for performance analyses within CPT. Goodness Index and Pearson's correlation from the output files were used to evaluate the model skill at different lead-times and different oceanic domains. An explanation of the set-up for model skill evaluation is explained in detail in paragraph 4.6 to 4.8.

4.2 Sea-Surface Temperature Data

The sea-surface temperature data for use with the CPT is available via the IRI data library. The monthly sea-surface temperatures from January 1950 to December 2006 were extracted from the IRI dataset library. Sea-surface temperatures can be downloaded from http://iridl.ldeo.columbia.edu. The SSTs used were obtained from National Oceanic and Atmospheric Administration (NOAA) National Climate Data Centre (NCDC) extended reconstructed global sea-surface temperature (ERSST), version 2 Improved extended reconstructed global sea-surface temperature data based on Comprehensive Ocean-Atmosphere Data Set (COADS) (Smith and Reynolds, 2004). The range of global SST data starts from 88˚S to 88˚N by 2˚ N; there are 89 grid points in the longitude selection and 0˚ to 2˚W by 2˚ E, there are 180 grid points in the latitude selection.

4.2.1   Accessing data for the Climate Predictability Tool

Surface temperature data from the most recent version of the Extended Reconstructed Sea-Surface Temperature dataset (NOAA NCDC ERSSTv2) can be downloaded from the above mentioned IRI website. The IRI data bank website has different types of data sets. It is very important to know what type of data is needed for downloading. The paragraph below illustrates how SSTs data was downloaded to be used in the CPT model.

Once the IRI website is opened then select the datasets by the category link at the bottom of the page. Click on the "Air-Sea Interface" link on the new page. Then select the "NOAA NCDC ERSST" link. Double click on the "version 2" link. Then the "the Sea-Surface Temperature" link can be selected. Click on the "Data Selection" link, after this selection then a longitude, latitude and time range setting box will appear. When selecting a part of the Oceanic domain the specific longitude and latitude for the selected domain must be entered in the latitude and longitude text boxes. Then carry on by selecting a time period, enter Jan 1950-2007 in the Time text box. Click on "Restrict Ranges". Then select time range (Jan 1950-2007) this means that only January months from 1950 to January 2007 will be extracted from the data bank. To select a different month or range of years, put the appropriate information in the "Time text" box using the same format (MmmYYYY to YYYY). Sub-domains of the data can be selected within CPT, so it is generally best to download data for as large an area as possible. This will, however, affect the size of the file downloaded in later steps. Click the "Stop Selecting" button. Click the "Data Files" link. Click the "CPT" link. Select of the "TSV" links to download the data (Smith and Reynolds, 2004). It is always best to download the compressed file, when downloading SST for the whole globe. When downloading these data from the ERSST dataset, the compressed file can be up to 10 times smaller than the uncompressed file.

4.3 Downloading Data for the Selected Oceanic Domains.

SSTs of the Atlantic, Indian and Pacific Oceans were downloaded following the steps in Section 4.2.1. The locations of the oceanic domains selected for this study are described in detail in Table 4.1 (Landman and Mason, 1999). According to the literature review, the oceanic domains shown from Fig. 4.2 to 4.5 have more influence to the South African

rainfall patterns. These pictures of the selected domains were obtained from the CPT model.

Table 4.1 Identification of the selected oceanic domains

South Atlantic Ocean		Equatorial Atlantic Ocean		Tropical Indian Ocean		Pacific Ocean	
10º S	45º S	6º N	6º S	6º N	6º S	14º S	46º S
20º W	20º E	48º E	104º E	40º W	8º E	20º W	16º E
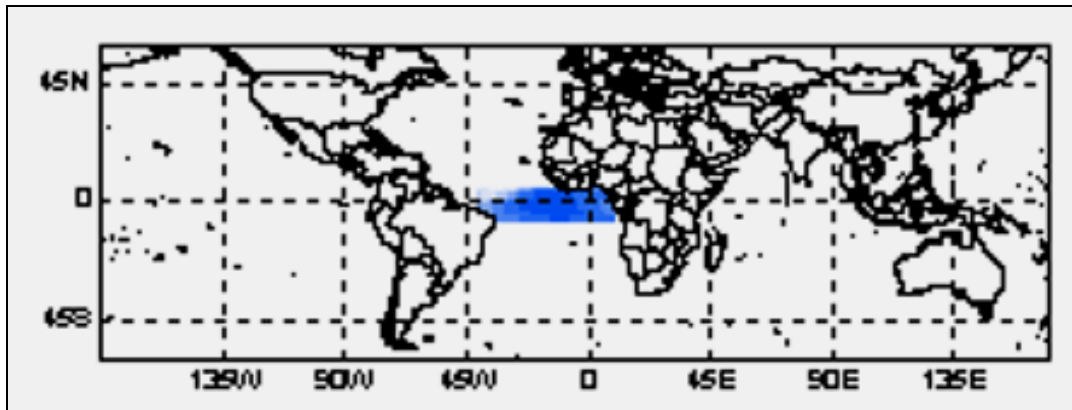
Fig. 4.2 Equatorial Atlantic Ocean domain from CPT
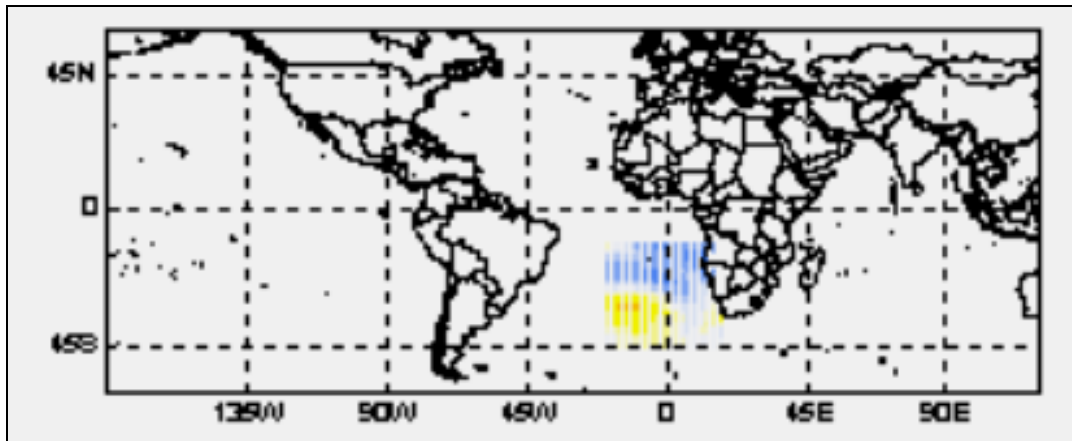
Fig. 4.3 South Atlantic Ocean domain from CPT
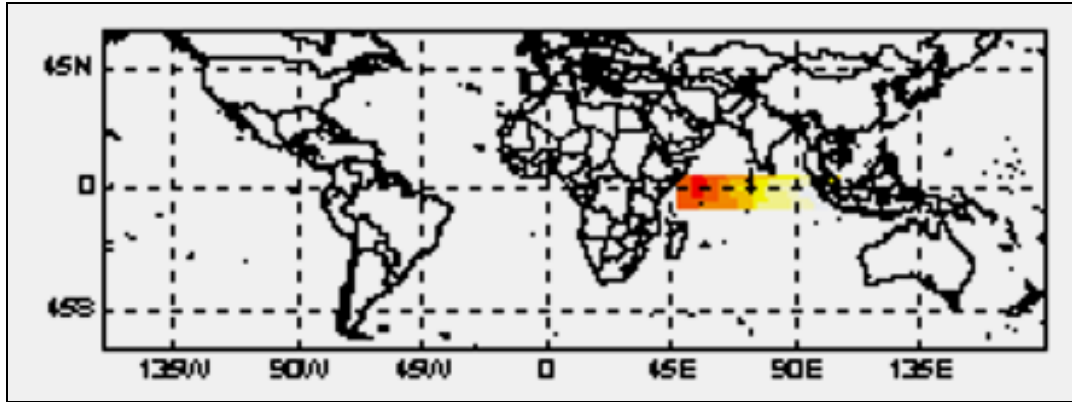
Fig. 4.4 Tropical Indian Ocean domain from CPT
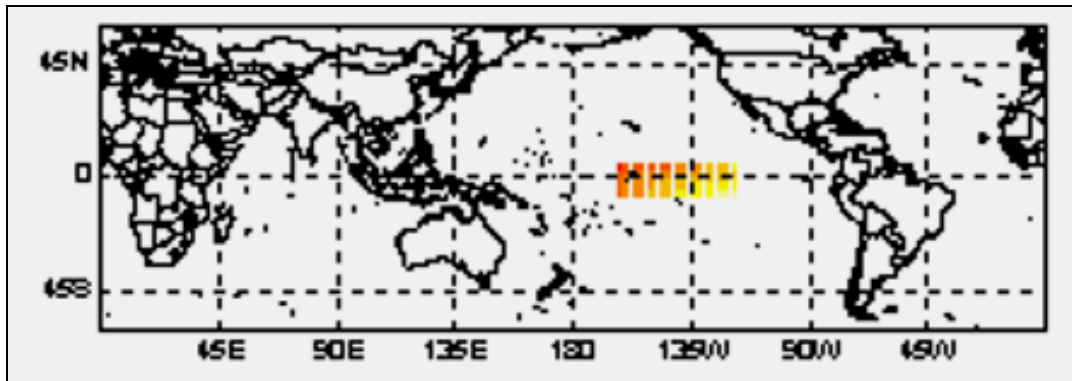
Fig. 4.5 Pacific Ocean domain from CPT

4.4 Stream Flow Data

A total of eight stream flow stations (Table 4.2) were selected within the upper Olifants catchment area. DWAF calls the stream flow stations gauging stations or weirs, for this study a weir will be called a stream flow station. Stream flow stations up stream before the dams were selected to reduce the effect of water storage dams on measured stream flow. Stream flow data was downloaded from DWAF website: http://www.dwaf.gov.za/hydrology/cgi-bin/his/cgihis.exe/station.

The stream flow station number is made up of six characters, for example: station number B1H012. The first two characters refer to the sub-drainage region (B1) in which the stream flow station is situated. So B1 in this study is the Groot Olifants sub-catchment and B2 is for the Wilger sub-catchment. The third character refers to the type of stream flow station (H in flowing water, R in stored/standing water and E for meteorological

stations). The last three characters are simply a serial number for the stream flow station in the sub-drainage region concerned.

Table 4.2 Selected stream flow stations in the upper Olifants catchment area (from DWAF website)

Sub-catchment	Station name	Station number	Latitude (S)	Longitude (E)	Data period
Groot Olifants	Rondebosch	B1H012	-25.808	29.587	1978/02-2006/12
	Aangewys	B1H017	-26.305	29.274	1989/12-2006/12
	Vaalkranz	B1H020	-26.105	29.332	1990/12-2003/11
	Middeldrift	B1H021	-26.136	29.270	1990/11-2007/03
Wilger	Waaikraal	B2H007	-25.995	28.663	1985/09-2006/12
	Witpoort	B2H006	-25.967	28.551	1984/11-2006/09
	Onverwacht	B2H014	-25.827	28.881	1990/12-2007/03
	Boschkop	B2H004	-25.925	28.586	1984/11-2006/12

4.4.1 Stream flow data downloading procedure

Before the stream flow data can be downloaded the stream flow stations must have been selected. To select stream flow station first open the DWAF webpage at http://www.dwaf.gov.za/HydroMpumalanga/. Then select a sub-catchment region from the drop down menu. For this study region B1 and B2 were used. Select either B1 or B2. Select a map on the top corner of the page to view stream flow stations location in the catchment. Then write down the selected stream flow station numbers. Once the stream flow stations names have been noted down then open the following webpage, http://www.dwaf.gov.za/hydrology. Select "river flow stations" to indicate that stream flow data would be downloaded. Enter the station number e.g. B1H012. Select "Access station" data. At this web page there is an option to select monthly and daily data. In this study monthly stream flow data was selected.

The downloaded monthly stream flow data is saved as a text file which can be imported to an excel spreadsheet for editing and rearranging. The downloaded monthly stream flow data starts from October each year going through to September of the following year and the last column gives the annual totals. The units for the monthly stream flow values are million cubic metres per month. The stream flow data is now ready to be compiled into the CPT format.

4.4.2   Preparing stream flow data for CPT use

The stream flow information shown in Table 4.2 can be obtained from station data source information downloaded from the DWAF webpage. The stream flow values were selected for the OND and JFM season. This means that for OND season, a sum for the three-month stream flows value for OND was calculated for each of the eight stream flow stations. The same was done for the JFM season. Stream flow data from 1990 to 2006 for OND and JFM was selected from the downloaded data. Stream flow station B1H020 has two years of missing stream flow data as compared to the other stream flow stations as stream flow data for this station ends in 2003 (Appendix 2).

The stream flow input file has to be prepared in the right format for CPT as shown in Table 4.3. The station name has to have the same characters as the input files (Mason, 1999). The first column is the year at the beginning of data, and then the second column is the actual stream flow data which correspond to the first station. In this example it would be data for station B1H012.

Table 4.3 Data input file for CPT, Stn stands for station name and Lat and Long represent Latitude and Longitude respectively

Stn	Stn_B1H012	Stn_B1H017	Station name without space and less than 16 characters		
Lat	-25.808	-26.305	In signed degrees		
Long	29.587	29.274			
1990	20.185	1.216	The first column is years and the second column is the sum of OND stream flow for each of the stations		
1991	11.270	0.540			
1992	0.881	5.228			
1993	2.054	13.370			
1994	11.490	0.445			
1995	0.440	17.825			

4.5 Rainfall Data

Fifteen rainfall stations in the upper Olifants catchment were selected (Table 4.4). The criterion for selecting the rainfall stations was based on the available rainfall data-set being longer than 30 years. The study area falls within the North-eastern Highveld rainfall region as described by Mason (1998); Landman *et al.* (2001) and Bartman, Landman and Rautenbach *(*2003). The targeted seasons are OND and JFM, which are

similar to the stream flow stations seasons. These seasons are important periods for water management and agricultural activities in the summer rainfall region of southern Africa. Moreover, the tropical atmospheric circulation becomes dominant during these peak austral summer rainfall months, and a higher forecast skill should consequently be possible (Mason, Joubert, Codijn and Crimp, 1996).

Table 4.4 Description of rainfall stations selected within the upper Olifants catchment

Station Name	Latitude (S)	Longitude (E)	Altitude (m)	Data length	Data Source
Bethal	-26.47	29.45	1640	1950-2007	ARC
Bronkhorstspruit	-25.80	28.73	1427	1950-2007	DWAF
Sundra POL	-26.18	28.55	1680	1950-2002	ARC
Vlakplaas	-26.23	28.70	1615	1950-2002	ARC
Witbank MUN	-25.87	29.23	1600	1950-2006	DWAF
Middelburg	-25.76	29.47	1447	1950-2002	SAWS
Wilgerivier	-25.80	28.85	1432	1950-2002	ARC
Blesbokfontein	-25.95	28.80	1495	1950-2002	ARC
Bankfontein	-25.66	29.62	1525	1950-2002	ARC
Roodepoort	-25.73	29.82	1737	1950-2002	ARC
Hendrina	-26.15	29.72	1615	1950-2004	ARC
Tweefontein	-26.49	29.67	1756	1950-2005	DWAF
Vandyksdrift	-26.10	29.32	1521	1950-2004	ARC
Secunda	-26.50	29.18	1628	1950-2005	ARC
Ogies POL	-26.05	29.07	1585	1950-2002	ARC

The rainfall data used in this study was patched using data from three different sources namely: Agricultural Research Council - Institute for Soil, Climate and Water (ARC-ISCW), DWAF and SAWS. Rainfall data for the selected stations was patched using the inverse distance method and closest station method (Moeletsi, 2004). The guidelines and stations used for data patching are explained in Appendix 3 and 4.

4.6 Setting-Up the Lead-Times

The lead-times were evaluated to determine the varying effect of sea-surface temperature during different months on the skill of the model to forecast stream flow. The lead-times

of zero to nine months were selected for evaluation. In this study a lead-time of 0 means the for the September months SSTs from 1990 to 1997 were used to forecast 1990 to 1997 OND stream flow. Operationally it would not really be practical to use zero month lead-time as there would not be enough time to distribute the forecast to the end users. The OND and JFM seasons were selected because they fall within the South African summer season (Lindesay, 1988; Landman and Mason, 1999).

According to Landman and Mason (1999) the OND season has been shown to have a high response to the southern Atlantic Ocean sea-surface temperatures. Even though Pathack *et al.* (1993) and Landman and Mason (1999) have mentioned that it is difficult to predict the rainfall for October month using only SSTs. But Walker (1990); Jury, Valentine and Lutjeharms (1993) and Mason (1995) stated that the South African seasonal rainfall is related to the SSTs anomalies of the oceans adjacent to South Africa. The month of October had to be included in the OND season as this season is within the austral summer season. However the January and March rainfall has been found to be predicted with better accuracy when using the equatorial Indian Ocean, therefore the JFM season was included for analysis also (Pathack *et al.,* 1993; Landman and Mason, 1999).

A schematic illustration of the definition of the predictor seasons for hind-casting the OND stream flow for 1990 to 1997 and JFM stream flow of 1991 to 1998 with different lead-times is shown in Table 4.5a and 4.5b.

Table 4.5a Hindcasting the OND stream flow at different lead-times for the 1990 to 1997 period (adapted from Landman and Mason, 1999)

Predictors: (SSTs) months		Lead-times
Sep 1990 to 1997	→	0
Aug 1990 to 1997	→	1
Jul 1990 to 1997	→	2
Jun 1990 to 1997	→	3
May 1990 to 1997	→	4
Apr 1990 to 1997	→	5
Mar 1990 to 1997	→	6
Feb 1990 to 1997	→	7
Jan 1990 to 1997	→	8
Dec 1990 to 1997	→	9

Table 4.5b Hindcasting the JFM stream flow at different lead-times for the 1990 to 1998 period (adapted from Landman and Mason, 1999)

Predictors: (SSTs) months		Lead-times
Dec 1990 to 1997	→	0
Nov 1990 to 1997	→	1
Oct 1990 to 1997	→	2
Sep 1990 to 1997	→	3
Aug 1990 to 1997	→	4
Jul 1990 to 1997	→	5
Jun 1990 to 1997	→	6
May1990 to 1997	→	7
Apr 1990 to 1997	→	8
Mar1990 to 1997	→	9

In Table 4.5a and 4.5b the predictor years are the sea-surface temperatures for the whole globe from 1990 to 1997 for each month as per lead-time. The predictand is the stream flow for the two selected seasons OND and JFM.

4.7 Estimating Forecast Skill

As described by Landman and Mason (1999), the cross-validation method was used to validate the performance of the model. Both the SSTs and the stream flow data sets were separated into two sets, called the training set and the testing set. For example, on each of the datasets if the original predictor and predictand fields have n observations, each time at index η, where $l \leq \eta \leq n$, then the ηth predictor and predictand fields were removed. An estimated observation of the predictand at time η is made when the remaining n-1 observations were used to train the model. The similar procedure is then repeated n times in sequence, leaving out a single field pair of n hindcasts series, then the errors the model made are accumulated to give the mean absolute test set error, which is used to evaluate the model (Elsner and Schmertmann, 1994; Landman and Mason 1999).

Model skill would be estimated using the Goodness Index for the catchment scale and Pearson correlation coefficient for the individual stream flow stations. The correlation coefficient is a variance-adjusted measure of model skill (Wilks, 2006). However, cross-

validation may still be biased. Since there is not always a direct relationship between seasons and specific climatological features like ENSO, therefore it is necessary that a validation should be performed over an independent training period. This is because the atmosphere behaves as one unit, consequently mixing occurs between different locations and interruption from other climate variables may also occur. Walker (1990) and Mason (1995) and Landman (1997) also mentioned that SST anomalies of the oceans bordering Southern Africa have a major effect on South African seasonal rainfall. Therefore the effects of the selected domains are evaluated in detail in chapter 6.

CHAPTER 5

Stream Flow Forecast Equation for OND and JFM Seasons

A CCA equation will be constructed to provide stream flow forecasts for eight stream flow measuring points in the upper Olifants catchment area. According to literature Global sea-surface temperatures have a great influence in the South African rainfall. Therefore the sea-surface temperature effect is expected to be carried on directly to stream flow. In this study sea-surface temperatures were used as the only predictors for stream flow. A monthly time interval of sea-surface temperatures will be used to incorporate evolutionary features as well as steady state properties of the predictor oceans, predicting three-month stream flow aggregates for both OND and JFM periods.

5.1 Comparison Between CCA and PCR

Before assessing the skill of the stream flow forecasting model, a comparison between the CCA and PCR methods was made to asses the feasibility of selecting a suitable model for a stream flow forecast. The CCA and PCR are functions found in the CPT (Mason, 1999). Fig. 5.1 illustrates the cross validation correlation values (Goodness Index) for the sum of monthly stream flow totals for OND and JFM between the eight selected stream flow stations and sea-surface temperatures up to lead-times of nine months for the period 1990-1997. The period of 1990 to 1997 is the training period which is used throughout the process of model set up before the validation and actual stream flow forecast is made. All the CCA correlations have a positive correlation which is statistically significant at the 95% level of confidence as compared to negative correlations from the PCR.

The Goodness Index of PCR for OND shows a strong correlation than the Goodness Index of PCR for JFM at all lead-times up to nine months (Fig. 5.1). The Goodness Index of CCA for OND is less than Goodness Index of CCA for JFM only at, the one and four month lead-times, but the Goodness Index of CCA for OND is higher than the Goodness Index of CCA for JFM at all other lead-times. The highest Goodness Index for CCA for OND is reached at lead-times of two and eight months and CCA for JFM at lead-times of zero and two months and with values of 0.494; 0.475 and 0.472; 0.433 respectively. The

41

lowest correlation value from CCA for OND is -0.015 at one month lead-time and for CCA for JFM it is at 0.019 a lead-time of nine months.
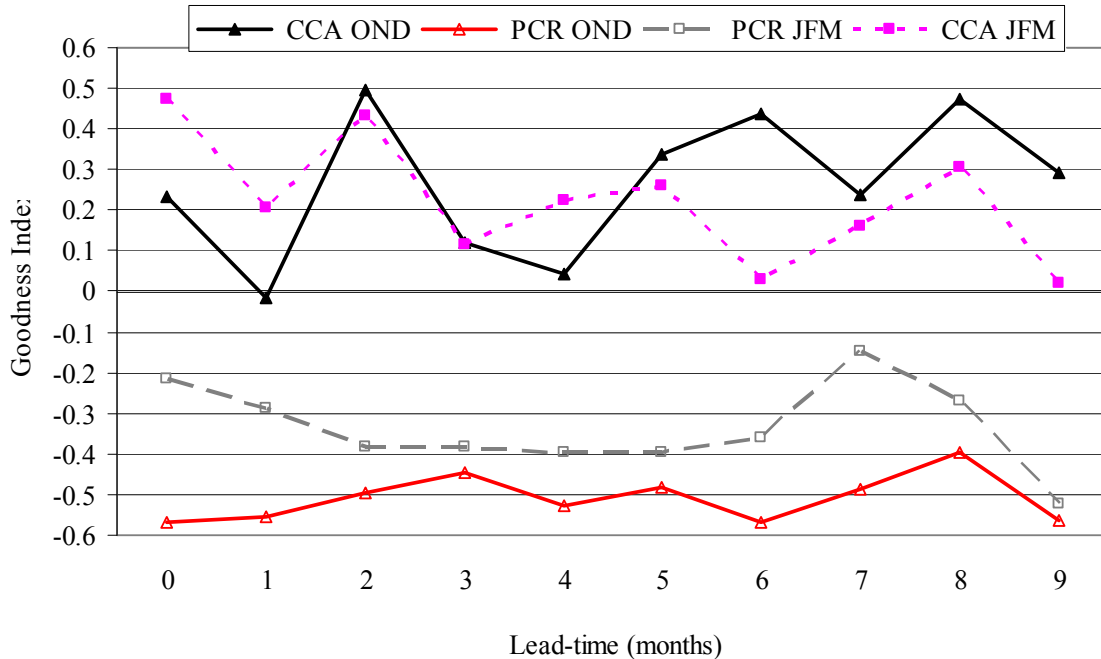
Fig. 5.1 Comparison of the cross-validated correlation between OND and JFM monthly sum of stream flow with sea-surface temperature obtained from CCA and PCA for the period of 1990-1997 for both seasons

In this study it has been decided that the PCR is not a good method to use as all Goodness Index correlation values are negative. In PCR each of the predictant variables is predicted individually so this means that separate regression models are made for each dependable variable, while in CCA the dependable variables are predicted simultaneously. Since in this study there are eight stream flow stations and there are basically two different tributaries of the Olifants River, so they are expected to be related to each other. Therefore PCR would not be a good method to be used. PCR is better suited for predicting either single predictand or a set of predictions that are not expected to have a strong relationship to each other (Mason, 1999). Therefore it is decided in the rest of this project to only use CCA for the prediction of stream flow from SSTs.

5.2 Comparison of Model Skill at Different Lead-Times

There are several methods for determining model output performance (Wilks, 2006). For both predictand seasons (OND and JFM), the highest skill is mostly associated with short (0 and 2-month) lead-times (Fig. 5.1). It should be noted that in this study only lead-times of up to ten months were considered. Box and Jenkins (1976) mentioned that the if the predictor data has an error effect then the error would be amplified more by longer lead-times, so for this reason it was decided to limit the study to ten months lead-times. In this section the effects of different lead-times on stream flow is analysed and discussed in detail.

Landman and Mason (1999) found that model skill with a correlation value greater than 0.5 could be considered to give good skill. Their model skill increased to 0.5 if it was calculated for El Niño years and increased to 0.58 for La Nina years (Landman and Mason, 1999). The data set available for this section of the upper Olifants is not long enough to divide into El Niño and La Nina years. In this study Pearson's correlation values of above 0.5 are considered to have significant skill and were selected for forecasting equations. The selection of correlation values would be determined during the training period from 1990 to 1997. The Pearson Correlation coefficient of stream flow predictability using global SSTs at different lead times during OND and JFM seasons is shown in Appendices 4 and 5.

5.3 Model Skill at Different Lead-Times during OND Season

Appendix 5 shows the cross validation correlations between observed OND sum of stream flows and global sea-surface temperatures at nine lead-times for the Groot Olifants and Wilger sub-catchments. The Pearson's correlation values shown in Appendix 5 were calculated by CPT using a CCA model at nine different lead-times. The B1 stream flow stations represent Groot Olifants sub-catchment and B2 stream flow stations represent Wilger sub-catchment. The individual stream flow stations in each of the two sub-catchments were considered when Pearson's correlation was used as the correlation method. The zero and two month lead-times have a higher Pearson correlation value for all the stream flow stations except for stream flow station B2H004 at a two months lead-time.

5.3.1   Groot Olifants sub-catchment during OND season

Fig 5.2 demonstrates a cross-validated correlation at different lead-times for the different stream flow stations in the Groot Olifants sub-catchment during the OND season. The Pearson's correlation is a measure of skill in the CCA model, a higher correlation value at a certain lead-time represents a high skill at that lead-time. The highest skill being above 0.5 means that at a specific lead-time it could be used for forecasting stream flow. Pearson's correlation values would be used as a measuring skill in this section. Stream flow station B1H012 has the highest correlation value at a lead-time of two months and the lowest correlation value at a lead-time of six months (Fig. 5.2).
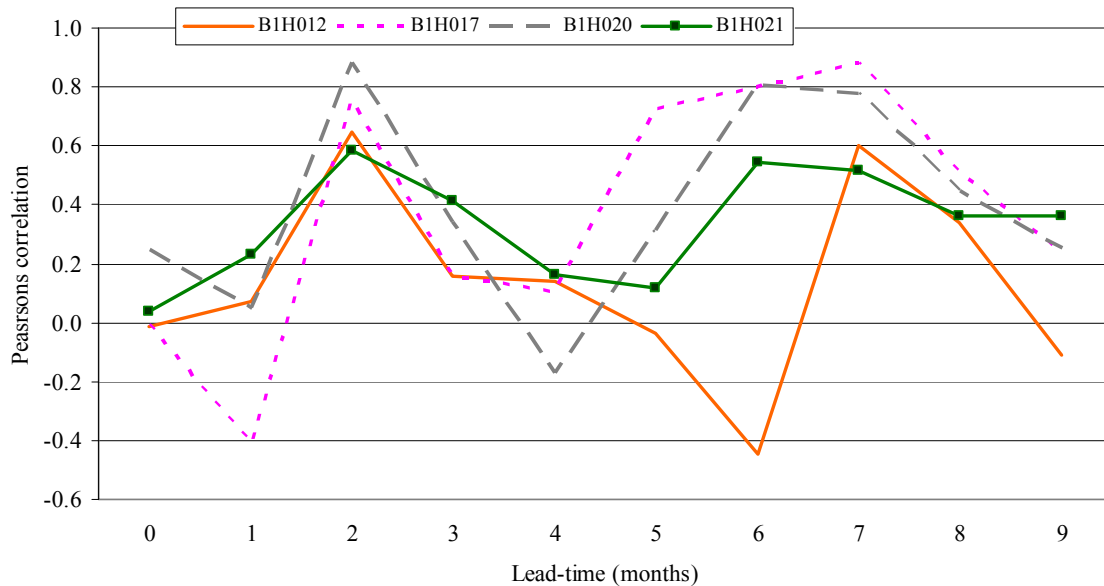
Fig. 5.2 Cross-validated correlations between OND stream flow sum and global SSTs for 1990-1997 at different lead-times for the four stream flow stations in the Groot Olifants sub-catchment

Stream flow station B1H017 has the highest correlation value at a lead-time of seven months, but this stream flow station also has correlation values of above 0.5 at a lead-time of two months five and six months. The lowest correlation value for stream flow station B1H017 is at a lead-time of one month. This means that for stream flow station B1H017 a lead-time of two five and seven months can be considered to be useful in stream flow forecasting (Fig. 5.2). Stream flow station B1H020 has the highest

44

correlation value at a lead-time of two months and the lowest correlation value at a lead-time of four months (Fig. 5.2), but also above 0.5 at seven months lead-time.

Stream flow station B1H021 has the highest correlation value at a lead-time of two months and the lowest correlation value at a lead-time of zero months. Since stream flow station B1H021 has correlation value greater than 0.5 during OND season at two, six and seven months lead-times, so this stream flow station has significant predictability at a lead time of two months during the OND season. In general a lead-time of two months has the highest correlation values in the Groot Olifants sub-catchment during the OND season because all the stream flow stations in the sub-catchment have a correlation value of above 0.58 at this lead-time of two months.

5.3.2 Wilger sub-catchment during OND season

Fig. 5.3 demonstrates how the cross-validated correlation varies with increasing lead-time in the Wilger sub-catchment.
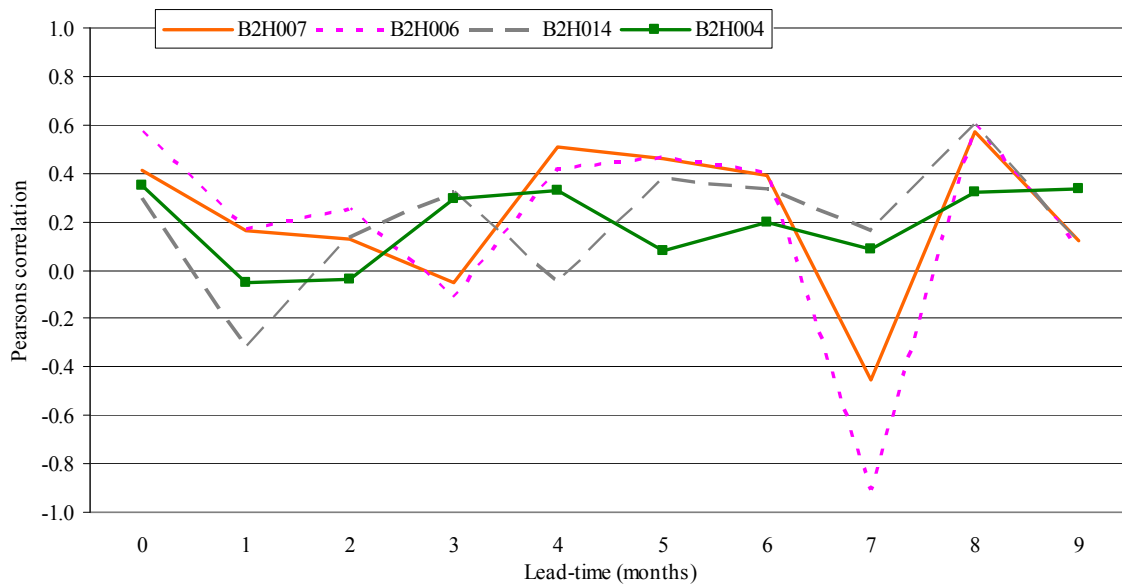
Fig. 5.3 Cross-validated correlations between OND stream flow sum and global SSTs for 1990-1997 at different lead-times for the four stream flow stations in the Wilger sub-catchment

Stream flow stations B2H007 and B2H014 have the highest correlation values at lead-time of eight months and the lowest correlation values for B2H007 and B2H014 stream flow stations are at lead-time of seven months and one month respectively. Stream flow

station B2H006 has higher correlation values at lead-times of zero and eight months and a stronger negative correlation value at a lead-time of seven months.

The correlation values for the Wilger sub-catchment are generally low when compared to the Groot Olifants sub-catchment as the Groot Olifants sub-catchment has a highest correlation value of 0.8806 while the Wilger sub-catchment only has the highest correlation value of 0.5989. This means that the Groot Olifants sub-catchment has more predictability skill than the Wilger sub-catchment when using global SSTs as the only stream flow predictors.

5.4 Model Skill at Different Lead-Times during JFM Season

Appendix 6 shows cross-validated correlations between observed and JFM sum of stream flows and global sea-surface temperatures at ten lead-times for the Groot Olifants and Wilger sub-catchments. Appendix 6 is discussed in detail in section 5.4.1 and 5.4.2.

5.4.1   Groot Olifants sub-catchment during JFM season

Fig. 5.4 demonstrates cross-validated correlation between JFM stream flow sum and global SSTs at ten lead-times in the Groot Olifants sub-catchment. Stream flow station B1H012 has a high correlation value at a lead-time of one and four months. Stream flow station B1H017 has the highest value at a lead-time of zero, five and eight months and the lowest value at a lead-time of nine months. Stream flow station B1H020 has the highest correlation value at a lead-time of zero and nine months and the lowest correlation value at a lead-time of six months. Stream flow station B1H021 has the highest value at a lead-time of zero months and the lowest value at a lead-time of seven months. Lead-time of zero months have correlation values above 0.50 on all the stream flow stations in the Groot Olifants sub-catchment for the JFM season except for stream flow station B1H012. Lead-time of seven months has the lowest correlation for all four of the stream flow stations in the Groot Olifants sub-catchment for the JFM season.

The results in Appendix 6 for the Groot Olifants sub-catchment show that there is no lead-time which has more than three correlation values greater than 0.50. This means that

one cannot select a lead-time to be used for stream flow predictions in the upper Olifants based on all the global SSTs only.
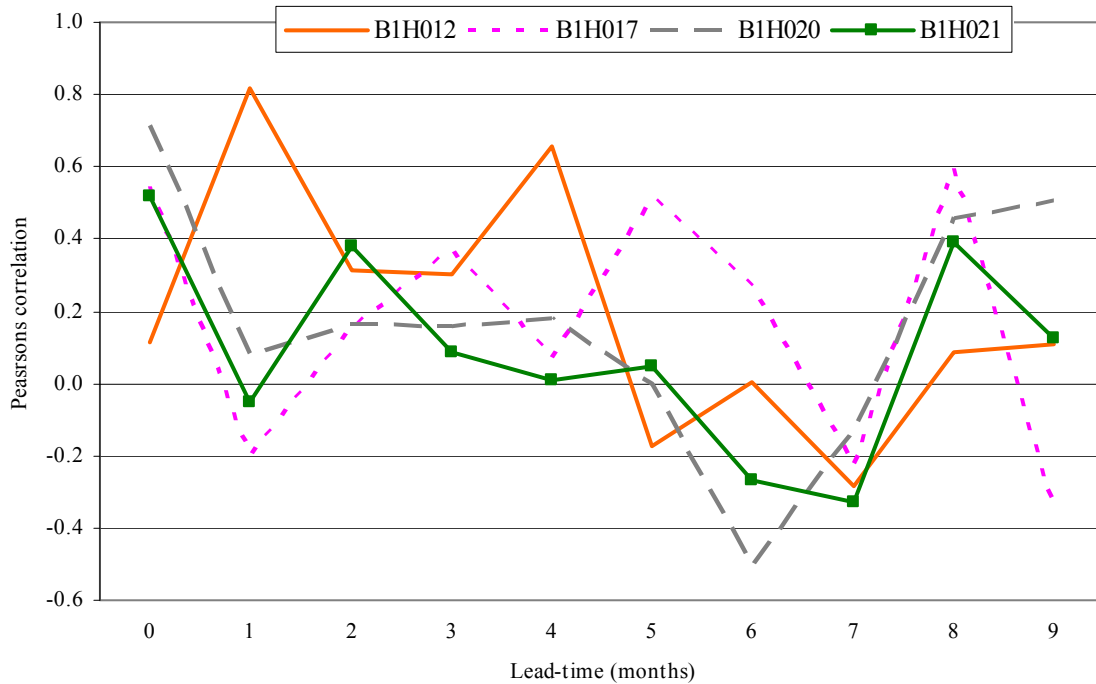
Fig. 5.4 Cross-validated correlations between JFM stream flow sum and global SSTs for 1990-1997 at different lead-times for the four stream flow stations in the Groot Olifants sub-catchment

5.4.2   Wilger sub-catchment during JFM season

Cross-validated correlation between JFM stream flow sum and global SSTs at nine lead-times in the Wilger sub-catchment are shown in Fig. 5.5. Stream flow station B2H007 has the highest correlation value (0.9600) at a lead-time of one month and the lowest correlation value at a lead-time of seven months. Stream flow stations B2H006 and BH014 both have the highest correlation value at lead-times of five months and the lowest correlation value at lead-times of seven months and six months respectively. The stream flow station B2H004 has the highest correlation values at lead-times of two and four months and the lowest correlation value at a lead-time of nine months. Stream flow stations B2H006 and B2H014 seem to follow a similar pattern at all lead-times except for a lead-time of six months and seven months. The results in Appendix 6 for the Wilger sub-catchment show that the shorter lead-times (lead-times of zero to two month) have higher correlation values. This means that one expects to have a better prediction skill in

the Wilger sub-catchment at shorter lead-times using global SSTs as the only stream flow predictor.
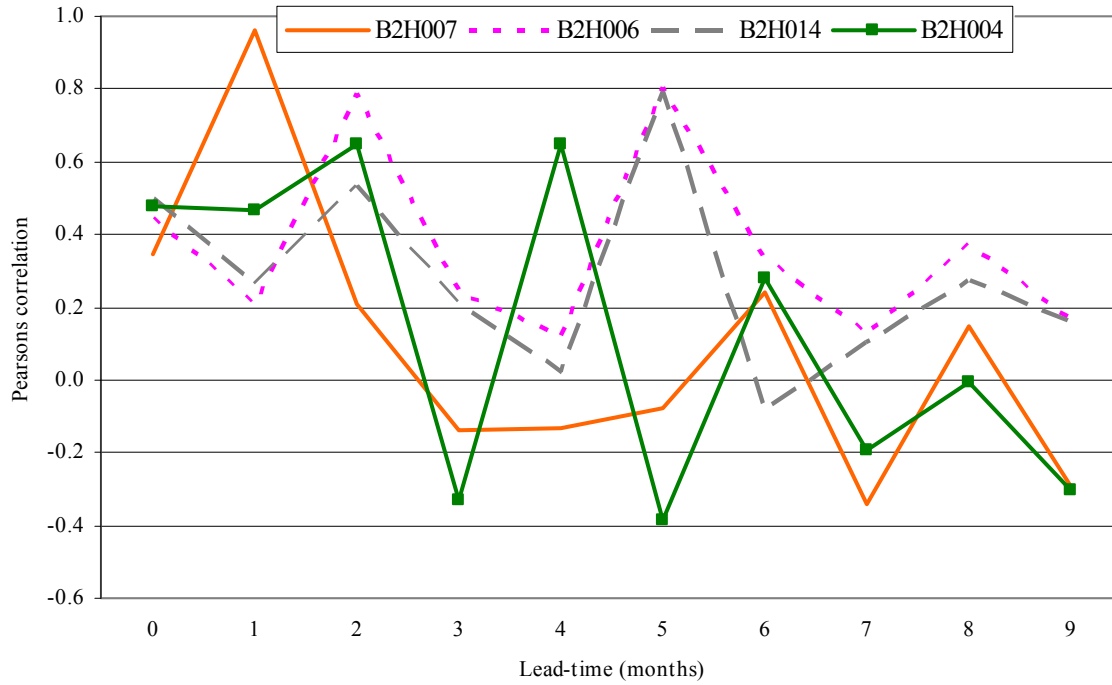
Fig. 5.5 Cross-validated correlations between JFM stream flow sum and global SSTs for 1990-1997 at different lead-times for the four stream flow stations in the Wilger sub-catchment

5.5 Correlation Values at Different Lead-Times in the Upper Olifants Catchment

A summary of the stream flow stations that have correlation values greater than 0.50 at different lead-times during the OND and JFM in the Groot Olifants and Wilger sub-catchments is given in Table 5.1. This summary of cross-validated correlation of stream flow at different lead-times using global SSTs as the main predictor which would be compared to a summary of cross-validated correlation of stream flow at different lead-times using the selected oceanic domains as the main predictor during the OND and JFM seasons in the Groot Olifants and Wilger sub-catchments.

5.5.1 A summary of cross-validated correlation of stream flow at different lead-times using global SSTs

Table 5.1 shows that the shorter lead-time of two months has the highest correlation values during the OND season in the Groot Olifants sub-catchment. During the same OND season in the Wilger sub-catchment, the longer lead-time of eight months has the

highest correlation values. During the JFM season the shorter lead-times of zero, one and two months have higher correlation values than the other lead-times.

Table 5.1 Selected cross validated Pearson's correlation values greater 0.50 for stream flow stations in the upper Olifants sub-catchments for the OND and JFM season

Season	Sub-catchment	Stream flow station	Lead-time 1	Lead-time 2	Correlation value 1	Correlation value 2
OND	Groot Olifants	B1H012	2	7	0.6460	0.6021
		B1H017	2	7	0.7549	0.8806
		B1H020	2	7,6	0.8790	0.8063
		B1H021	2	7,6	0.5858	0.5452
	Wilger	B2H007	4	8	0.5104	0.5732
		B2H006	7	8	-0.9105	0.5989
		B2H014	8	-	0.5971	-
		B2H004	No correlation			
JFM	Groot Olifants	B1H012	1	4	0.8170	0.6550
		B1H017	8	0	0.5985	0.5434
		B1H020	0	9	0.7131	0.5096
		B1H021	0	-	0.5180	-
	Wilger	B2H007	1	-	0.9600	-
		B2H006	5	2	0.8008	0.7870
		B2H014	5	2	0.7917	0.5330
		B2H004	4	2	0.6469	0.6480

During the OND season, the lead-times of two and six months have the highest correlation in the Groot Olifants sub-catchment while all the lead-times have lower correlation values in the Wilger sub-catchment. This shows a good correlation of global SSTs and OND stream flow in the Groot Olifants sub-catchment, therefore good forecasting skill is expected in this catchment especially at lead-times of two and six months for stream flow stations B1H017, B1H020 and B1H021. This means a forecast could be made in July and March prior to the start of the rainy season in October. But it shows that the model will not have a good skill for a lead-time of nine months.

During the JFM season the lead-time of zero months has a good correlation in the Groot Olifants sub-catchment except for stream flow station B1H012 that has a correlation value of 0.1120 however, a lead time of zero months is not very useful in practical

predictions. The lead-time of two months has a good correlation value in the Wilger sub-catchment for stream flow stations B2H006, B2H014 and B2H004 excluding stream flow station B2H007 that has a correlation value of 0.2080. It means that the best forecasting skill during the JFM season would be achieved when a lead-time of two months would be used in the Wilger sub-catchment, which would mean that a forecast could be made in October the previous year. In general the lead-times of six and nine months would not have good skill as they have low correlation values in both the Groot Olifants and the Wilger sub-catchments.

In general the OND season has the highest correlation values at lead-times of two and six months in the Groot Olifants sub-catchment, except at stream flow station B1H012 that has the highest correlation value at a lead-time of seven months. Since zero and nine months lead-times have no value greater than 0.05 this means that it would not be feasible to issue a zero and nine months stream flow forecast using global SSTs as the only predictant for stream flow in the Groot Olifants during the OND season. It will also be unfeasible to issue a zero, two, six and nine months stream flow forecast in the Wilger sub-catchment during OND season, because of a weak correlation between stream flow and global SSTs.

Results of the lead-times with the highest cross-validated correlations from this chapter will be used for the stream flow hindcasting in chapter 7.

CHAPTER 6

Evaluation of Oceanic Domains for Forecasting Skill

6.1 Typical Synoptic-Scale Circulation Pattern for Southern Africa

Although pressure, wind and rainfall patterns are constantly changing, there are certain basic patterns in the pressure and wind fields that occur regularly. Furthermore, seasonal variations exist in the location of certain pressure systems. There is, for example, a large variation in the location of the South Atlantic and Indian High pressure cells through the course of the year. In the Indian Ocean, the High pressure cell is subjected to a large annual variation in its latitudinal movement. Whereas in the Atlantic Ocean both the latitudinal and longitudinal variations are seasonal. On average the South Atlantic High pressure cell is located 3º further north than the Indian Ocean High pressure cell, but both cells shift 5 to 6º northwards in the winter. The annual longitudinal shift of the Atlantic High is 7 to 13º, while the Indian Ocean High is subject to a considerably larger longitudinal shift of 24 to 30º. The latter, therefore, has a much larger effect on the weather and climate of South Africa (Taljaard, 1996).

Different oceans carry unique climate signals, and therefore significant improvement in the forecast skill should be attained by combining the oceans into a single model (Barnett and Preisendorfer, 1987). SSTs measured at different oceans are related to the rainfall patterns of the different months as well as different geographical regions or zones (Diga, 2005). A reasonable forecasting model, with high forecast skill, must first be developed and cross-validated. Then this candidate model can be tested operationally to forecast future values of the predictand, depending on the upcoming observations of the predictor variables (Wilks, 2006). The model can also be tested with an independent set of historical data. Due to the location of South Africa, surrounded by water, model skill might be expected to improve if the equatorial oceans adjacent to South Africa coastline and the equatorial Pacific Ocean are considered separately instead of a global set of sea-surface temperatures (as done in chapter five) (Landman and Mason, 1999). Four oceanic domains were evaluated in this study using cross-validation correlation for a possible

effect on stream flow during each of the OND and JFM seasons. SSTs used for this section differ from those used in section 5.2, because those SSTs were taken from the whole globe.

Oceanic domains were selected (detail in section 4.3) in order to evaluate the contribution effects of temperatures of each different ocean to the individual stream flow stations in the upper Olifants catchment. In this chapter a Pearson's correlation value of above 0.5 is considered to have significant skill and was used to select the forecasting equation. The selection of correlation values would be determined during the training period of 1990 to 1997. The Goodness Index correlation value will be used to represent a correlation between specific oceanic domains SSTs and the sum of stream flow at a station for either OND or JFM season as shown in Fig. 6.1 and 6.2. The Pearson correlation value will be used to represent a 'correlation value' between the four selected oceanic domains and the sum of stream flow at a station for both OND and JFM seasons. The effect of each of the selected oceanic domain to be considered for the sum of OND and JFM stream flow prediction over the whole Upper Olifants catchment will be evaluated in section 6.2 and 6.3. The effect of each of the selected oceanic domains at each of the selected stream flow measuring points in both sub-catchment of the Wilger and Groot Olifants during the OND and JFM seasons will be evaluated in sections 6.4 and 6.5.

6.2 OND Season at Selected Domains for the Upper Olifants Catchment

The Goodness Index values for different oceanic domains at different monthly lead-times to predict the OND season stream flow in the upper Olifants catchment vary greatly (Fig. 6.1). The equatorial Atlantic Ocean (Eq Atl OND) domain has the highest Goodness of fit value at a lead-time of seven months. The southern Atlantic Ocean (S Atl OND) has the highest Goodness of fit value at a lead-time of three months although it is less than 0.50. The equatorial Indian Ocean (Eq Ind OND) has the highest correlation value at a lead-time of six months and is less than 0.4 at all lead-times so does not meet the required criteria for a good model. The equatorial Pacific Ocean (Eq Pac OND) has the highest Goodness of fit value at a lead-time of seven months being just above 0.4. These high Goodness of fit values show that the mentioned domains have the best skill at the stated

lead-times but probably do not constitute sufficient correlation to be used in a forecasting model. The lowest correlation values occur at a lead-time of eight months for all selected oceanic domains when predicting the OND season. This means that there is little of no skill for stream flow forecast at a lead-time of eight months (i.e. previous January) from any of the selected domains during OND season. The correlation behaviours of the individual stream flow stations and the effects of the oceanic domains in the upper Olifants catchment is not illustrated in Fig. 6.1, these correlations effects will be illustrated in section 6.4 and 6.5 for OND season and JFM season respectively.
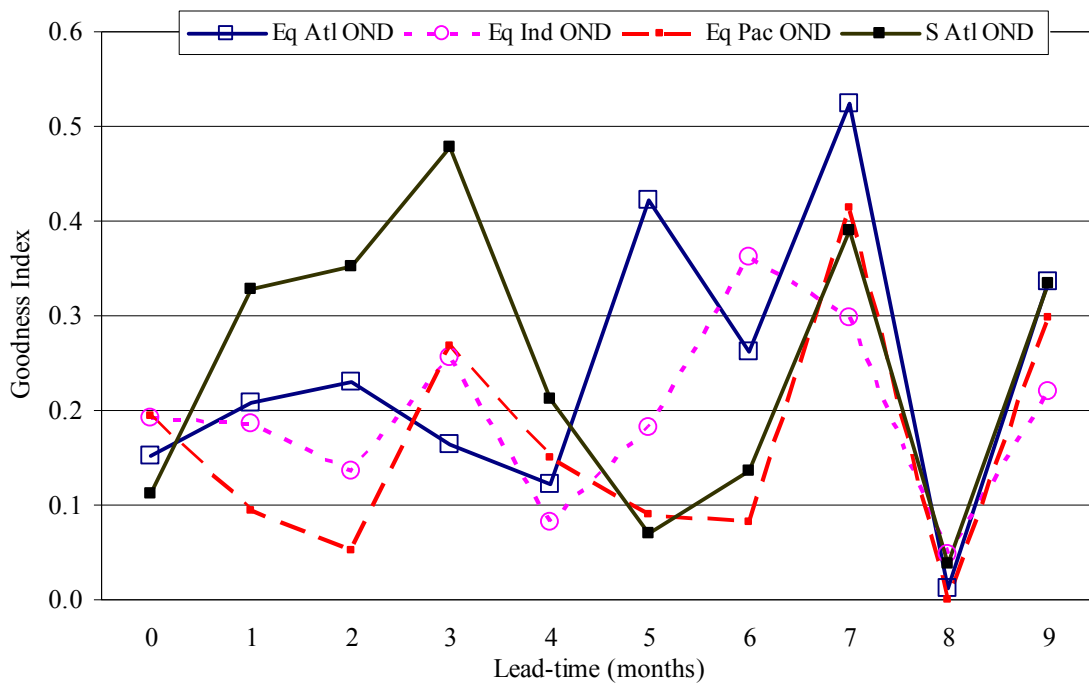
Fig. 6.1 Comparison of the oceanic domains Goodness Indices between the sum of the upper Olifants catchment stream flows and sea-surface temperatures at different lead-times for the OND season

6.3 JFM Season at Selected Domains in the Upper Olifants Catchment

None of the Goodness Index values (Fig. 6.2) are above 0.5 for any of the oceanic domains used to predict the JFM season across the whole catchment. The equatorial Atlantic Ocean (Eq Atl JFM) domain has a higher Goodness of fit value at lead-times of seven and eight months but is still less than 0.50 and the lowest Goodness of fit value at any lead-time is that of one month. The equatorial Indian (Eq Ind JFM), Southern Atlantic (S Atl JFM) and equatorial Pacific Oceans (Eq Pac JFM) have the highest

Goodness of fit value at a lead-time of zero months which is just less than 0.40 and the lowest Goodness of fit value at a lead-time of four months, except for the S Atl JFM which occurs at a lead-time of six months. The Eq Ind JFM and Eq Pac JFM have a similar stream flow to SSTs Goodness of fit pattern at lead-time of zero, four, five and seven months, while the Eq Atl JFM and S Atl JFM have different SST stream flow correlation patterns. However, it appears that there is not any one oceanic domains that stand out to be used as a reasonable predictor or a single forecast tool for all the stream flow gauges together during JFM across the whole of the upper Olifants catchment of Mpumalanga.
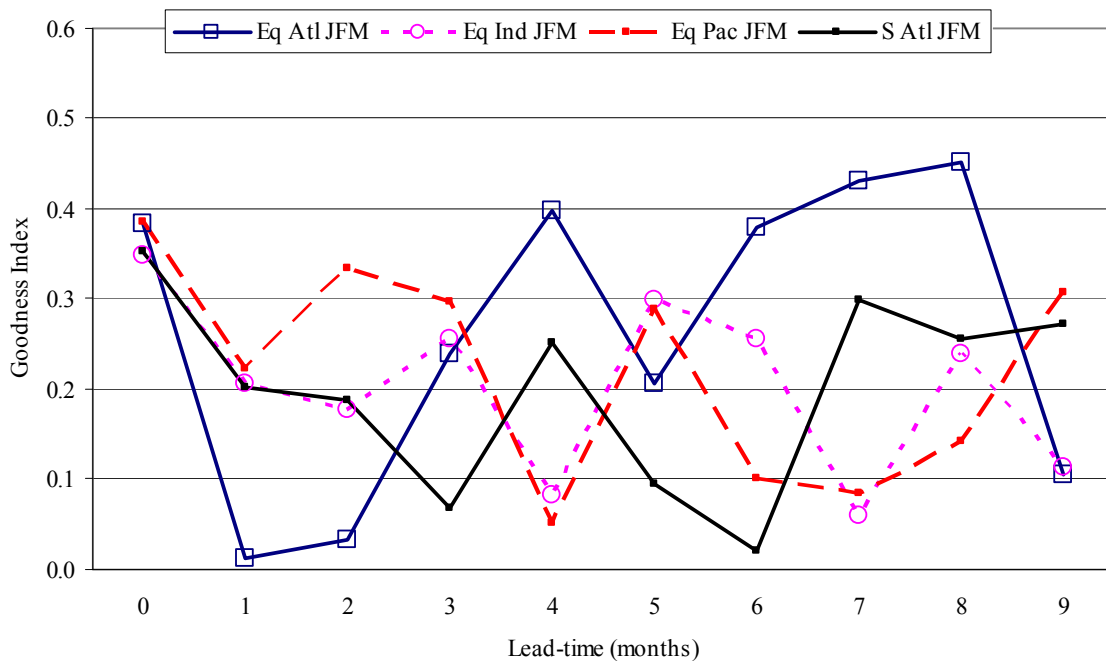
Fig. 6.2 Comparison of the oceanic domains Goodness Indices between the sum of the upper Olifants catchment stream flows and sea-surface temperatures at different lead-times for the JFM season

The equatorial Atlantic Ocean (Eq Atl JFM) Goodness of fit values for both OND and JFM seasons both show higher Goodness of fit values between stream flow and SSTs at lead-time of seven months, this means that there could be some forecasting skill when the equatorial Atlantic Ocean SSTs are used in a forecasting model. The Atlantic and Pacific Oceans show the best Goodness of fit at a lead-time of seven months while the Indian Ocean shows the best correlation at a lead-time of six months for the OND season (Fig.

6.1). The Goodness of fit could indicate that a forecast might be good at a catchment scale for decision making purposes. Sub-catchment correlations will be discussed in section 6.4 and 6.5.

6.4 Correlations between SSTs from the Selected Oceanic Domains and Individual Stream Flow during the OND Season

The results in section 5.5 shows that the global SSTs have a different effect on the OND and JFM season at different lead times, therefore it is deemed necessary in this study to evaluate the effect of different oceanic domains on forecasting at specific stream flow gauges. The effects of different selected oceanic domains during the OND season on individual monitoring sites are evaluated in section 6.4.1 to 6.4.4. In this section, a discussion of cross-validated Pearson's correlation values for individual stream flow stations in the Wilger and Groot Olifants sub-catchments using each of the selected oceanic domains during the OND season are discussed. The correlation values that are above 0.5 will be considered for inclusion in the construction of the forecasting equations.

6.4.1   Equatorial Atlantic Ocean cross-validated correlations

The cross-validated correlation between SSTs and the OND stream flow sum in Wilger and Groot Olifants sub-catchments using the equatorial Atlantic Ocean domain are listed in Appendix 7.1. The Pearson's correlation values were calculated from CPT using a CCA at ten lead-times. The individual stream flow stations will be discussed using Fig. 6.3 and 6.4.

The equatorial Atlantic Ocean sea-surface temperatures cross-validated correlations with the sum of stream flows for OND period at ten lead-times for the four stream flow stations in the Groot Olifants sub-catchment are shown in Fig. 6.3. Stream flow stations B1H017 and B1H020 both have the highest correlation values (approximately 0.80) at a lead-time of five months and low correlation values at a lead-time of zero months. The lead-times where stream flow station correlation values are high means that the model has a good skill when determining the OND stream flow using the equatorial Atlantic Ocean SSTs. Stream flow stations B1H017, B1H020 and B1H021 show similar patterns from a lead-time of two months to a lead-time of eight months except for stream flow

station B1H021 at a lead-time of six months which has the highest correlation value (approximately 0.80) although it was lower at the other lead-times. The stream flow station B1H021 has negative correlation values at lead-times of zero and four months. It will be very interesting to compare how the negative correlations affect the verification results in chapter seven.

Fig. 6.3 Equatorial Atlantic Ocean sea-surface temperatures cross-validated correlations with sum of OND stream flows at ten lead-times for the four stream flow stations in the Groot Olifants sub-catchment

The equatorial Atlantic Ocean SSTs cross-validated correlation with the sum of the stream flows for the OND season at different ten lead-times for the Wilger sub-catchment are shown in Fig. 6.4. Stream flow stations B2H007, B2H014 and B2H006 have high correlation values (near 0.8) at lead-times of zero, four and nine months. Stream flow station B2H004 has a higher correlation value at a lead-time of two months. Stream flow stations B2H007, B2H014 and B2H006 give similar prediction results using the equatorial Atlantic Ocean SSTs as the main stream flow predictor in the Groot Olifants

catchment, except at a lead-time of six months where stream flow station B2H014 has a higher correlation value.

Fig. 6.4 Equatorial Atlantic Ocean sea-surface temperatures cross-validated correlations against the sum of OND stream flows at ten lead-times for the four stream flow stations in the Wilger sub-catchment

6.4.2   Southern Atlantic Ocean cross-validated correlations

The cross-validated correlations between SSTs and OND stream flow sum in the Wilger and Groot Olifants sub-catchments for the Southern Atlantic Ocean domain are listed in Appendix 7.2. The Pearson's correlation values were calculated from the CPT using the CCA at ten different lead-times.

The Southern Atlantic Ocean sea-surface temperatures cross-validated correlations with the sum of the stream flows for the OND period at ten different lead-times for the Groot Olifants sub-catchment are shown in Fig. 6.5. Stream flow stations B1H017 and B1H020 have the highest correlation values at lead-times of one and seven months while stream flow stations B1H012 and B1H021 have the highest correlation values at a lead-time of

nine months. It is difficult to try to imagine any possible physical connection between the occurrences in the Southern Atlantic Ocean and the stream flow in various parts of a small catchment in South Africa. With lead-times as long as seven or nine months. If it was a systematic time scale of few days, one could maybe begin to explain the physical logic according to air-mass movement near the Antarctic to the African continent.
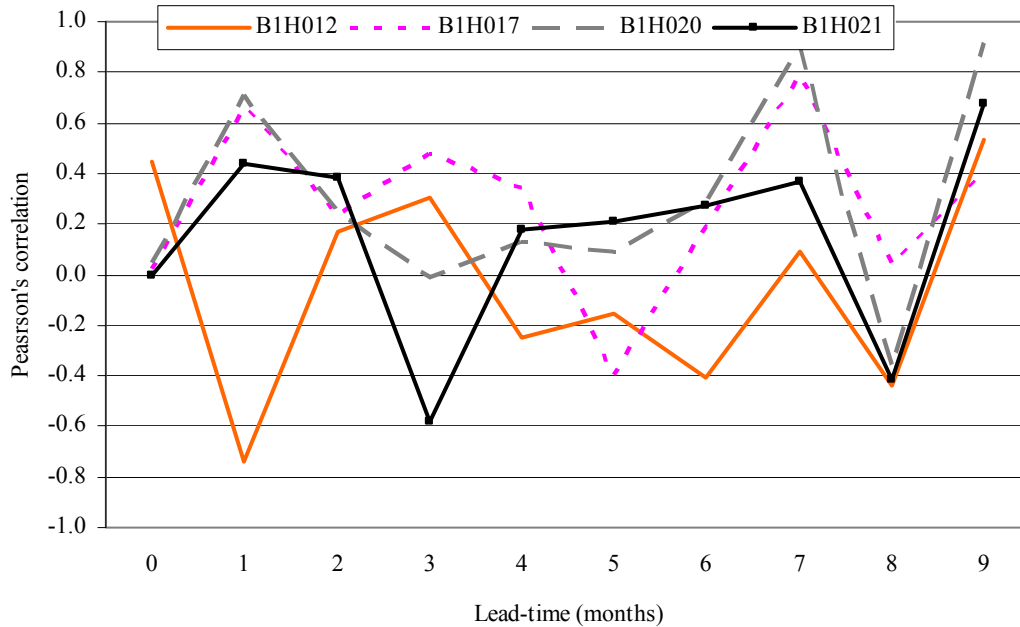
Fig. 6.5 Southern Atlantic Ocean sea-surface temperatures Cross-validated correlations against the sum of OND stream flows at ten lead-times for the four stream flow stations in the Groot Olifants sub-catchment

The Southern Atlantic Ocean SSTs cross-validated correlations with the sum of the stream flows for the OND season at different ten months lead-times for the four stream flow stations in the Wilger sub-catchment area are illustrated in Fig. 6.6. It should be noted that there are few negative correlations between stream flow and SSTs in this area. Stream flow stations B2H007, B2H006 and B2H014 have correlation values higher than 0.80 at a lead-time of three months. Stream flow correlation value for B2H004 has the highest correlation value greater than 0.5 only at a lead-time of one month. After lead-time of four months correlation values for the stream flow stations are all below 0.50 so cannot be considered as useful models. Therefore one can expect to get a good skill at shorter lead-times for all the stream flow stations during the OND season in the Wilger

sub-catchment when the southern Atlantic Ocean SSTs are used as the main predictors. Stream flow stations B2H007, B2H006 and B2H014, follow a similar pattern throughout all the ten lead-times. Looking closely at these three stream flow stations (B2H007, B2H006 and B2H014), stream flow station B2H007 has a higher correlation value at all the ten lead-times except for lead-time of four to seven months.
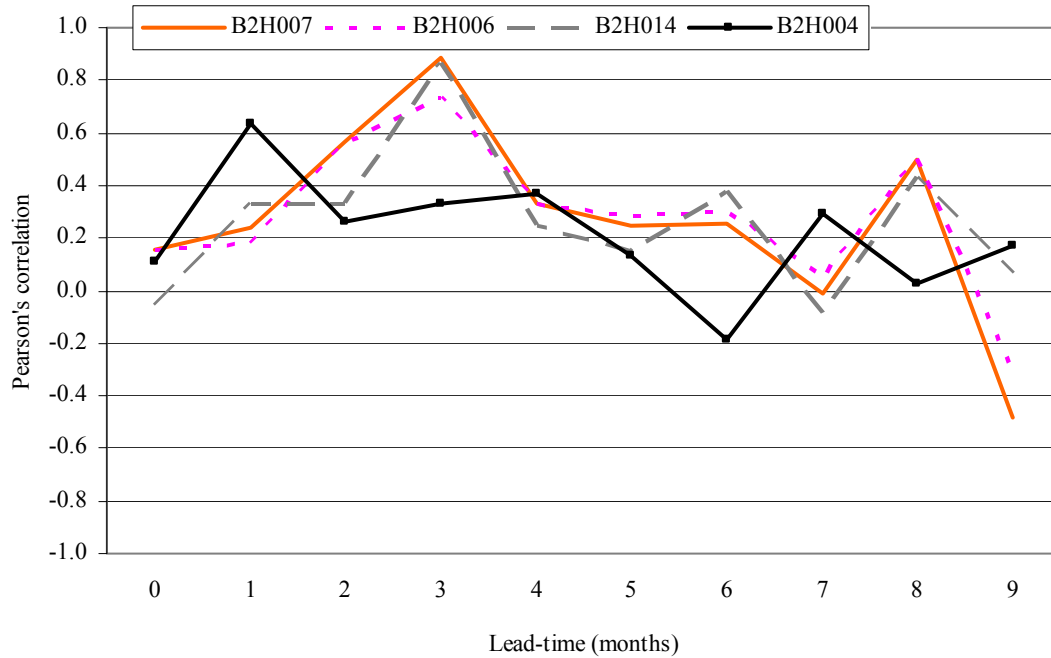
Fig. 6.6 Southern Atlantic Ocean sea-surface temperatures cross-validated correlations between sum of OND stream flows and at ten lead-times for the four stream flow stations in the Wilger sub-catchment

6.4.3   Equatorial Indian Ocean cross-validated correlations

The Pearson's correlation values were calculated from CPT using a CCA at ten different lead-times. The equatorial Indian Ocean sea-surface temperatures cross-validated correlations with the sum of the stream flows for OND season at different ten months lead-times in the Groot Olifants sub-catchment are shown in Fig. 6.7 (actual list in Appendix 7.3). Stream flow station B1H012 has its highest correlation value greater than 0.60 at lead-time of two months. Stream flow stations B1H021, B1H017 and B1H020 have the highest correlation values (near 0.8) at lead-times of nine and zero months except for stream flow station B1H021 which does not have a high correlation value at a lead-time of zero months. Stream flow stations B1H017 and B1H020, all located close together, have a similar pattern, where correlation values for stream flow station B1H017

are lower than stream flow correlation value for stream flow station B1H020, except at a lead-time of two months where stream flow station B1H017 has a higher correlation value than that of stream flow station B1H020.
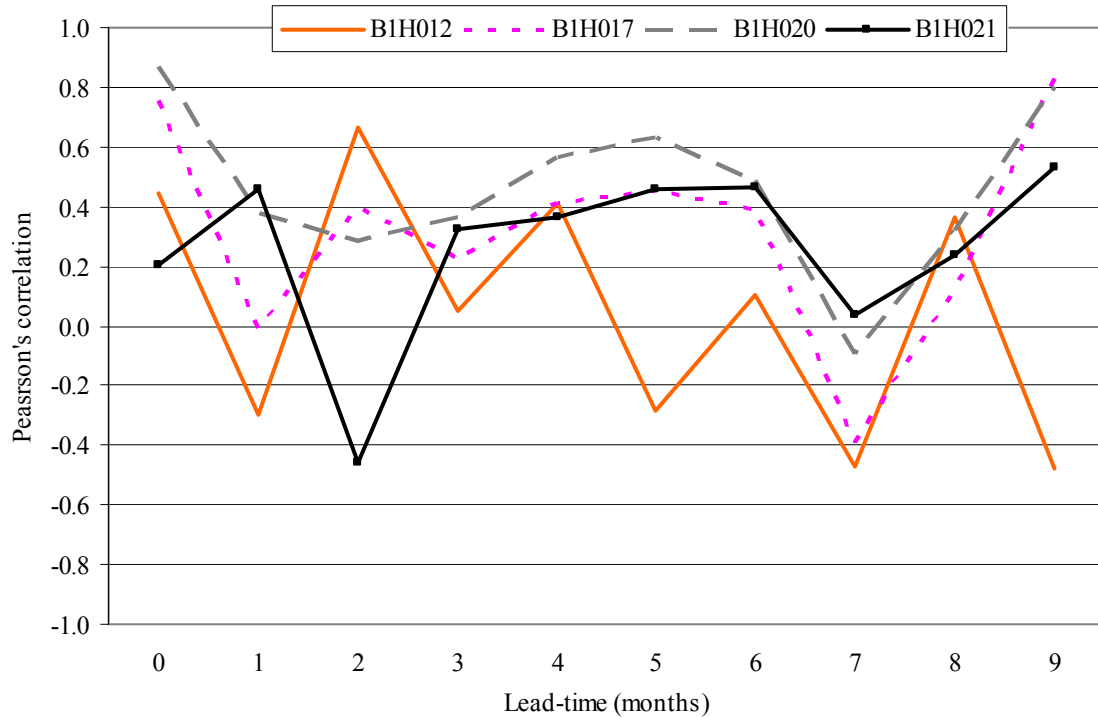
Fig. 6.7 Equatorial Indian Ocean cross-validated correlations between sum of OND stream flows and sea-surface temperatures at ten lead-times for the four stream flow stations in the Groot Olifants sub-catchment

Consider the equatorial Indian Ocean sea-surface temperatures cross-validated correlation with the sum of the stream flows for OND season at different ten lead-times for the four stream flow stations in the Wilger sub-catchment as shown in Fig. 6.8 (actual values in Appendix 7.3). None of these four stream flow stations has a correlation value as high as 0.6. Stream flow station B2H014 has the highest correlation value which is slightly less than 0.6 at a lead-time of one month. While stream flow station B2H004 has its highest correlation value also less than 0.6 at a lead-time of two months. This means no equatorial Indian Ocean model has sufficient skill to be used for forecasting the Wilger river stream flow during the OND season. Possibly with a larger dataset a model may be able to have a better predictability. These models will still be tested in chapter seven.
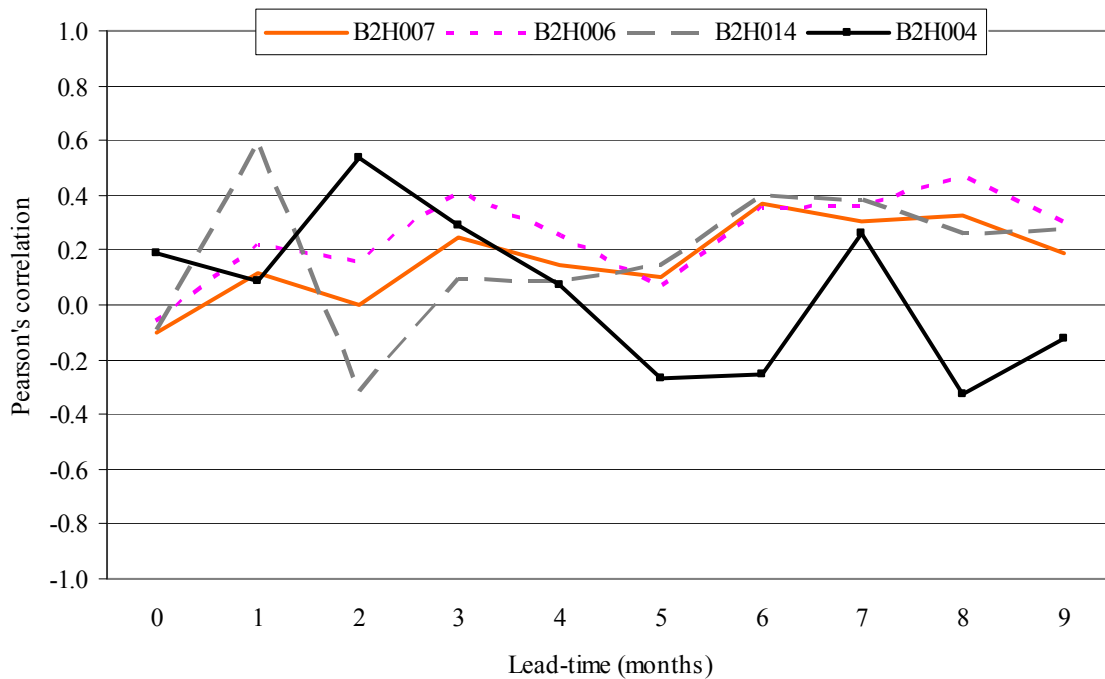
Fig. 6.8 Equatorial Indian Ocean sea-surface temperatures cross-validated correlations with the sum of OND stream flows at ten lead-times for the four stream flow stations in the Wilger sub-catchment

6.4.4   Equatorial Pacific Ocean cross-validated correlations

The Pearson's correlation values were calculated from the CPT using a CCA at ten different lead-times. The equatorial Pacific Ocean SSTs cross-validated correlations with the sum of the stream flows for OND period at ten lead-times for each of the four stream flow stations in the Groot Olifants sub-catchment are illustrated in Fig. 6.9 and values listed in Appendix 7.4. Stream flow station B1H012 has the highest correlation value at a lead-time of zero months being the only value greater than 0.6 for this stream flow station. Stream flow stations B1H017 and B1H020 have high correlation (values greater than 0.6) at lead-times of zero, two, three and six months. These two stream flow station also have large negative correlation values less than -0.6, it would be interesting to see how this negative correlation affect the skills scores tested in chapter seven especially the bias test. Stream flow station B1H021 has the highest correlation values at lead-times of zero, one, two, three and sixth months although those at zero and one month are not greater than 0.5. Stream flow stations B1H017 and B1H021 have a strong correlation at a lead-time of four months. Stream flow station B1H021 has slightly less strong correlation

at a lead-time of eight months. All the stream flow stations in the Groot Olifants sub-catchment have a negative correlation at a lead-time of nine months, concluding that with a long lead-time the opposite effect dominates.
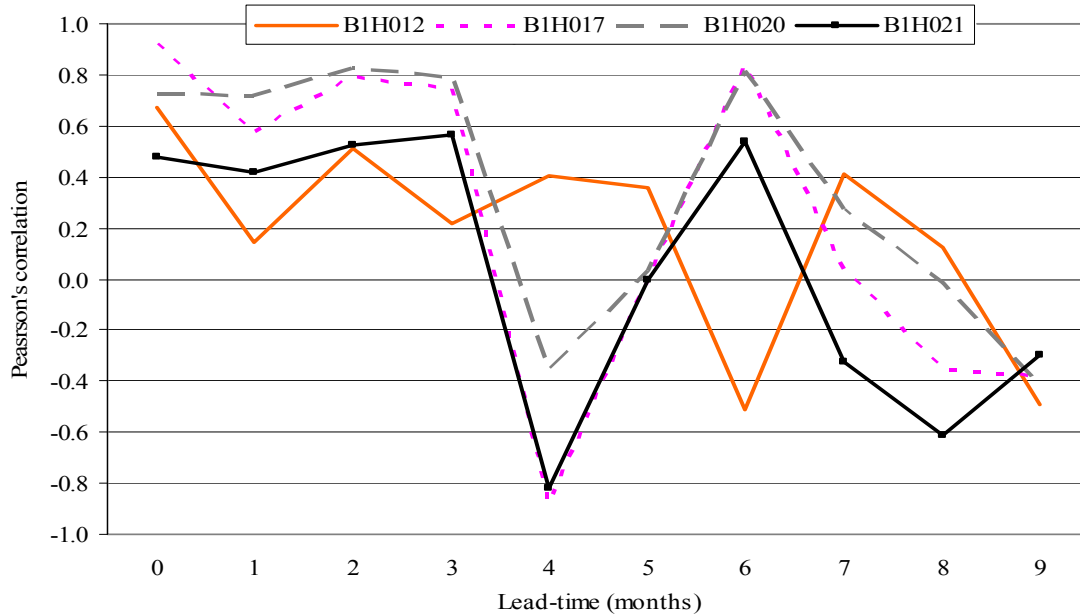
Fig. 6.9 Equatorial Pacific Ocean sea-surface temperatures cross-validated correlations against the sum of OND stream flows at ten lead-times for the four stream flow stations in the Groot Olifants sub-catchment

The equatorial Pacific Ocean sea-surface temperatures cross-validated correlations with the sum of the stream flows for OND season at different ten lead-times for the four stream flow stations in the Wilger sub-catchment are illustrated in Fig. 6.10. Stream flow station B2H007 and B2H006 have high correlation values greater than 0.6 at lead-times of eight, nine and four months. Stream flow station B2H014 has a high correlation value greater than 0.6 at a lead-time of both four and eight months. Stream flow station B2H004 does not have any positive correlation value greater than 0.5. However there is a very strong correlation (-0.8) at a lead time of three months and a less strong correlation at a lead time of nine months, indicating that if the equatorial Pacific Ocean SSTs become warmer (cool down) then the stream flow at station gauge B2H004 will be expected to decrease (increase) at a three months lead-time.
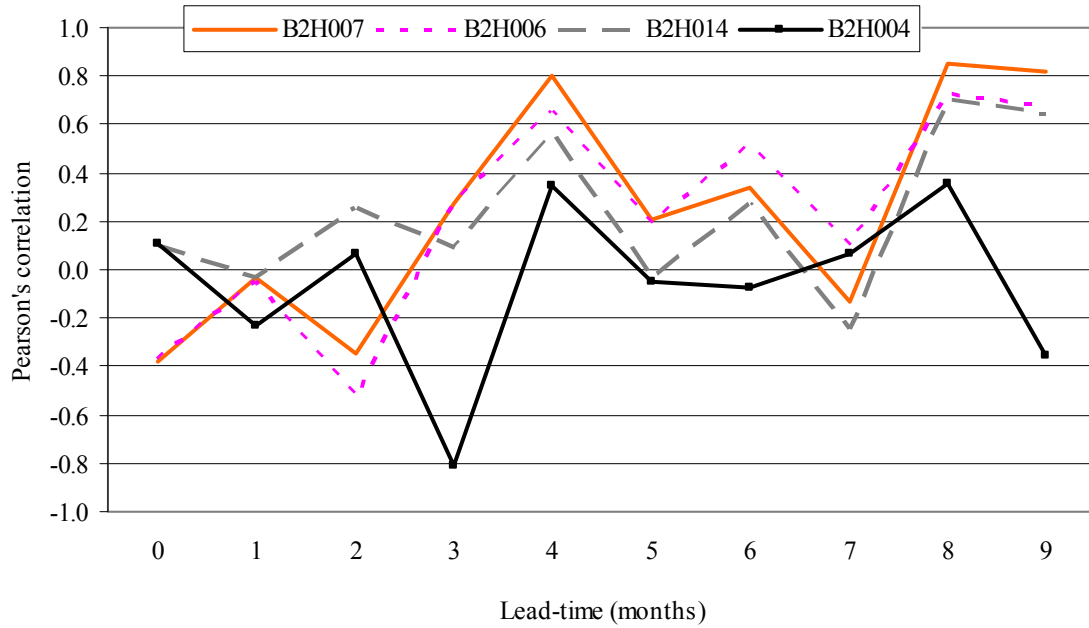
Fig. 6.10 Equatorial Pacific Ocean cross-validated correlations between sum of OND stream flows and sea-surface temperatures at ten lead-times for the four stream flow stations in the Wilger sub-catchment.

6.5 Correlations between SSTs from the Selected Oceanic Domains and Stream Flow during the JFM Season

The importance of evaluating the effects JFM season on stream flow using different SSTs from different oceanic domains has been elaborated in chapter five whereby global SSTs and OND season cannot give convincing correlation to some of the stream flow stations. But as shown by rainfall vs. stream flow analysis (Fig. 3.3 and 3.4); for the JFM season data (r^2 0.4690) indicating a closer relationship during the JFM than the OND season (r^2 0.0538). Therefore different relationships with SSTs also expected during different seasons. The effects of different oceanic domains on the predictability of JFM stream flow in both the Wilger and Groot Olifants at ten different lead-times will be evaluated in this section.

6.5.1 Equatorial Atlantic Ocean cross-validated correlations

The complete list of cross-validated correlations between SSTs and JFM stream flow sum in the Wilger and Groot Olifants sub-catchments from the equatorial Atlantic Ocean domain are shown in Appendix 8.1. The Pearson's correlation values were calculated

from the CPT using the CCA at ten different lead-times. The stream flow stations will be discussed in next paragraph.

The equatorial Atlantic Ocean sea-surface temperatures cross-validated correlations with the sum of the stream flows for the JFM season at ten different lead-times for the four stream flow stations in the Groot Olifants sub-catchment are shown in Fig. 6.11. Stream flow station B1H012 has a strong correlation value at the lead-time of eight months which is -0.7186. Stream flow stations B1H017 and B1H020 have higher positive correlation values greater than 0.6 at lead-time of seven and eight months. Stream flow station B1H021 has the highest correlation value at a lead-time of eight months. These strong correlations at the outlined lead-times from the mentioned stream flow stations means that these stream flow stations have a good forecasting skill. Generally B1H012 has the lowest correlations compared to other stations throughout lead-times greater than two months.
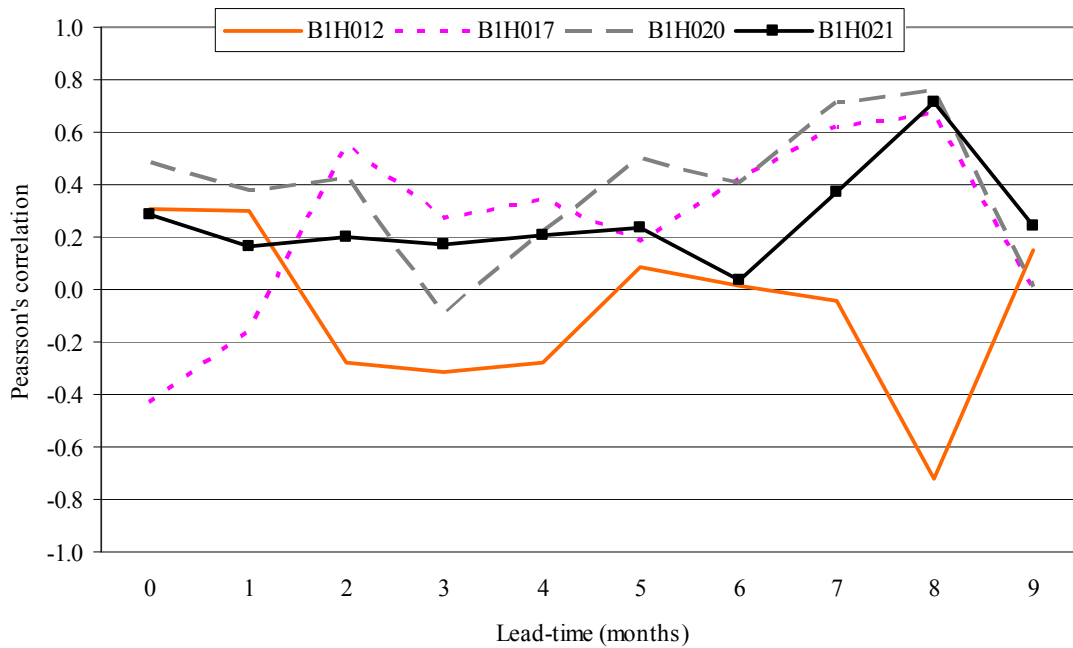
Fig. 6.11 Equatorial Atlantic Ocean sea-surface temperatures cross-validated correlations with the sum of JFM stream flows at ten lead-times for the four stream flow stations in the Groot Olifants sub-catchment

The equatorial Atlantic Ocean sea-surface temperatures cross-validated correlations with sum of the stream flows for JFM period at ten different lead-times for the four stream flow stations in the Wilger sub-catchment are shown in Fig. 6.12. Stream flow stations B2H006 and B2H014 have the highest correlation values near 0.8 at lead-time of eight and six months. Stream flow stations B2H007 and B2H004 which are located near to each other but at different streams, have no absolute correlation value higher than 0.5. This means that there is no significant skill to determine stream flow at stations B2H007 and B2H004 using equatorial Atlantic Ocean SSTs during the JFM season. Stream flow stations B2H006 and B2H014 have a similar pattern which might caused by the fact that these two stream flow stations are not far apart from one another as compared to the distance to the other steam flow stations in the Wilger sub-catchment (Fig. 3.1).
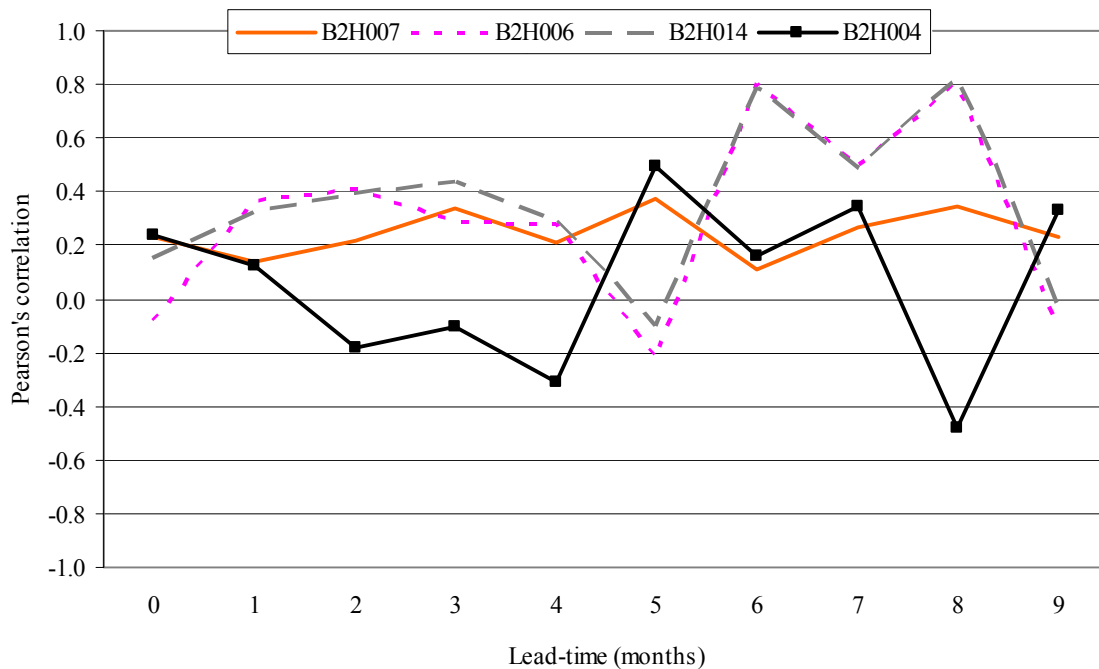
Fig. 6.12 Equatorial Atlantic Ocean cross-validated correlations between sum of JFM stream flows and sea-surface temperatures at ten lead-times for the four stream flow stations in the Wilger sub-catchment

6.5.2   Southern Atlantic Ocean Cross-validated correlations

These Pearson's correlation values were calculated from the CPT using the CCA at ten different lead-times. The Southern Atlantic Ocean sea-surface temperatures cross-

validated correlation with the sum of the stream flows for the JFM season at ten lead-times for the four stream flow stations in the Groot Olifants sub-catchment are shown in Fig. 6.13 and data given in Appendix 8.2. Stream flow station B1H020 has the highest correlation values at lead-times of one, two and six months. Stream flow station B1H017 has highest correlation value at lead-times of eight months and with a strong negative correlation value at a lead-time of six months.
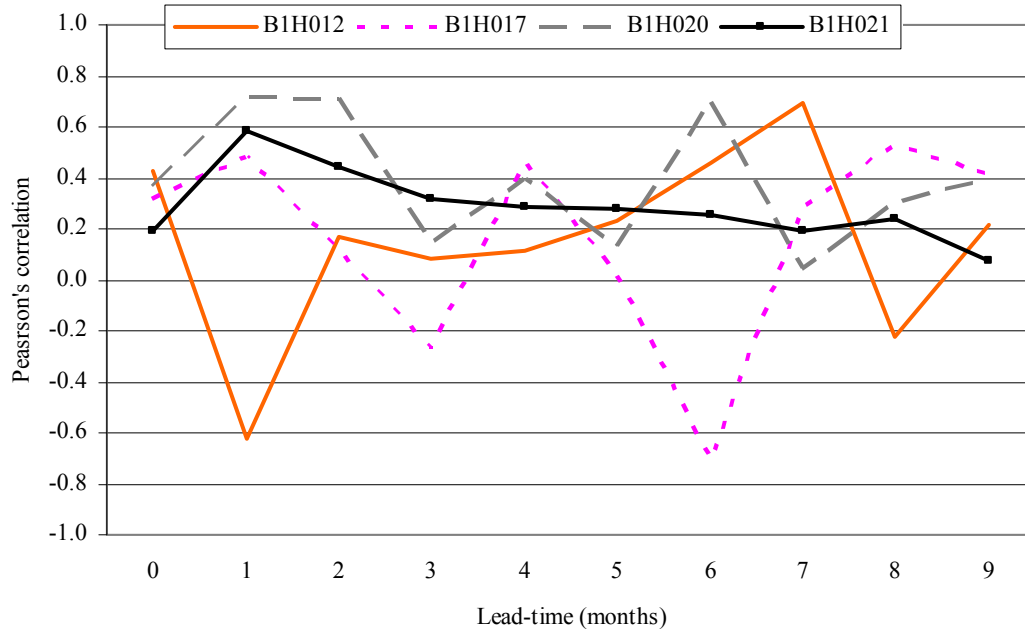
Fig. 6.13 Southern Atlantic Ocean sea-surface temperatures cross-validated correlation against the sum of JFM stream flows at ten lead-times for the four stream flow stations in the Groot Olifants sub-catchment.

Stream flow stations B1H012 has the highest correlation value at a lead-time of seven months and a good negative correlation value at lead-time of one month, therefore the Southern Atlantic Ocean sea-surface temperatures and stream flow relationship is expected to be negative at that time. This means that the B1H012 stream flow value is expected to increase if the Southern Atlantic Ocean sea-surface temperatures decrease. B1H021 has its highest correlation value (0.5834) at a lead-time of one month being the only one above a value of 0.5.

The Southern Atlantic Ocean sea-surface temperatures cross-validated correlation with the sum of the stream flows for the JFM period at ten lead-times for the four stream flow stations in the Wilger sub-catchment are shown in Fig. 6.14. Stream flow station B2H004 has the highest correlation value (0.7816) at a lead-time of zero months and next highest correlation value (0.5543) at a lead-time of two months. These two lead-times could possibly be used for a prediction model. The other stream flow stations in the Wilger sub-catchment do not have any correlation value that is greater than 0.5, therefore the Southern Atlantic oceanic domain can not be used for stream flow predictions during the JFM season. There are no obvious significant correlation similarities between the Wilger and Groot Olifants sub-catchment as illustrated by Fig. 6.13 and 6.14.
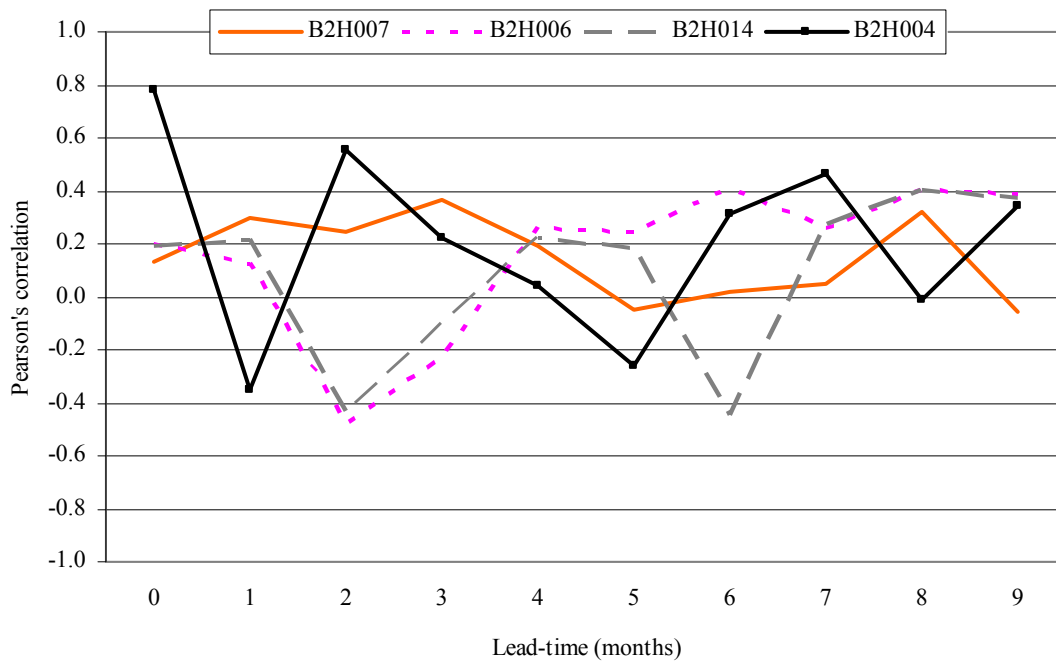
Fig. 6.14 Southern Atlantic Ocean sea-surface temperatures Cross-validated correlation with the sum of JFM stream flows at ten lead-times for the four stream flow stations in the Wilger sub-catchment

6.5.3   Equatorial Indian Ocean cross-validated correlations

The detail of cross-validated correlations between equatorial Indian Ocean domain SSTs and JFM stream flow sum in the Wilger and Groot Olifants sub-catchments are given in Appendix 8.3 and plotted in a graph in Fig. 6.15. The Pearson's correlation values were calculated from CPT using a CCA at ten different lead-times. Stream flow station

B1H017 has the higher correlation values greater than 0.6 at lead-times of zero and one months. B1H020 has a strong negative correlation at a lead-time one and five months. Stream flow stations B1H012, B1H020 and B1H021 do not have a positive correlation value that is greater than correlation value of 0.5. This means that the model does not have significant skill that could be used in the stream flow forecast during the JFM season from the equatorial Indian Ocean sea-surface temperatures.
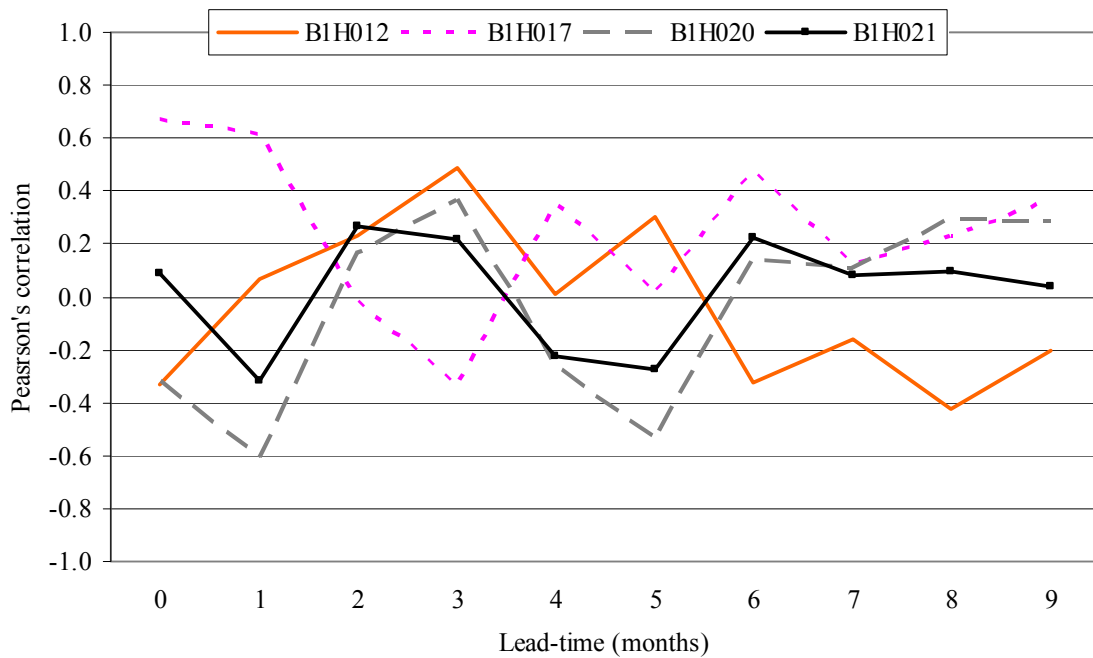
Fig. 6.15 Equatorial Indian Ocean sea-surface temperatures cross-validated correlations with the sum of JFM stream flows at ten lead-times for the four stream flow stations in the Groot Olifants sub-catchment

The equatorial Indian Ocean sea-surface temperatures cross-validated correlations with the sum of the stream flows for the JFM season at ten lead-times for the four stream flow stations in the Wilger sub-catchment are shown in Fig. 6.16. Stream flow stations B2H006 and B2H014 have the highest correlation values near 0.8 at a lead-time of zero months. Stream flow station B1H004 has the highest correlation value at a lead-time of five month and a strong negative at a zero month. Stream flow station B2H007 does not have any correlation value that is higher than the selected minimum correlation value of 0.5 at any of the ten lead-times and so probably will not be able to be predicted from the

equatorial Indian Ocean. In Fig. 6.15 and 6.16, most of the correlation values are not higher than 0.5 in either the Wilger or the Groot Olifants sub-catchments. However there are more lead-times having negative correlation values in the Groot Olifants Catchment than in the Wilger catchment. This means that the Groot Olifants sub-catchment is more negatively correlated to the Equatorial Indian Ocean sea-surface temperatures than the Wilger sub-catchment and therefore the Groot Olifants stream flow will be expected to increase (decrease) as the Equatorial Indian Ocean sea-surface temperature decreases (increases) during the JFM season.
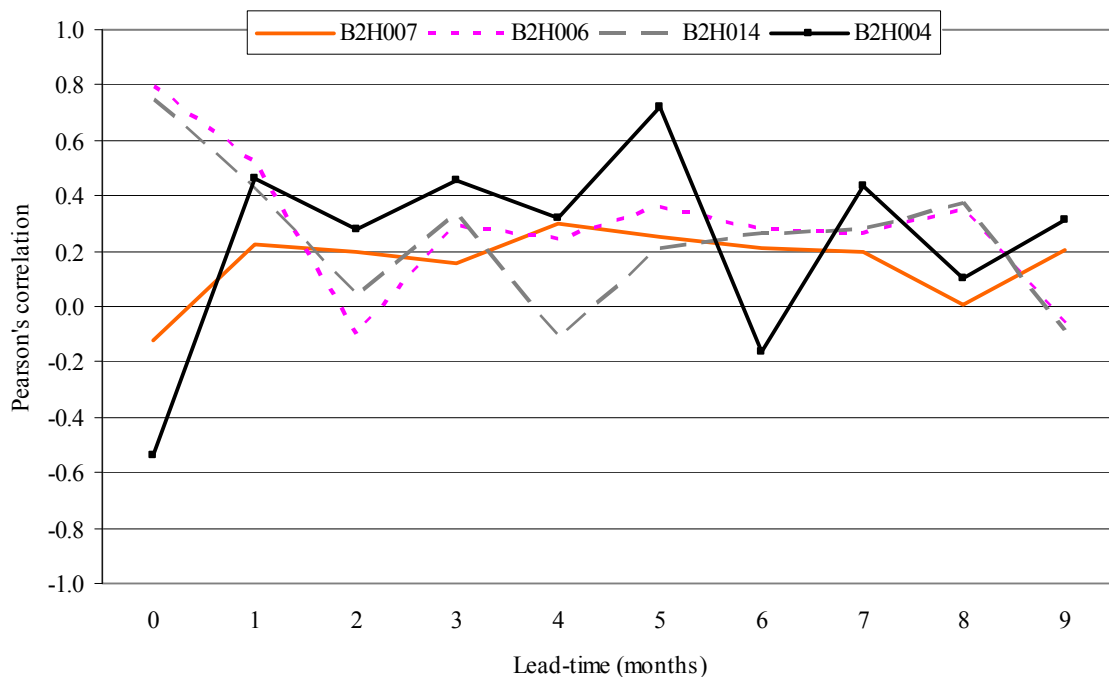
Fig. 6.16 Indian Ocean sea-surface temperatures cross-validated correlations with the sum of JFM stream flows at ten lead-times for the four stream flow stations in the Wilger sub-catchment

6.5.4   Equatorial Pacific Ocean cross-validated correlations

The list of cross-validated correlations between the equatorial Pacific Ocean domain SSTs and JFM stream flow sum in the Wilger and Groot Olifants sub-catchments are given in Appendix 8.4. These Pearson's correlation values were calculated from CPT using a CCA at ten lead-times. The equatorial Pacific Ocean sea-surface temperatures cross-validated correlations with the sum of the stream flows for the JFM season at ten lead-times for the four stream flow stations in the Groot Olifants sub-catchment are

shown in Fig. 6.17. Stream flow station B1H012 has higher correlation values greater than 0.6 at lead-times of eight and three months. Stream flow station B1H017 has the highest correlation values at lead-times of zero and nine months. Stream flow stations B1H020 and B1H021 only have poor negative correlation values at zero month lead-time that are numerically greater than the correlation value of 0.5, that could be selected in the forecasting model from the equatorial Pacific Ocean sea-surface temperatures.
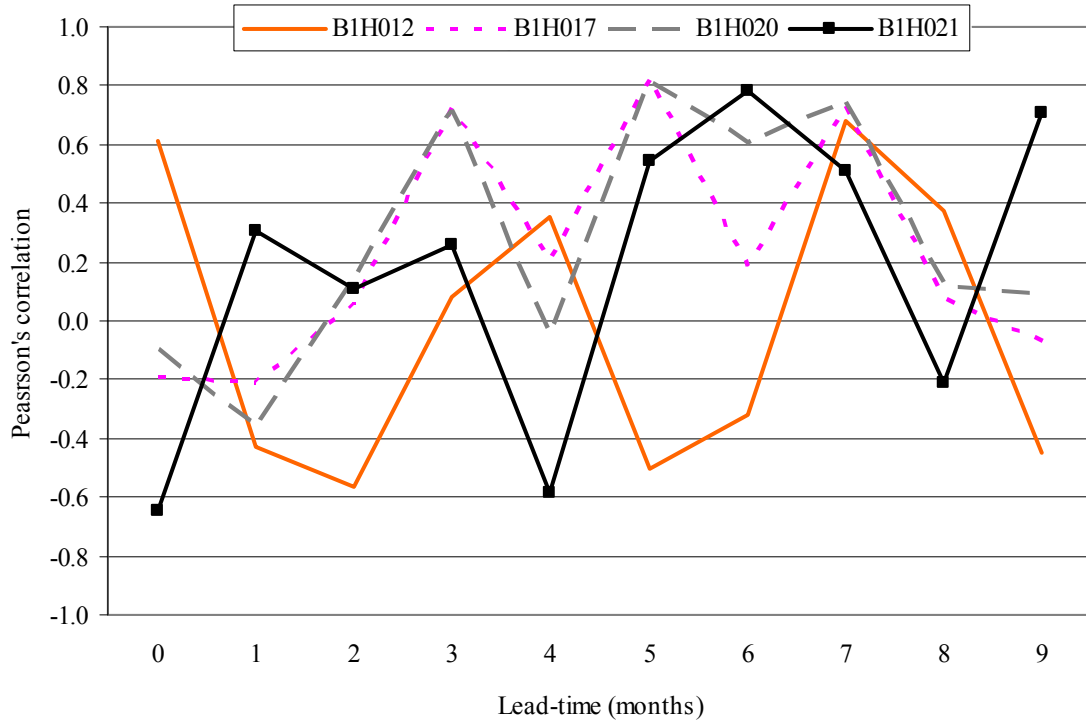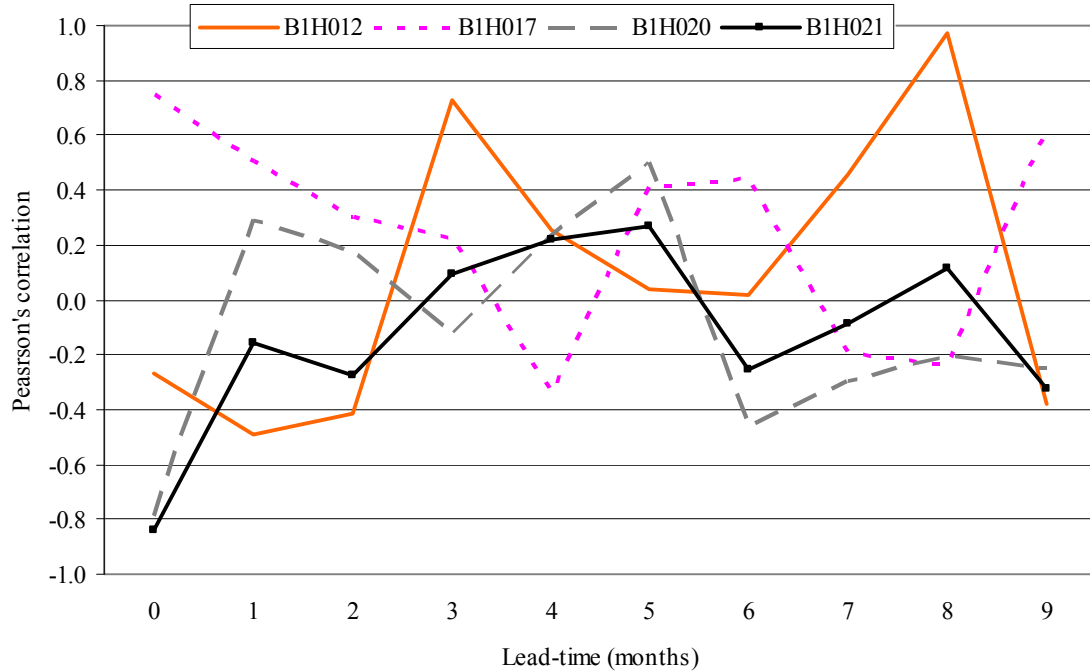

Fig. 6.17 Equatorial Pacific Ocean sea-surface temperatures cross-validated correlations against the sum of JFM stream flows at ten lead-times for the four stream flow stations in the Groot Olifants sub-catchment

The equatorial Pacific Ocean sea-surface temperatures cross-validated correlations with the sum of the stream flows for the JFM period at ten lead-times for the four stream flow stations in the Wilger sub-catchment are shown in Fig. 6.18. Stream flow stations B2H006 has the highest correlation values at lead-times of zero and nine months. Stream flow station B2H014 only has the highest correlation value (0.8994) at a lead-time of zero months. Stream flow station B2H004 has the highest correlation values (greater than 0.5) at lead-times of three, seven and eight months. Stream flow station B2H007 does not have a correlation value greater than 0.5 that could be included in the model. Stream flow stations B2H006, B2H007 and B2H014 follow a similar pattern from lead-time zero to

lead-time six months. The correlation value these stations starts high at a lead-time of zero months then decreased to a lead-time of two months then increased slightly trough the lead-time of six months, except for the stream flow station B2H014 which decreases from a lead-time of five month to a lead-time of six months. Although B2H14 and B2H007 are far apart, some of the stream flow running to each of them come from a region very close together and then diverge.

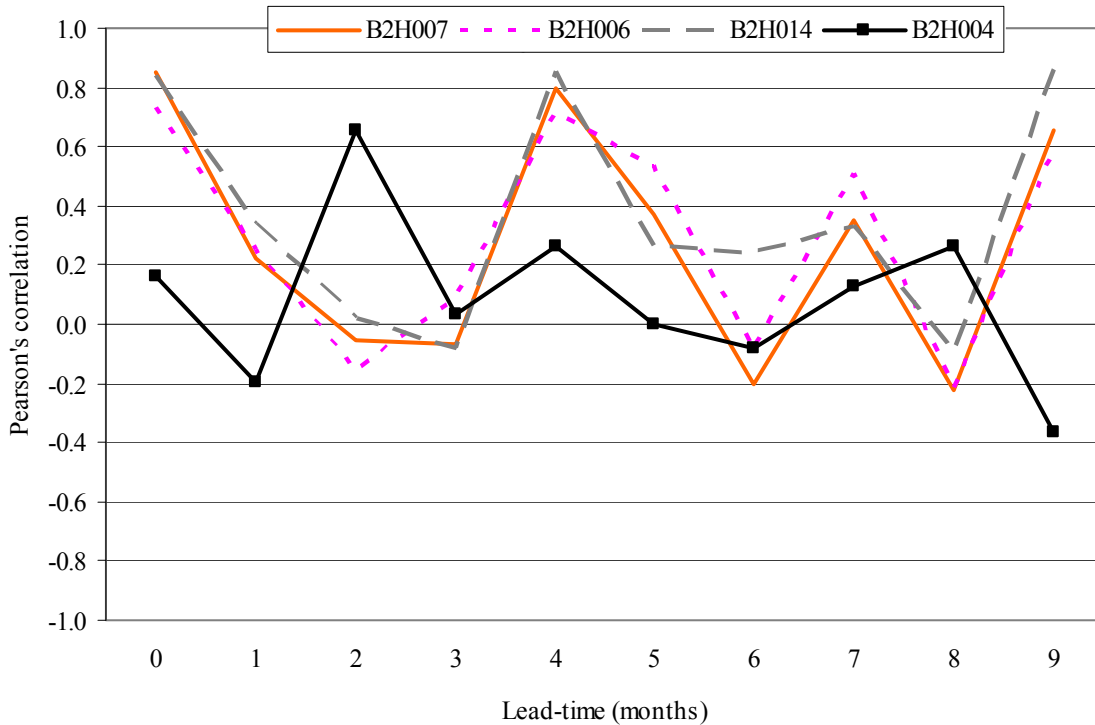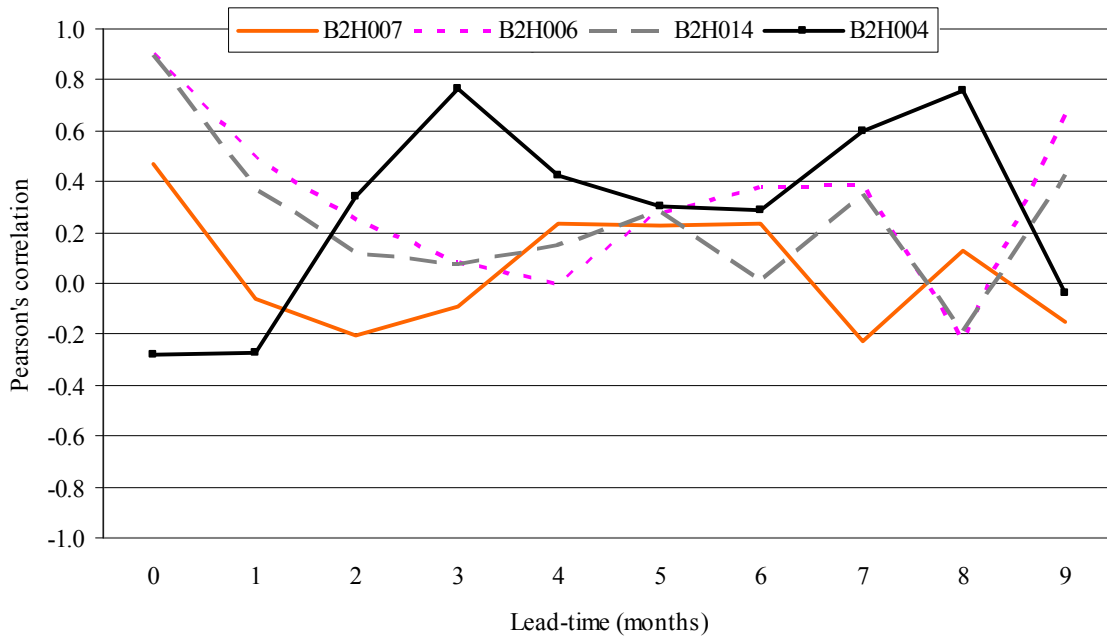**Fig. 6.18 Equatorial Pacific Ocean sea-surface temperatures cross-validated correlations with the sum of JFM stream flows at ten lead-times for the four stream flow stations in the Wilger sub-catchment**

6.6 Selected Correlation Values at Different Oceanic Domains in the Upper Olifants Catchment

In an attempt to distil out the correlation relationships that have some meaning and could be used for model development, the summary table was constructed. The correlation values greater than 0.5 at ten different lead-times for the OND and JFM seasons are summarised in Table 6.1 and 6.2. The equatorial Atlantic Ocean sea-surface temperatures and Southern Atlantic Ocean sea-surface temperatures show higher correlation values than the other oceanic domains at longer lead-times (between lead-times of six and nine months) for the Groot Olifants sub-catchment and shorter lead-times (between lead-times

of zero and six months) for the Wilger sub-catchment. This means that a good verification skill is expected during verification stage in chapter seven to have confidence in the forecasted stream flow in the Groot Olifants and Wilger sub-catchment when using the equatorial and southern Atlantic Ocean SSTs as the main predictors in CPT model for the OND season.

During the JFM season (Table 6.2), the equatorial Atlantic Ocean has the highest correlation values at lead-time of eight months for both Groot Olifants and Wilger sub-catchments except for stream flow stations B2H007 and B2H004. The equatorial Indian Ocean does not have that much of a distinctive trend of lead-time periods and the correlation values for the Wilger sub-catchment. In general, during the OND season (Table 6.1) the Wilger sub-catchment does not have a strong correlation as was seen when comparing rainfall and stream flow directly also (Fig 3.3). However, during the JFM season the Groot Olifants sub-catchment does have strong correlation values when either the equatorial Atlantic Ocean SSTs or the Southern Atlantic SSTs are correlated to stream flow at longer lead-times. The equatorial Pacific Ocean has strong correlation values at shorter lead-times in the Groot Olifants sub-catchment and longer lead-times in the Wilger sub-catchment during the OND season (Table 6.1). The equatorial Pacific Ocean sea-surface temperature correlations with the stream flow for the OND season in Wilger sub-catchment has strong correlation at the three of the four stream flow stations at the lead-times of eight, nine and four months (Table 6.1).

In general, the equatorial Atlantic, Southern Atlantic and equatorial Indian Ocean did not show any negative correlation to the Wilger sub-catchment during the OND season (Table 6.1). The equatorial Pacific Ocean has the highest correlation values in five out of eight stream flow stations at a lead-time of zero months, but they are not useful. Stream flow stations B1H012 and B2H004 both have strong correlation values at lead-times of three and eight months before the JFM season (Table 6.2). When constructing the verification chapter the outcomes from chapter five and six will be evaluated, especially how the use of different lead-times at different oceanic domains can be trusted for operational purpouses. The other important limiting factor that has to be kept in mind

during the verification process is the effect of the relatively short period of stream flow data.

Table 6.1 A summary of the stream flow stations that have a correlation value greater than 0.50 at the selected Oceanic domains and different lead-times during the OND in the Groot Olifants and Wilger sub-catchments

Oceanic domain	Sub-catchment	Stream flow station	Lead-time 1	Lead-time 2	Lead-time 3	Correlation value 1	value 2	value 3
Equatorial Atlantic	Groot Olifants	B1H012	7	0	2	0.6771	0.6108	-0.5677
		B1H017	5	7	3	0.8254	0.7291	0.7210
		B1H020	5	7	3	0.8157	0.7450	0.7165
		B1H021	6	9	0	0.7834	0.7049	-0.6433
	Wilger	B2H007	0	4	9	0.8531	0.7946	0.6526
		B2H006	0	4	9	0.7311	0.7139	0.5935
		B2H014	9	4	0	0.8634	0.8481	0.8377
		B2H004	2	-	-	0.6544	-	-
South Atlantic	Groot Olifants	B1H012	9	1	-	0.5319	-0.7399	-
		B1H017	7	1	-	0.7896	0.6610	-
		B1H020	9	7	1	0.9138	0.9052	0.7089
		B1H021	9	3	-	0.6761	-0.5802	-
	Wilger	B2H007	3	2	-	0.8840	0.5667	-
		B2H006	3	2	-	0.7315	0.5578	-
		B2H014	3	-	-	0.8667	-	-
		B2H004	1	-	-	0.6340	-	-
Equatorial Indian	Groot Olifants	B1H012	2	-	-	0.6624	-	-
		B1H017	9	0	-	0.8357	0.7531	-
		B1H020	0	9	5	0.8653	0.8011	0.6310
		B1H021	9	-	-	0.5286	-	-
	Wilger	B2H007	No correlation					
		B2H006						
		B2H014	1	-	-	0.5912	-	-
		B2H004	2	-	-	0.5380	-	-
Equatorial Pacific	Groot Olifants	B1H012	0	2	6	0.6693	0.5140	-0.5094
		B1H017	0	4	6	0.9224	-0.8795	0.8416
		B1H020	2	6	3	0.8272	0.8157	0.7918
		B1H021	4	8	3	-0.8168	-0.6140	0.5643
	Wilger	B2H007	8	9	4	0.8516	0.8183	0.7994
		B2H006	8	9	4	0.7293	0.6739	0.6505
		B2H014	8	9	4	0.7055	0.6448	0.5590
		B2H004	3	-	-	-0.8070	-	-

Table 6.2 A summary of the stream flow stations that have a correlation value greater than 0.50 at the selected Oceanic domains and different lead-times during the JFM in the Groot Olifants and Wilger sub-catchments

Oceanic domain	Sub-catchment	Stream flow station	Lead-time 1	Lead-time 2	Lead-time 3	Correlation value 1	value 2	value 3
Equatorial Atlantic	Groot Olifants	B1H012	8	-	-	-0.7186	-	-
		B1H017	8	7	2	0.6706	0.6206	0.5501
		B1H020	8	7	5	0.7600	0.7150	0.5034
		B1H021	8	-	-	0.7128	-	-
	Wilger	B2H007	No correlation					
		B2H006	8	6	-	0.8013	0.7974	-
		B2H014	8	6	-	0.8242	0.7844	-
		B2H004	No correlation					
South Atlantic	Groot Olifants	B1H012	7	1	-	0.6913	-0.6260	-
		B1H017	6	8		-0.7112	0.5297	-
		B1H020	1	2	6	0.7205	0.7082	0.7020
		B1H021	1	-	-	0.5834	-	-
	Wilger	B2H007	No correlation					
		B2H006						
		B2H014						
		B2H004	0	2	-	0.7816	0.5543	-
Equatorial Indian	Groot Olifants	B1H012	No correlation					
		B1H017	0	1	-	0.6692	0.6146	-
		B1H020	1	5	-	-0.6061	-0.5379	-
		B1H021	No correlation					
	Wilger	B2H007	No correlation					
		B2H006	0	1	-	0.7946	0.5182	-
		B2H014	0	-	-	0.7509	-	-
		B2H004	5	0	-	0.7224	-0.5346	-
Equatorial Pacific	Groot Olifants	B1H012	8	3	-	0.9744	0.7301	-
		B1H017	0	9	1	0.7504	0.6233	0.5086
		B1H020	0	-	-	-0.7909	-	-
		B1H021	0	-	-	-0.8371	-	-
	Wilger	B2H007	No correlation					
		B2H006	0	9	-	0.8994	0.6683	-
		B2H014	0	-	-	0.8974	-	-
		B2H004	3	8	7	0.7683	0.7592	0.5969

CHAPTER 7

Stream Flow Hindcasting in the Upper Olifants Catchment

When developing a forecast it is very important to take into consideration the effect of SSTs from different oceanic domains affecting the upper Olifants rainfall and stream flow patterns during the OND and JFM season. Lead-times with high correlation values for the individual oceans have already been determined in chapter five and six. Secondly the highest correlation values between different oceanic SSTs and stream flow at various lead-times in the upper Olifants were selected for hindcasting stream flow during the OND and JFM. The hindcasting period was from 1998 to 2005. Lead-times of seven and eight months were selected for the equatorial Atlantic Ocean, lead-time of two months was selected for the Southern Atlantic Ocean. In the Indian Ocean lead-times of two and nine months were selected for the OND and JFM respectively. In the Pacific Ocean lead-times of two and nine months were selected for both OND and JFM seasons.

7.1. Threshold Values of Stream Flow

The values in Table 7.1 were used to determine thresholds for the above normal, normal and below normal limits throughout this chapter. Table 7.1 shows threshold limits that were set for each stream flow station for each of the seasons to determine above and below normal scenarios as below 33.33% being below normal and above 66.66% being above normal and between 33.33 and 66.66% being the near normal part. The stream flow stations with the highest correlation values were selected to be used for the stream flow forecasting during the OND and JFM season. Global SSTs and SSTs from the four selected domains were used as the main input for eight years to make the equations (1990 to 1997) in the upper Olifants catchment stream flow at a lead-time of two months. The threshold values are calculated automatically in the CPT model depending on the above normal, below normal and normal scenarios and the length of hindcasting period. The values in Table 7.1 were used to determine thresholds for the above normal, normal and below normal limits throughout this chapter.

Table 7.1 Stream flow threshold limits for the OND and JFM season using global SSTs as the main predictand for hindcasting stream flow in the upper Olifants catchment. The upper and lower limit values are in million cubic meters per season (OND and JFM)

Catchment	Station	JFM		OND	
		Upper limit	Lower limit	Upper limit	Lower limit
Groot Olifants Sub-catchment	B1H012	28.87	6.01	20.19	2.05
	B1H017	27.96	2.63	14.84	1.22
	B1H020	1.88	0.97	1.21	0.17
	B1H021	6.61	1.84	33.58	6.75
Wilger Sub-catchment	B2H007	3.79	0.54	4.12	1.34
	B2H006	2.15	0.21	0.78	0.26
	B2H014	33.19	3.76	15.01	1.13
	B2H004	4.01	0.35	0.75	0.33

The following stream flow stations B1H012, B1H017 and B1H020 which are in the Groot Olifants sub-catchment had some years of missing data. Stream flow station B1H012 has missing data during the year 2004 for the OND period (Appendix 2.1). Stream flow station B1H017 has a missing value during the year 2005 for the JFM period (Appendix 2.2). Stream flow station B1H020 has missing values from the years 2003 to 2005 for both OND and JFM seasons (Appendix 2.1 and 2.2).

7.2 Hit Scores for OND and JFM Retro-Active Stream Flow Hindcasts using Global SSTs

A cross-validation method was used to evaluate the CPT performance at ten different lead-times and for four different oceanic domains during OND and JFM in both the Wilger and Groot Olifants sub-catchments (i.e. 10x4x2 = 80). Model skill was estimated using Pearson's correlation coefficient between the predicted and observed indices for each of the selected stream flow stations in both the Wilger and Groot Olifants sub-catchments (Wilks, 2006). A summary of the two months lead-time retro-active hit scores of stream flow hindcasting for the upper Olifants catchment during OND and JFM seasons from 1998 to 2005 are given in Table 7.2. A good score is any hit score that is greater than 0.5. Throughout the main upper Olifants catchment during OND season only three years (2000, 2003 and 2005) did not give a good scores (greater than 0.5) and three years (1998, 2000 and 2001) did not give a good scores for the JFM season. These results can be used to get

an overview of the stream flow at secondary catchment scale (B1 and B2). Tertiary and quaternary catchments can be compared to monitor stream flow from the upper parts of the catchment to the lower parts of the upper Olifants catchment. Two of the eight years (2004 and 2005) in the Groot Olifants during OND season gave poor scores while the other six years (1998 to 2003) obtained good scores. In the Wilger sub-catchment three years (2002, 2003 and 2005) do not give a good score, however the other years gave good scores.

During the JFM season the main upper Olifants catchment gave low scores in the years 1998, 2000 and 2001. In the Groot Olifants sub-catchment two years gives low scores in the year 2000 and 2001. In the Wilger sub-catchment there are two years with a low score 1998 and 2000. In the first one year of hindcasting period the model performed better as there are only two out of twelve scores below 0.50 across the entire catchment (1998 during the JFM season in the main catchment and the Wilger sub-catchment). During the year 1999 the model gave good hit scores in all the catchments as there were no hit scores below 0.5. In the years 2002 and 2004 the model performed well during the OND and JFM seasons except for the low scores in the Groot Olifants and the Wilger sub-catchment, 0.00 and 0.25 respectively.

Table 7.2 Hit scores averaged yearly per main catchment and sub-catchment at a lead-time of two months during the OND and JFM seasons using global SSTs as predictors (Appendix 10)

	OND			JFM		
Years	**Main Catchment**	**Sub-catchments**		**Main Catchment**	**Sub-catchments**	
	Upper Olifants	**Groot Olifants**	**Wilger**	**Upper Olifants**	**Groot Olifants**	**Wilger**
1998	0.75	0.50	1.00	0.38	0.50	0.25
1999	0.75	0.75	0.75	0.75	0.50	1.00
2000	0.38	0.50	0.75	0.13	0.25	0.00
2001	0.63	0.50	0.75	0.25	0.00	0.50
2002	0.50	0.50	0.25	0.63	0.75	0.50
2003	0.43	0.67	0.25	0.86	0.67	1.00
2004	0.50	0.00	0.75	0.71	0.67	0.75
2005	0.14	0.00	0.25	1.00	1.00	1.00

It has been seen in the previous chapters that the individual stream flow gauge stations in the sub-catchments have different correlation values compared to the whole of the Upper

Olifants catchment correlation values. It is with this thought that the hit scores for the individual stream flow stations were also investigated. Table 7.3 shows the eight years of stream flow hit scores averages in the upper Olifants and Wilger sub-catchments, at a lead-time of two months during OND and JFM seasons. During the OND season the Groot Olifants sub-catchment stream flow station B1H021 gives a poor hit score while stream flow station B1H012 and B1H020 obtained poor hit scores during the JFM season. For the Wilger sub-catchment the stream flow station at B2H006 during OND and B2H007 during JFM also obtained low hit scores.

Table 7.3 Eight year averages of hit scores per stream flow station at a lead-time of two months in the upper Olifants catchment for the OND and JFM season using the global SSTs as predictors

Catchment	Station	OND	JFM
Groot Olifants Sub-catchment	B1H012	0.57	0.38
	B1H017	0.63	0.57
	B1H020	0.60	0.40
	B1H021	0.25	0.75
Wilger Sub-catchment	B2H007	0.75	0.38
	B2H006	0.25	0.63
	B2H014	0.63	0.63
	B2H004	0.50	0.75

7.3 Retro-Active Stream Flow Hindcasts at Selected Oceanic Domains

The stream flow stations with the highest correlation values between selected oceanic domains and the eight stream flow stations were selected to be used for the stream flow forecasting during the OND and JFM seasons. Since this is a pioneering study, lead-times with higher correlation values were selected for both OND and JFN and then used for the hindcasting model. Threshold values did not change, the same threshold values as previously listed in Table 7.1 will again be used in this section.

7.3.1 Stream flow hindcast using Equatorial Atlantic Ocean SSTs

The lead-times of seven and eight months were selected for the hindcast using the equatorial Atlantic Ocean during the OND and JFM periods because these two lead-times had a high correlation value during the cross-validation period. Since this is a first investigative study all lead-times cannot be used. Table 7.4 gives hit scores for hindcast lead-times of seven and eight months using the equatorial Atlantic Ocean SSTs. This means that for the OND season, with a lead-time of seven months, by the beginning of March one

can have a predicted stream flow for the OND season. For the JFM at a lead-time of seven months it means that by the beginning of June one could forecast the expected stream flow for the JFM season.

In 1999, 2003 and 2005 the lead-times of seven and eight months for the JFM season gave good scores for the whole catchment and in both the sub-catchments as there is no hit score below 0.50 in these years for this season. In 2002 and 2004 the model shows a good score when using lead-times of seven months during the JFM season for the whole of the upper Olifants catchment and the two sub-catchments. For the OND season during the years 1998 and 2001, the model shows good skill when using lead-times of eight and seven months, for the whole catchment and in both sub-catchments.

Table 7.4 Hit scores averaged yearly per sub-catchment at lead-time of seven and eight months during the OND and JFM season using equatorial Atlantic Ocean SSTs as the predictors (Appendix 11)

Year	OND			JFM		
	Upper Olifants	**Groot Olifants**	**Wilger**	**Upper Olifants**	**Groot Olifants**	**Wilger**
	Seven months lead-time					
1998	0.88	0.75	1.00	0.25	0.25	0.25
1999	0.50	0.25	0.75	0.75	0.75	0.75
2000	0.88	1.00	0.75	0.13	0.25	0.00
2001	0.75	0.50	1.00	0.38	0.00	0.75
2002	0.25	0.25	0.25	0.50	0.50	0.50
2003	0.14	0.33	0.00	0.71	0.67	0.75
2004	0.50	0.00	0.75	0.71	0.67	0.75
2005	0.14	0.00	0.25	0.83	1.00	0.75
	Eight months lead-time					
1998	1.00	1.00	1.00	0.50	0.25	0.75
1999	0.38	0.25	0.50	0.75	0.75	0.75
2000	0.63	1.00	0.25	0.00	0.00	0.00
2001	0.63	0.50	0.75	0.50	0.25	0.75
2002	0.38	0.50	0.25	0.38	0.25	0.50
2003	0.29	0.67	0.00	0.86	0.67	1.00
2004	0.33	0.00	0.50	0.57	0.33	0.75
2005	0.14	0.00	0.25	0.67	0.50	0.75

Eight year averages of hit scores per stream flow station at lead-times of seven and eight months in the upper Olifants catchment for each of the OND and JFM season using the equatorial Atlantic Ocean SSTs are shown in Table 7.5. When using seven months lead-

time for hindcasting during the OND season the following stream flow stations in the Groot Olifants sub-catchment obtained good scores B1H017 and B1H020 and the Wilger sub-catchment at gauges B2H007, B2H006 and B2H014. During the JFM the following stream flow stations in the Groot Olifants sub-catchment obtained good scores B1H017 and B1H021, and the Wilger sub-catchment at B2H006, B2H014 and B2H004 for seven months lead-time.

When using eight months lead-time for hindcasting during the OND season the following stream flow stations in the Groot Olifants sub-catchment gave good scores for B1H012, B1H017 B1H020 and B2H006 in the Wilger sub-catchment. Then during the JFM only one stream flow station gave a good score B1H017 in the Groot Olifants sub-catchment but B2H006, B2H014 and B2H004 obtain high score in the Wilger sub-catchment.

Table 7.5 Eight year averages of hit scores per stream flow station at lead-times of seven and eight in the upper Olifants catchment for the OND and JFM season using equatorial Atlantic Ocean SSTs as the predictors

Catchment	Station	Seven months Lead-time		Eight months lead-time	
		OND	**JFM**	**OND**	**JFM**
Groot Olifants Sub-catchment	**B1H012**	0.38	0.38	0.50	0.25
	B1H017	0.71	0.57	0.86	0.57
	B1H020	0.60	0.20	0.60	0.20
	B1H021	0.13	0.63	0.25	0.38
Wilger Sub-catchment	**B2H007**	0.75	0.25	0.38	0.38
	B2H006	0.63	0.75	0.63	0.88
	B2H014	0.63	0.50	0.38	0.63
	B2H004	0.38	0.75	0.38	0.75

The Wilger sub-catchment has good hit scores at a lead-time of seven months during the OND and JFM, except for stream flow station B2H004 and B2H007 which had hit scores of below 0.50 during OND and JFM respectively. Again the Wilger sub-catchment has good hit scores at a lead-time of eight months during the JFM, except for stream flow station B2H007 which had hit scores of below 0.50. This means for the OND season, at a lead-time of seven months by the beginning of March one can have a predicted stream flow for the OND season except at stream flow station B2H004 and at a lead-time of eight

months by the beginning of February one can have a good prediction of stream flow for the OND season except at stream flow station B2H007. For the JFM at a lead-time of seven months means that by the beginning of June one could predict the expected stream flow for the JFM season except for stream flow station B1H021.

7.3.2 Stream flow hindcast using Southern Atlantic Ocean SSTs

The lead-time of two months has been selected for the hindcast using the Southern Atlantic Ocean SSTs during the OND period because it had a high correlation value during the cross-validation period. The whole of the upper Olifants catchment area has good hit scores during the OND period from 1998 to 2003 except for the year 2004 and 2005 which have hit scores lower than 0.50 as shown in Table 7.6. During the JFM periods the upper Olifants catchment has good hit scores, except for 1999 and 2000.

Table 7.6 Hit scores averaged yearly per sub-catchment at lead-time of two months during the OND and JFM season using Southern Atlantic Ocean SSTs as the predictors (Appendix 12)

Year	OND			JFM		
	Upper Olifants	Groot Olifants	Wilger	Upper Olifants	Groot Olifants	Wilger
1998	0.75	1.00	0.50	0.50	0.50	0.50
1999	0.63	0.75	0.50	0.25	0.25	0.25
2000	0.63	0.50	0.75	0.25	0.25	0.25
2001	0.50	0.50	0.50	0.50	0.25	0.75
2002	0.50	0.25	0.75	0.75	0.50	1.00
2003	0.71	0.67	0.75	0.57	0.67	0.50
2004	0.33	0.00	0.50	0.71	0.67	0.75
2005	0.29	0.33	0.25	0.67	0.50	0.75

The Groot Olifants sub-catchment has good hit scores at a lead-time of two months in general, except for 2002, 2004 and 2005 during OND season and 1999 to 2001 during the JFM season. The Wilger sub-catchment also has good hit scores at a lead-time of two months, except for 2005 during OND season and 2000 and 2001 during the JFM season. The eight year average hit scores per stream flow station at a lead-time of two months in the upper Olifants catchment are shown in Table 7.7. The model gives a good hit score for each stream flow station during the OND season for the two sub-catchments, except for the stream flow stations B1H021 and B2H006 which both have low hit skill scores (0.38).

Table 7.7 Eight year averages of hit scores per stream flow station at lead-times of two months in the upper Olifants catchment for the OND and JFM season using Southern Atlantic Ocean SSTs as the predictors

Catchment	Station	OND	JFM
Groot Olifants Sub-catchment	**B1H012**	0.57	0.63
	B1H017	0.63	0.43
	B1H020	0.60	0.00
	B1H021	0.38	0.50
Wilger Sub-catchment	**B2H007**	0.50	0.38
	B2H006	0.38	0.63
	B2H014	0.75	0.63
	B2H004	0.63	0.75

During the JFM stream flow stations B1H017, B1H020, and B2H007 have skill scores below 0.50. since there are only two values below 0.5 during the OND season therefore the OND season will have good skill score as compared to the JFM season which has three values lower than 0.50.

7.3.4 Stream flow hindcast using Equatorial Indian Ocean SSTs

The lead-time of two months has been selected for the hindcast using the equatorial Indian Ocean during the OND and a lead-time of one month was selected for the JFM season (Table 7.8) according to results in chapter six.

Table 7.8 Hit scores averaged yearly per sub-catchment at lead-time of two months during the OND and lead-time of one months during the JFM season using the equatorial Indian Ocean SSTs as the predictors (Appendix 13)

Year	OND at two months lead-time			JFM at one months lead-time		
	Upper Olifants	Groot Olifants	Wilger	Upper Olifants	Groot Olifants	Wilger
1998	1.00	1.00	1.00	0.50	0.50	0.50
1999	0.63	0.75	0.50	0.25	0.25	0.25
2000	0.88	0.75	1.00	0.63	0.50	0.75
2001	0.38	0.50	0.25	0.38	0.25	0.50
2002	0.25	0.50	0.00	0.50	0.25	0.75
2003	0.29	0.33	0.25	0.57	0.67	0.50
2004	0.50	0.00	0.75	0.71	0.67	0.75
2005	0.14	0.33	0.00	1.00	1.00	1.00

The OND season at a lead-time of two months has good hit scores from the years 1998 to 2000, for the whole catchment and 1998 to 2002 in the Groot Olifants sub-catchment.

The JFM season at a lead-time of one month had a good hit score during the five of the eight years 1998, 2000 and 2003 to 2005, with 2005 having the highest hit scores for the two sub-catchments. The Wilger has good scores for all the eight years during the JFM at one months lead-time except for the year 1999 at 0.25.

The eight year OND and JFM average hit scores per stream flow station at a lead-time of two months in the upper Olifants catchment using equatorial Indian Ocean SSTs are shown in Table 7.9. The Wilger sub-catchment has a good hit score for both OND and JFM season, except for the B2H006 stream flow station with low hit score during OND and B2H007 stream flow station with low hit score during JFM season.

Table 7.9 Eight year averages of hit scores per stream flow station at lead-time of two months during the OND and lead-time of one month during the JFM season using the equatorial Indian Ocean SSTs as the predictors

Catchment	Station	OND	JFM
Groot Olifants Sub-catchment	B1H012	0.86	0.50
	B1H017	0.75	0.43
	B1H020	0.40	0.00
	B1H021	0.25	0.63
Wilger Sub-catchment	B2H007	0.50	0.38
	B2H006	0.38	0.88
	B2H014	0.50	0.88
	B2H004	0.50	0.50

7.3.5 Stream flow hindcast using Equatorial Pacific Ocean SSTs

The lead-times of two and nine months were selected for this hindcast because they gave the highest correlation value between the stream flow and Pacific Ocean SSTs during the OND and JFM seasons. Table 7.10 illustrates the annual hit scores (1998 to 2005) for the Groot Olifants and Wilger sub-catchments at a lead time of two and nine months. The equatorial Pacific Ocean SSTs were the predictors while the stream flow stations in the Groot Olifants and Wilger sub-catchment were the predictant.

There are five years with hit scores above 0.50 during the OND season at a lead-time of two months in the Groot Olifants sub-catchment while the OND season at a lead-time of nine months has only three years of hit score above 0.50. The Wilger sub-catchments have equal number of years (5) with hit scores above 0.50 during the OND season for the lead-times of two and nine months. During the JFM season there are four years with hit scores above 0.50 at a lead-time of two months in the Groot Olifants sub-catchment while the JFM season at a lead-time of nine months has only two years of hit scores above 0.50 so should not be used.

Table 7.10 Hit scores averaged yearly per sub-catchment at lead-times of two and nine months during the OND and JFM season using the equatorial Pacific Ocean as the predictors (Appendix 14)

Year	OND			JFM		
	Upper Olifants	**Groot Olifants**	**Wilger**	**Upper Olifants**	**Groot Olifants**	**Wilger**
	Two months lead-time					
1998	0.75	0.50	1.00	0.63	0.50	0.75
1999	0.50	0.50	0.50	0.75	0.75	0.75
2000	0.50	0.75	0.25	0.25	0.25	0.25
2001	0.63	0.50	0.75	0.38	0.00	0.75
2002	0.25	0.50	0.00	0.25	0.00	0.50
2003	0.14	0.33	0.00	0.86	0.67	1.00
2004	0.67	0.00	1.00	0.57	0.33	0.75
2005	0.43	0.33	0.50	0.67	1.00	0.50
	Nine months lead-time					
1998	0.50	0.50	0.50	0.50	0.25	0.75
1999	0.38	0.75	0.75	0.75	1.00	0.50
2000	0.88	1.00	0.50	0.63	0.75	0.50
2001	0.25	0.25	0.25	0.38	0.00	0.75
2002	0.25	0.25	0.25	0.63	0.50	0.75
2003	0.29	0.33	0.25	0.86	0.67	1.00
2004	0.29	0.00	0.50	0.71	1.00	0.50
2005	0.50	0.25	0.50	0.67	0.50	0.75

The Wilger sub-catchment has only one year (2000) of a hit score below 0.50 during the JFM season at a lead-time of two months while at a lead-time of nine months the hit score is above 0.50 for all the years. The Wilger sub-catchment has the highest hit scores for the OND and JFM seasons showing that the equatorial Pacific Ocean plays a major role as an

indicator of the stream flow in the Wilger sub-catchment, especially at a lead-time of nine months.

The eight years (1998 to 2005) OND and JFM season hit scores per stream flow station at a lead-time of two and nine months in the upper Olifants catchment using the equatorial Pacific Ocean SSTs are shown in Table 7.11. Stream flow station B1H020 in the Groot Olifants sub-catchment has poor hit scores all being below 0.50 for the lead-time of two and nine months during both the OND and JFM seasons. The good hit score for the five years during OND at a lead time of two months was mainly contributed by the stream flow stations B1H012 and B1H017 as these two stream flow stations have hit scores of above 0.50.

Although Table 7.10 shows that the Wilger sub-catchment has the highest hit scores at lead-times of two and nine months during the OND and JFM season, it should be read in conjunction with Table 7.11 which shows the hit scores for the individual stream flow stations. Stream flow station B2H014 has a low hit score during the OND at a lead-time of two months and stream flow station B2H007 has a low hit score during the JFM season at a lead-time of two months. For the lead-time of nine months stream flow stations B2H004 and B2H014 have a lower hit score during the OND season.

Table 7.11 Eight years stream flow stations hit scores averages at a lead-time of two and nine months for OND and JFM season in the upper Olifants catchment using equatorial Pacific Ocean SSTs as the predictor

Catchment	Station	Two months lead-time		Nine months lead-time	
		OND	JFM	OND	JFM
Groot Olifants Sub-catchment	B1H012	0.57	0.38	0.50	0.63
	B1H017	0.63	0.29	0.86	0.57
	B1H020	0.40	0.20	0.40	0.40
	B1H021	0.25	0.63	0.25	0.63
Wilger Sub-catchment	B2H007	0.50	0.38	0.50	0.75
	B2H006	0.50	0.75	0.50	0.75
	B2H014	0.38	0.63	0.25	0.50
	B2H004	0.63	0.88	0.13	0.75

The Pearson's correlation was used in chapter five and six to evaluate the association between SSTs and stream flow at different lead-times. The strength of the relationship between SSTs and stream flow will be assessed for a two months lead-time using the following verification measures: Bias Measure; Percent Correct and Heidke Score. A two month lead-time was assessed in this study because of the high correlation values for both the Wilger and Groot Olifants sub-catchments when using different oceanic domains.

7.4 Bias in the Upper Olifants Catchment

The bias measure is the number forecast divided by the number observed for each category. The bias measures the ability of the model to forecast events at the same frequency as found in the sample. The details of the calculation of the bias (Jolliffe and Stephenson, 2003) are given in Appendix 9.1, together with the contingency tables used to calculate the basis in Table 7.12.

The performance of stream flow forecast in the upper Olifants at a lead-time of two months for each of the selected oceanic domains for OND is shown in Table 7.12. Bias greater than one implies over-forecasting the event; bias less than one implies under-forecasting the event and a bias equal to one shows there is no bias at all. In both the sub-catchments OND stream flow is over-estimated in the forecast of above and especially near normal stream flow from all the oceanic domains and under-forecasted for below normal forecasts.

Table 7.12 Bias measure for stream flow forecast during the OND season at a lead-time of two months in the upper Olifants catchment

OND	Groot Olifants sub-catchment			Wilger sub-catchment		
Oceanic domain	Above normal	Near-normal	Below normal	Above normal	Near-normal	Below normal
Equatorial Atlantic	0.75	2.78	0.00	1.91	1.43	0.07
Southern Atlantic	1.50	2.20	0.00	1.29	1.13	0.50
Equatorial Indian	1.20	2.20	0.00	2.22	0.76	0.10
Equatorial Pacific	1.25	2.44	0.07	1.27	1.44	0.42

The bias forecast measure for the upper Olifants sub-catchments during the JFM season is shown in Table 7.13 where the near-normal category has high biased values in the whole upper Olifants catchment, whereby the southern Atlantic Ocean has the highest bias value

(7.667) in the Wilger sub-catchment. For the Wilger catchment OND (Table 7.12) shows more bias at the above normal category and in JFM (Table 7.13) at near-normal.

This means that the model would more frequently give a forecast for above normal during OND season and near-normal forecast in the JFM season for the Wilger sub-catchment. So these models would need to be used with caution taking into considering these bias factors.

Table 7.13 Bias measure for stream flow forecast during the JFM season at a lead-time of two months in the upper Olifants catchment

JFM	Groot Olifants sub-catchment			Wilger sub- catchment		
Oceanic domain	Above normal	Near-normal	Below normal	Above normal	Near-normal	Below normal
Equatorial Atlantic	2.111	0.800	0.111	1.375	4.500	0.150
Southern Atlantic	0.909	1.556	0.500	0.667	7.667	0.150
Equatorial Indian	1.333	1.200	0.444	0.909	6.333	0.167
Equatorial Pacific	2.333	0.545	0.125	1.750	6.000	0.000

7.5 Percent Correct

As describe by Jolliffe and Stephenson (2003) the Percent correct is a proportion of the whole sample of correct forecasts and it is as the summation of the diagonal elements of a contingency table (Appendix 9.1) divided by the total number of events. Table 7.14 shows the percent correct values for the upper Olifants catchment at a lead-time of two months.

Table 7.14 Two months lead-time Proportion Correct values for a stream flow forecast in the upper Olifants catchment

Season	Oceanic domain	Groot Olifants sub-catchment	Wilger sub-catchment
OND	Equatorial Atlantic	32.14	34.38
	Southern Atlantic	39.29	53.13
	Equatorial Indian	50.00	25.08
	Equatorial Pacific	42.86	28.13
JFM	Equatorial Atlantic	53.57	25.00
	Southern Atlantic	46.43	21.88
	Equatorial Indian	53.57	31.25
	Equatorial Pacific	50.00	21.88

The percent correct value of 32.14% in the Groot Olifants means that the forecast was 32.14% correct when using Equatorial Atlantic SSTs to predict stream flow during the OND season. The Indian Ocean has a higher value of the percent correct in the Olifants for both the seasons in the Groot Olifants sub-catchment (50.0 and 53.6%). The southern Atlantic Ocean has the highest value of percent correct in the Wilger sub-catchment for OND. The Groot Olifants has higher proportion correct values than the Wilger catchment across all eight years.

7.6 Heidke Skill Score

The Heidke Skill score is described as a percent correct adjusted to account for the proportion of forecast that would have been correct by chance in the absence of skill (Jolliffe and Stephenson, 2003). The Heidke Skill score is most often associated with chance as the standard of comparison and is popular as a verification statistics (Stanski *et al.,* 1989). Table 7.15 shows Heidke's scores for the upper Olifants during the OND and JFM seasons using SSTs from different oceanic domains. The southern Atlantic Ocean and equatorial Indian Ocean both have Heidke scores above 0.26 during the OND season in the Wilger and Groot Olifants respectively.

Table 7.15 Heidke scores for a two months lead-time forecast for the upper Olifants during OND and JFM seasons

Season	Oceanic domain	Groot Olifants sub-catchment	Wilger sub-catchment
OND	Equatorial Atlantic	0.0274	0.0522
	Southern Atlantic	0.1185	0.2615
	Equatorial Indian	0.2659	-0.0436
	Equatorial Pacific	0.1869	-0.0620
JFM	Equatorial Atlantic	0.3053	0.0448
	Southern Atlantic	0.1860	0.0488
	Equatorial Indian	0.3000	0.1233
	Equatorial Pacific	0.2476	0.0676

The Heidke score shows that the model is expected to give a good forecast when using the equatorial Indian Ocean (0.30), equatorial Pacific Ocean (0.24) and equatorial Atlantic Ocean (0.31) SSTs to forecast stream flow in the Groot Olifants catchment during the JFM season at a lead-time of two months. The Heidke skill score confirms that overall the Groot

Olifants stream flow can be forecasted with more skill than the stream flow in the Wilger catchment at a lead time of two months during the JFM season.

7.7 Conclusion and Recommendations

Good hit skill score from the Southern Atlantic Ocean were found and at a lead-time period of two months for both OND and JFM seasons in the upper Olifants catchment. However higher hit skill scores were found to be associated with below normal southern Atlantic SSTs during OND in the Wilger sub-catchment because the model has less bias (under forecasting) at below normal forecasts. The southern Atlantic Ocean is well known to have a great impact on South Western Cape rainfall in South Africa. However a reasonable Heidke score has been found at a lead-time of two months in the Wilger sub-catchment during the OND summer season. The hit score may be as a result of frequent occurrence of changing SST over the Southern Atlantic Ocean. This could alter the steepness of the temperature gradient to the southwest of the subcontinent which may impact on cyclogenesis and the intensity and subsequent movement of westerly troughs and cut-off lows which brings rainfall to the north eastern interior of South Africa (Taljaard and Steyn, 1991).

Equatorial Atlantic Ocean was biased for both the OND and JFM season. This means that the stream flow would either give over-forecasted or near-normal forecast when using the equatorial Atlantic Ocean as the main predictor. The Percent correct shows that 32.14 and 34.38 percent is adjusted to account for the proportion of a forecast that would have been correct by chance in the absence of the skill when the Equatorial Atlantic Ocean were used as the main predictor during the OND season. A change in SSTs over the equatorial Atlantic Ocean should influence the strength of the easterly trades and particularly that of the southwesterly monsoon during the austral summer (Allan, 2000; Taljaard and Steyn, 1991).

The equatorial Indian Ocean gave a good skill score at short lead-times of two months when they are used as the main predictors of stream flow in the upper Olifants. In general the Wilger sub-catchment gave a better hit score using equatorial Indian Ocean SSTs at

lead-time of two months. The good skill might be influenced by the air from the Atlantic Ocean High (AOH) which meets that from the Indian Ocean High (IOH), where a moisture boundary (also called a moisture front or dry-line) forms. Uplift occurs along this moisture front due to the undercutting effect of the colder/dryer air (from AOH), often affecting the rainfall distribution over the entire north eastern region of South Africa (Taljaard, 1970).

The equatorial Pacific Ocean gave a good score at shorter and longer lead-times of two and nine months for both the seasons. The equatorial Pacific Ocean has a major role to play during the El Niño and La Nina periods. Although El Niño and La Nina events are characterized by warmer or cooler than average sea-surface temperatures in the tropical Pacific, they are also associated with changes in wind, pressure, and rainfall patterns. The distance between Pacific Ocean and southern Africa plays a major role in the lead-time variability when compared to the Indian and Atlantic Ocean which are not far away from southern Africa. So one would expect longer lead-times to have a stronger effect if equatorial Pacific Ocean SSTs are used as the main predictor for the OND and JFM seasons.

The oceanic domains adjacent to the southern African continent gave a good skill score at shorter lead-times while the Pacific Ocean gave a good skill at both shorter and longer lead-times. Further research on different oceanic domains with more years data should improve the forecasting skill as it was shown in the upper Olifants catchment that different oceanic domains affect stream flow differently. The skill of the model could be improved by incorporating logical hydrological parameters into the GCMs as well or using a regional climate model with downscaling from the larger GCM grid.

These forecasting equations need to be further tested in real time in the next few years as at present only a limited number of years of data was available. As there is also longer data set of stream flow data for selected weirs (namely B1H012 from 1978; B1H017 from 1989 and B2H007 from 1985, B2H004 & B2H006 from 1984) this could give up to 20 years of information. When more data sets have been collected then one will be able to divide the years up into El Niño and La Nina events and it can then be ascertained if there are better forecast from different ENSO phases. These forecasts results would have to be further

packaged for distribution to the hydrologist and water resource managers if one could be confident with the prediction. They can begin to test the usefulness and appropriateness of this information. Other important factors that can be included in the model for future analysis are the local soil land types and hydrological factors. The vegetation cover has an impact on the stream flow was not included in the model so it would be interesting to investigate these aspects.

References

ALLAN, R.J., 2000. ENSO and climate variability in the last 150 years. *El Niño and the Southern Oscillation: Multiscale Variability, Global and Regional Impacts.* (ed. Diaz, H.F. & Markgraf, V) Cambridge University Press, pp. 3-56.

ANDERSON, T.W., 1984. *An Introduction to Multivariate Statistical Analysis.* Wiley, New York, pp. 675.

ARC-ISCW GISLIB., 2004. Agricultural Research Council - Institute for Soil Climate and Water, Geographical Information Systems Library Databank, Pretoria.

BARNETT, T.P. & PREISENDORFER, R.W., 1987. Origins and levels of monthly and seasonal forecast skill for United States air temperature determined by canonical correlation analysis. *Mon. Wea. Rev.* 115, 1825-1850.

BARNSTON, A.G., 1994. Linear statistical short-term climate predictive skill in the Northern Hemisphere. *J. Climate* 7, 1513-1564.

BARNSTON, A.G. & SMITH, T.M., 1996. Specification and prediction of global surface temperature and precipitation from global SST using CCA. *J. Climate* 9, 2660-2697.

BARNSTON, A.G., THIAO, W. & KUMAR, V., 1996. Long-lead forecasts of seasonal precipitation in Africa using CCA. *Wea. Forecast.* 11, 506-520.

BARTMAN, A.G., LANDMAN, W.A & RAUTENBACH, C.J.W., 2003. Recalibration of general circulation model output to austral summer rainfall over southern Africa. *Int. J. Climat.* 23, 1407-1419.

BEVEN, K.J. & HORNBERGER, G.M., 1982. Assessing the effect of spatial patterns of precipitation in modelling stream flow hydrographs. *Water Resour. Bul.* 18, 823-829.

BOX, G.P. & JENKINS, G.M., 1976. *Time Series Analysis Forecasting and Control.* Holden Day, Johannesburg, pp. 398.

BROWN, R.G., 1964. *Smoothing, Forecasting and Prediction of Discrete Time Series.* Prentice-Hall Inc, United States of America, pp. 468.

References

CHIEW, F.S.H., PIECHOTA, T.C., DRACUP, J.A. & MCMAHON, T.A., 1998. El Niño/Southern Oscillation and Australian rainfall, stream flow and drought: Links and potential for forecasting. *J. Hydrol.* 204, 138-149.

CHU, P. S. & HE, Y., 1994. Long-range prediction of Hawaiian winter rainfall using canonical correlation analysis. *Int. J. Climatol.* 14, 659-669.

COLBERG, F., REASON C.J.C. & RODGERS, K., 2004. South Atlantic response to ENSO induced climate variability in an OGCM. *J. Geophys. Res.* 109, C12015.

COOK, C., REASON, C.J.C. & HEWITSON, B.C., 2004. Wet and dry spells within particular wet and dry summers in the South African summer rainfall region. *Climate Res.* 26, 17-31.

CORRADINI, C., 1985. Analysis of the effects of orography on surface rainfall by a parameritised numerical model. *J. Hydrol.* 77, 19-30.

COSGROVE, W. & RIJSBERMAN, F., 2000. World Water Vision: Making Water Everybody's Business. Earthscan publications Ltd, UK, pp. 15-30.

DAWDY, D.R. & BERGMAN, J.M., 1969. Effect of rainfall variability on stream flow simulation. *Water Resour. Res.* 5, 958-966.

DENT, M.C., 2000. Strategic issues in modelling for integrated water resource management Southern Africa. *Water SA.* 26, 513-519.

DENT, M.C., LYNCH, S.D. & TURBOTON, H., 1990. Detailed delineation of rainfall regions in South Africa. *Weather SA.* 16, 1-4.

DENT, M.C., SCHULZE, R.E & ANGUS, G.R., 1988. Crop water requirements, deficits and water yield for irrigation planning in Southern Africa. *Water Research Commission,* Pretoria, *Report* 118/1/88. pp. 183.

DIGA, M.G., 2005. *Using Seasonal Climate Outlook to Advice on Sorghum Production in the Central Rift Valley of Ethiopia.* Ph.D. thesis, University of Free State, Bloemfontein, South Africa, pp. 171.

DONIGIAN, A.S., BICKNELL, B.R., PATWARDHAN, A.S., LINKER, L.C., ALEGRE, D.Y., CHANG, C., REYNOLD, R. & CARSELS, R., 1991. Chesapeake Bay Program. Watershed Model Application to Climate Bay Nutrient Loadings. US Environmental Protection Agency, Annapolis, Maryland, pp. 137.

DROSDOWSKY, W., 1994. Analog (nonlinear) forecasts of the Southern Oscillation Index time series. *Wea. Forecast.* 9, 78-84.

References

DWAF, 1997. White Paper on Environmental Management Policy Government Gazette, July, Cape Town, South Africa.

DWAF, 2007. Department of Water Affairs and Forestry. http://www.dwaf.gov.za . Last visited April 2007.

ELSNER, J.B. & SCHMERTMANN, C.P., 1994. Assessing forecast skill through cross-validation. *Wea. Forecast*, 9, 619-624.

ENGELBRECHT, F.A., 2005. Simulations of climate and climate change over southern and tropical Africa with the conformal-cubic atmospheric model. chap. 4. In *Potential Impacts and Vulnerabilities of Climate Change on Hydrological Responses in southern Africa,* ed. R.E. Schulze, WRC Report 1430/1/05. Water Research Commission, Pretoria, pp. 51-69.

FITZPATRICK, R.W., HAHNE, H.C.H., KRISTEN, W.F.A. & HAWKER, L.C., 1986. Soil mineralogy. In land types of the maps 2526 Rustenburg, 2528 Pretoria. (ed. du Plessis H.M.) *Mem. Agric. Nat. Resour. SA. No.8.* pp 391.

FLORENCHIE, P., REASON, C.J.C., LUTJEHARMS, J.R.E., ROUAULT, M. & ROY, C., 2004: Evolution of interannual warm and cold events in the southeast Atlantic Ocean. *J. Climate* 17, 2318-2334.

GLANTZ, M.H., KATZ, R.W. & NICHOLLS, N., 1991. *Teleconnections Linking Worldwide Climate Anomalies*. Cambridge University Press, Cambridge. pp 535.

GODDARD, L. & MASON S.J., 2002. Sensitivity of seasonal climate forecasts to persisted SST anomalies. *Climate Dyn.* 19, 619-631.

HAHNE, H.C.M. & FITZPATRICK, R.W., 1985. Soil Mineralogy. *In Land Types Maps* 2628 East Rand*, 2630 Mbabane.* (Ed. Mac Vicar, C.N.) *Mem. Agric. Nat. Resour. S.A.* 5, pp. 261.

HALL, M.J. & BARCLAY, P.A., 1975. Methods of determining areal rainfall from observed data. *In: Precipitation in Catchment Hydrology,* ed. Chapman, T.G and Dunin, F.X., Australian Academy of Science, Canberra, pp. 45-67.

HAMLIN, M.J., 1983. The significance of rainfall in the study of hydrological processes at basin scale. *J. Hydrol.* 65, 73-94.

HARRISON, M.S., 1984. A generalised classification of South African summer rainfall rain bearing synoptic systems. *J. Climatol.* 4, 547-560.

References

HEWITSON, B.C., TADROSS, M. & JACK, C., 2005. Scenarios from the University of Cape Town. In *Potential Impacts and Vulnerabilities of Climate Change on Hydrological Responses in southern Africa,* (ed. Schulze, R.E.) WRC Report 1430/1/05. Water Research Commission, Pretoria, pp. 38-62.

HIRST, A.C. & HASTENRATH, S., 1983. Atmosphere-Ocean mechanisms of climate anomalies in the Angola-tropical Atlantic sector. *J. Phys. Oceanogr.* 13, 1146-1157.

JACKSON, J.E., 1991. *A User's Guide to Principal Components*. Wiley, New York, pp. 569.

JOHNSTON, R.J., 1992. *Multivariate Statistical Analysis in Geography*. Longman, New York, pp. 280.

JOLLIFFE, I.T. & STEPHENSON, D.B., 2003. *Forecast Verification. A Practitioner's Guide in Atmospheric Science*. Willey, London, pp. 240.

JURY, M.R., 1996. Regional teleconnection patterns associated with summer rainfall over South Africa, Namibia and Zimbabwe. *Int. J. Climatol.* 16, 135-153.

JURY, M.R., 2002. *Development of Statistical Forecast Models of Summer Climate and Hydrological Resources over Southern Africa.* Water Research Commission Report No. 903/1/02, pp. 116.

JURY, M.R., MC QUEEN, C. & LEVEY, K., 1994. SOI and QBO signals in the African region. *Theor. Appl. Climatol.* 50, 103-115.

JURY, M.R. & PATHACK, B.M.R., 1991. A study of climate and weather variability over the tropical southwest Indian Ocean. *Met. Atmos. Phys.* 47, 37-48.

JURY, M.R., VALENTINE, H.R. & LUTJEHARMS, J.R.E., 1993. Influence of the Agulhas current on summer rainfall along the southeast coast of South Africa. *J. Appl. Met.* 32, 1282-1287.

KRUGER, A.C., 2004a. Climate of South Africa. Climate Controls. South African Weather Bureau. WS44, Pretoria, South Africa, pp. 21.

KRUGER, A.C., 2004b. Climate of South Africa. Climate Regions. South African Weather Bureau. WS45, Pretoria, South Africa, pp. 19.

LANDMAN, W.A., 1997. *A Study of Rainfall Variability of South Africa as Revealed by Multivariate Analysis.* Unpublished M.Sc. dissertation, University of Pretoria, South Africa, pp. 134.

References

LANDMAN, W.A. & MASON, S.J., 1999. Change in the association between Indian Ocean sea-surface temperatures and summer rainfall over South Africa and Namibia. *Int. J. Climatol*. 19, 1477-1492.

LANDMAN, W.A. & MASON, S.J., 2001. Forecast of near-global sea-surface temperatures using canonical correlation analysis. *J. Climate* 14, 3819-3833.

LANDMAN, W.A., MASON, S.J., TYSON, P.D. & TENNANT, W.J., 2001. Retro-active skill of multi-tiered forecasts of summer rainfall over southern Africa. *Int. J. Climatol.* 21, 1-9.

LÉVITE, H. & SALLY, H., 2002. Linkages between productivity and equitable allocation of water. *Phys. Chem. Earth.* 27, 825-830.

LINDESAY, J.A., 1988. South African rainfall, the Southern Oscillation and a Southern Hemisphere semi-annual cycle. *J. Climatol*. 8, 17-30.

LOUGH, J., 1986. Tropical Atlantic sea-surface temperatures and rainfall variations in sub-Saharan Africa. *Mon. Wea. Rev.* 114, 561-570.

LOW, A.B. & REBELO, A.G., 1996. Vegetation of South Africa, Lesotho and Swaziland. Published by the Department of Environmental Affairs and Tourism. Pretoria. pp. 39-43.

LYNCH, S.D. & DENT, M.C., 1990. Appropriate record lengths for the estimation of mean annual and mean monthly precipitation in South Africa. *Water SA*. 16, 93-98.

MASON, S.J., 1976. Towards the understanding and prediction of climatic variation. *Q. J. Roy. Soc.* 102, 473-498.

MASON, S.J., 1990. Temporal variability of sea-surface temperatures around Southern Africa: a possible forcing mechanism for the 18-year rainfall oscillation. *S. Afr. J. Sci*. 86, 243-252.

MASON, S.J., 1995. Sea-surface temperature South African rainfall associations, 1910–1989. *Int. J. Climatol*. 15, 119-135.

MASON, S.J., 1998. Seasonal forecasting of South African rainfall using a non-linear discriminant analysis model. *Int. J. Climatol*. 18, 147-164.

MASON, S.J., 1999. The Climate Predictability Tool. http://www.iri.columbia.edu. Last visited April 2007.

MASON, S.J. & JOUBERT, A.M., 1997. Simulated changes in extreme rainfall over southern Africa. *Int. J. Climatol.* 17, 291-301.

References

MASON, S.J., JOUBERT, A.M., COSIJN, C. & CRIMP, S.J., 1996. Review of seasonal forecasting techniques and their applicability to southern Africa. *Water SA*. 22, 203-209.

MASON, S.J. & JURY, M., 1997. Climate variability and change over southern Africa: A reflection on underlying processes. *Prog. Phys. Geogr.* 21, 23-50.

MASON, S.J. & LINDESAY, J.A., 1993. A note on the modulation of Southern Oscillation–Southern African rainfall associations with the Quasi-Biennial Oscillation. *J. Geophys. Res.*, 98, 8847-8850.

MASON, S.J., LINDESAY, J.A. & TYSON, P.D., 1994. Simulating drought in southern Africa using sea-surface temperature variations. *Water SA*. 20, 15-22.

MO, K.C. & PAEGLE, J.A., 2001. The Pacific–South American modes and their downstream effects. *Int. J. Climatol.* 21, 1211-1229.

MOELETSI, M.E., 2004. *Agroclimatic Characterization of Lesotho for Dryland Maize Production.* M.Sc. thesis, Agrometeorology, University of Free State, Bloemfontein, South Africa, pp.175.

MOURA, A.D., BENGTSSON, L., BUIZER, J., BUSALACCHI, A., CANE, M.A., LAGOS, P., LEETMAA, A., MATSUMO, T., MOONEY, K., MOREL, P., SARACHIK, E.S., SHUKLA, J., SUMI, A. & PATTERSON, M., 1992. International Research Institute for Climate Prediction: A proposal. 1100 Wayne Avenue, Suite 1255, Silver Spring, MD 20910, USA, pp. 51.

MULENGA, H.M., ROUAULT, M. & REASON, C.J.C., 2003. Dry summers over NE South Africa and associated circulation anomalies. *Climate Res.* 25, 29-49.

NICHOLSON, S.E. & ENTEKHABI, D., 1986. The quasi-periodic behavior of rainfall variability in Africa and its relationship to the southern oscillation. *Geo. Phys. and Bio-Climat.* A34, 311-348.

NICHOLSON, S.E. & ENTEKHABI, D., 1987. Rainfall variability in equatorial and southern Africa: relationships with sea-surface temperatures along the southwestern coast of Africa. *J. Clim. Appl. Meteorol.* 26, 561-578.

NICHOLSON, S.E. & KIM. J., 1997. The relationship of the El Niño Southern Oscillation to African rainfall. *Int. J. Climatol.* 17, 117-135.

PARKER, D.E., FOLLAND, C.K. & WARD, M.N., 1988. Sea-surface temperature anomaly patterns and prediction of seasonal rainfall in the Sahel region of Africa. In

References

Recent Climate Change: A Regional Approach, (ed. Gregory, S.) Belhaven Press, London, pp. 166-178.

PATHACK, B.M.R., JURY, M.R., SHILLINGTON, F.A. & COURTNEY, S., 1993. South African Summer Rainfall Variability and its Association with Marine Environment. Water Research Commission Report 278/1/94.

PHILANDER, S.G., 1990. *El Niño, La Nina and the Southern Oscillation.* Academic Press. London, pp. 293.

PRESTON-WHITE, R.A. & TYSON, P.D., 1988. *The Atmosphere and Weather of Southern Africa.* Oxford University Press. Cape Town, pp. 326.

RAUTENBACH, C.J. DE W. & MPHEPY, J., 2005. Observed rainfall trends over South Africa: 1960–2001. Eskom Research Report RES/RR/04/25332, Johannesburg.

RAUTENBACH, C.J. DE W. & SMITH, I.N., 2001. Teleconnections between global sea-surface temperatures and the variability of observed and model simulated rainfall over southern Africa. *J. Hydrol.* 254, 1-15.

REASON, C. J.C., ALLAN, R.J., LINDESAY, J.A. & ANSELL, T. J., 2000. ENSO and climatic signals across the Indian Ocean basin in the global context: Part I, Interannual composite patterns. *Int. J. Climatol.* 20, 1285-1327.

REASON, C.J.C., ENGELBRECHT, F., LANDMAN, W.A., LUTJEHARMS, J.R.E., PIKETH, S., RAUTENBACH, C.J. DE W. & HEWITSON, B.C., 2006b. A review of South African research in atmospheric science and physical Oceanography during 2000-2005. *S. Afr. J. Sci.* 102, 1-11.

REASON, C.J.C., HACHIGONTA, S. & PHALADI, R.F., 2005. Interannual variability in rainy season characteristics over the Limpopo region of southern Africa. *Int. J. Climatol.* 25, 1835-1853.

REASON, C.J.C. & JAGADEESHA, D., 2005. A model investigation of recent ENSO impacts over southern Africa. *Met. Atmos. Phys.* 89, 181-205.

REASON, C.J.C., JAGADEESHA, D. & TADROSS, M., 2003. A model investigation of interannual winter rainfall variability over south-western South Africa and associated Ocean-atmosphere interaction. *S. Afr. J. Sci.* 99, 75-80.

REASON, C.J.C., LANDMAN, W. & TENNANT, W., 2006a. Seasonal to decadal prediction of South African climate and its links with variability of the Atlantic Ocean. *Bull. Amer. Meteo. Soc.* 87, 941-955.

References

REASON, C.J.C. & MULENGA, H.M., 1999. Relationship between South African rainfall and SST anomalies in the south western Indian Ocean. *Int. J. Climatol.* 19, 1651-1673.

REASON, C.J.C. & ROUAULT, M., 2002. ENSO-like decadal patterns and South African rainfall. *Geophys. Res. Lett.,* 29, 1638, doi:10.1029/2002GL014663.

REITSMA, R., ZIGURS, I., LEWIS, C., SLOANE, A. & WILSON, V., 1996. Experimentation with simulation model in water-resources negotiations. *J. Water Resour. Planning and Manage.* 122, 64-70.

ROCHA, A. & SIMMONDS, I., 1997. Interannual variability of south-eastern African summer rainfall. Part I: relationships with air-sea interaction processes. *Int. J. Climatol.* 7, 235-266.

ROPELEWISKI, C.F. & HALPERT, M.S., 1987. Global and region scale precipitation patterns associated with the El Niño/Southern Oscillation. *Mon. Wea. Rev.* 115, 1606-1626.

ROUAULT, M., FLORENCHIE, P., FAUCHEREAU, N. & REASON, C.J.C., 2003. South east Atlantic warm events and southern African rainfall. *Geophys. Res. Lett.* 30, 1-4.

RSA (REPUBLIC OF SOUTH AFRICA), 1997. Water Policy White Paper. Government Gazette, April 1997, Cape Town, South Africa.

RSA (REPUBLIC OF SOUTH AFRICA), 1998. National Water Act. Government Gazette, vol. 398. 26 August 1998, no 19182. Cape Town, South Africa.

SCHALEKAMP, M., 1994. The problems associated with reversing water pollution trends in large river systems. SA Inst. of Civ. Eng. Special Symp. *50 Years of Water Engineering in South Africa.*

SCHULZE, B.R., 1994. Climate of South Africa. General Survey. Weather Bureau, Department of Environmental Affairs. WBR 28, Pretoria, South Africa, pp. 330.

SCHULZE, R.E., 1983. Agrohydrology and Climatology of Natal. Water Research Commission, Pretoria, pp. 138.

SCHULZE, R.E., MAHARAJ, M., LYNCH, S.D., HOWE, B.J. & MELVIL-THOMSON, B., 1997. South African Atlas of Agrohydrology and Climatology. Water Research Commission, Pretoria, Report TT82/96, pp. 276.

SINGH, D., BHADRAM, C.V.V. & MANDAL, G.S., 1995. New regression model for Indian Monsoon rainfall. *Meteorol. Atmos. Phys.*, 55, 77-86.

References

SMITH, T.M. & REYNOLDS, R.W., 2004. Improved Extended Reconstruction of SST. *J. Climate* Last visited April 2007, http://iridl.ldeo.columbia.edu/SOURCES/.NOAA/.NCDC/.ERSST/.version2/.SST

STANSKI, H.R., WILSON, L.J. & BURROWS, W.R., 1989. *Survey of Common Verification Methods in Meteorology.* 2nd Ed. Ontario, Canada, pp. 21-35.

STATS SA, 2003. Statistic South Africa. http://www.info.gov.za/aboutsa/landpeople.htm Mid-year Estimates, statistics release P0302. Last visited September 2006.

TADROSS, M.A., JACK, C. & HEWITSON, B.C., 2005. On RCM-based projections of change in southern African summer climate. *Geophys. Res. Lett.,* 32, L23713, doi: 10.1029/2005GL024460.

TALJAARD, J.J., 1970. Die waterinhound van die atmosfeer oor suidelike Afrika (The water content of yhr atmosphere over southern Africa) Water Year, 1970. Convention Water for the Future. RSA.

TALJAARD, J.J., 1981. Upper-air circulation, temperature and humidity over Southern Africa. S.A. Weather Bureau, Department of Environmental Affairs, Pretoria. Technical Paper no. 10, pp. 37-42.

TALJAARD, J.J., 1996. Atmospheric circulation systems, synoptic climatology and weather phenomena of South Africa. S.A. Weather Bureau, Department of Environmental Affairs, Pretoria. Technical Paper no. 32, pp. 98.

TALJAARD, J.J. & STEYN, P.C.L., 1991. Relationships between atmospheric circulation and rainfall in the South African region. S.A. Weather Bureau, Department of Environmental Affairs, Pretoria. Technical Paper no. 24, pp. 62.

TENNANT, W.J., 2003. An assessment on intra-seasonal variability from 13-yr GCM simulations. *Mon. Wea. Rev.* 131, 1975-1991.

TENNANT, W.J. & REASON, C.J.C., 2005. Associations between the global energy cycle and regional rainfall in South Africa and Southwest Australia. *J. Climate* 18, 3032-3047.

TURTON, A.R. & LICHTENTALER, S., 1999. Water demand management, natural resource reconstruction and traditional value system: A case study from Yemen School of Oriental and African Studies, University of London. Occasional Paper no. 4, pp. 1-14.

References

TYSON, P.D., 1986. *Climatic Change and Variability in Southern Africa.* Oxford University Press, Cape Town, pp. 220.

TYSON, P.D., DYER, T.G.J. & MAMETSE, M.N., 1975. Secular changes in South African rainfall: 1880–1972. *Q. J. Roy. Met. Soc.* 101, 817-833.

VENEGAS, S.A., MYSAK, L.A. & STRAUB, D.N., 1997. Atmosphere-Ocean coupled variability in South Atlantic. *J. Climate* 10, 2904-2920.

VILJOEN, M.F. & BOOYSEN, H.J., 2006. Planning and management of flood damage control: The South African experience. *Irrig. Drain.* 55, S83-S91.

WALKER, N.D., 1990. Links between South African summer rainfall and temperature variability of the Agulhas and Benguela currents systems. *J. Geophys. Res.* 95, 3297-3319.

WALKER, N.D. & LINDESAY, J.A., 1989. Preliminary observations of Oceanic influences on the February–March 1988 floods in central South Africa. *S. Afr. J. Sci.* 85, 164-169.

WILBY, R.L. & WIGLEY, T.M.L., 1997. Downscaling general circulation model output: A review of methods and limitations. *Prog. Phys. Geogr.* 21, 530-548.

WILKS, D.S., 2006. *Statistical Methods in the Atmospheric Sciences*, 2nd Ed. Academic Press, Elsvier, pp. 562.

WMO., 1966. World Meteorological Organization. International list of selected, supplementary and auxiliary ships. 10th ed. WMO 47 (WMO/OMM 47, TP. 18).

ZHANG, Y., WALLACE, J.M. & BATTISTI, D.S., 1997. ENSO-like interdecadal variability. *J. Climate* 10, 1004-1020.

ZHAOBO, S., 1994. Empirical statistical techniques in seasonal forecasting. *WMO. Bull.* 43, 216-220.

Appendices

Appendix 1: Soil Description of the Upper Olifants Catchment (Hahne and Fitzpatrick, 1985)

1.1 Top soil layer description in the upper Olifants catchment

Lat (S)	Long (E)	Land Type	Soil form	Soil Series	Top soil layer								Area Km2
					Depth (mm)	OM (%)	Sand (%)	Silt (%)	Clay (%)	CEC	PH	
-25.78	29.60	Bb14	Hutton	Msinga	0-250	0.8	65	6	22	48	4.9	230
-25.62	29.65	Ba14	Hutton	Vimy	0-300	2.0	34	8	49	117	4.9	600
-26.02	28.88	Ba5	Hutton	Msinga	0-350	0.6	66	8	29	60	5.1	560
-26.17	29.10	Bb4	Glencoe	Glencoe	0-410	0.2	86	2	12	28	4.4	90
-26.22	29.30	Bb4	Glencoe	Klipstapel	0-450	0.5	89	2	8	30	4.6	1950
-26.22	29.30	Bb4	Avalon	Avalon	0-430	0.6	76	5	18	5	5.3	160
-26.35	29.30	Bb4	Swartland	Rosehill	0-280	1.0	67	6	27	179	6	90
-26.67	28.98	Bb3	Avalon	Bezuidenhout	0-320	0.9	73	6	18	67	5.5	90

1.2 Soil layer number three description in the upper Olifants catchment

Lat (S)	Long (E)	Land Type	Soil form	Soil Series	Third soil Layer						
					Depth (mm)	OM %	Sand %	Silt %	Clay %	CEC	PH
-25.78	29.60	Bb14	Hutton	Msinga	250-500	0.7	64	6	24	38	4.7
-25.62	29.65	Ba14	Hutton	Vimy	300-1200	0.8	27	7	66	89	5.1
-26.02	28.88	Ba5	Hutton	Msinga	760-1100+	0.3	51	11	37	51	4.8
-26.17	29.10	Bb4	Glencoe	Glencoe	730-1150	0.2	76	5	21	28	5.4
-26.22	29.30	Bb4	Glencoe	Klipstapel	450-900	0.2	86	2	13	17	4.4
-26.22	29.30	Bb4	Avalon	Avalon	940-1200+	0.3	61	8	32	60	5.5
-26.35	29.30	Bb4	Swartland	Rosehill	610-950+	0.2	62	10	32	236	7.1
-26.67	28.98	Bb3	Avalon	Bezuidenhout	850-1200+	0.2	44	6	51	159	5.2

Appendix 2: Selected Stream Flow Stations in the Upper Olifants Catchment Area From 1990 to 2005 for the OND and JFM Seasons

Source Website: http://www.dwaf.gov.za/hydrology.

2.1 OND stream flow data in the upper Olifants catchment (m^3 sec^{-1})

Stn	Stn_B1H012	Stn_B1H017	Stn_B1H020	Stn_B1H021	Stn_B2H007	Stn_B2H006	Stn_B2H014	Stn_B2H004
LAT (S)	26.47	25.80	26.18	26.23	25.87	25.77	25.80	25.95
LONG (E)	29.587	29.274	29.332	29.27	28.663	28.551	28.881	28.586
1990	20.185	1.216	1.027	19.690	0.787	0.118	12.960	0.753
1991	11.270	0.540	0.095	0.990	2.133	0.426	8.118	0.165
1992	0.881	5.228	0.171	6.751	1.386	0.258	0.879	0.325
1993	2.054	13.370	1.205	26.060	1.343	0.286	15.010	0.387
1994	11.490	0.445	0.062	1.379	0.365	0.172	1.125	0.588
1995	0.440	17.825	1.045	69.31	11.100	1.536	42.52	0.077
1996	25.344	14.844	1.316	33.581	4.115	0.781	12.890	2.125
1997	25.760	38.670	2.831	63.39	6.520	1.288	22.740	0.750
1998	41.950	7.696	1.988	17.172	8.479	1.620	18.507	1.509
1999	16.688	2.276	1.294	4.891	8.397	0.199	1.897	1.379
2000	12.554	10.487	1.684	26.58	4.508	1.342	37.150	0.203
2001	25.200	1.331	0.942	2.585	1.629	0.555	5.543	2.097
2002	4.398	5.172	0.007	5.832	0.253	0.273	0.341	0.816
2003	0.339	2.202	-999	3.866	0.218	0.150	0.199	0.171
2004	-999	0.931	-999	3.666	3.595	0.401	1.769	0.054
2005	7.616	0.922	-999	2.321	4.062	0.252	0.246	0.631

2.2 JFM stream flow data in the upper Olifants catchment (m^3 sec^{-1})

Stn	Stn_B1H012	Stn_B1H017	Stn_B1H020	Stn_B1H021	Stn_B2H007	Stn_B2H006	Stn_B2H014	Stn_B2H004
LAT (S)	26.47	25.80	26.18	26.23	25.87	25.77	25.80	25.95
LONG (E)	29.587	29.274	29.332	29.27	28.663	28.551	28.881	28.586
1990	52.700	27.96	1.788	46.410	2.606	2.936	34.270	0.502
1991	28.870	0.024	0.143	0.758	0.131	0.156	3.759	4.34
1992	1.179	2.626	0.971	5.340	0.541	0.210	3.759	0.121
1993	6.005	9.487	1.552	17.900	3.790	0.495	12.1300	0.346
1994	9.260	2.313	0.373	5.663	0.263	0.183	2.487	0.600
1995	2.464	49.600	3.916	160.100	36.840	6.769	85.400	0.046
1996	114.000	17.583	2.624	44.770	10.063	2.147	33.188	7.749
1997	13.200	31.417	1.879	49.440	2.683	1.038	11.360	4.012
1998	16.500	2.240	0.718	17.439	1.056	0.389	11.643	1.234
1999	17.482	41.890	4.210	79.700	36.570	5.076	75.300	0.299
2000	134.300	2.095	0.197	3.188	1.262	0.786	3.720	7.680
2001	2.035	1.179	0.037	3.105	0.987	0.408	4.285	0.869
2002	2.281	9.164	0.502	11.138	0.851	0.465	2.060	0.388
2003	2.1580	15.02	-999	24.85	4.436	1.892	9.925	0.376
2004	16.330	6.061	-999	11.270	1.754	1.776	8.900	2.822
2005	33.860	-999	-999	101.200	10.31	2.167	33.75	2.968

Appendix 3: Selected Rainfall Stations in the Upper Olifants Catchment from 1950 to 2002 during the OND and JFM Season

3.1 OND rainfall in the upper Olifants catchment (mm)

Stn	G101	G102	G103	G104	G105	G106	G107	G108	G109	G110	G111	G112	G113	G114	G115
LAT (S)	26.47	25.80	26.18	26.23	25.87	25.77	25.80	25.95	25.67	25.73	26.15	26.4	26.1	26.5	26.05
LONG (E)	29.45	28.73	28.55	28.78	29.23	29.47	28.85	28.80	29.62	29.82	29.72	29.77	29.32	29.18	29.07
1950	75	64	202	219	104	74	105	111	73	80	70	122	109	132	96
1951	200	151	132	145	136	100	131	142	96	130	77	196	142	119	103
1952	95	97	96	105	263	230	76	81	222	193	89	102	275	86	181
1953	123	220	204	221	332	288	156	167	278	311	205	145	348	148	275
1954	163	187	123	133	178	192	172	183	188	227	254	172	187	213	211
1955	79	111	74	79	82	138	130	137	137	136	133	90	87	99	91
1956	133	123	146	158	133	207	152	160	206	262	187	142	139	165	156
1957	107	139	202	219	153	145	136	143	143	110	116	124	160	234	235
1958	104	171	83	90	98	88	120	127	87	91	59	108	102	130	137
1959	123	131	117	124	130	138	105	110	136	166	176	165	135	89	92
1960	81	29	43	46	65	123	42	43	122	237	106	120	70	44	208
1961	83	84	75	82	108	182	71	75	178	141	62	58	113	126	123
1962	38	89	42	47	13	44	76	80	43	132	29	28	14	29	66
1963	91	174	107	118	82	101	168	177	99	182	43	137	84	128	125
1964	90	69	73	80	86	115	47	49	113	109	109	130	89	101	92
1965	107	101	151	164	115	130	84	88	127	230	184	133	122	191	152
1966	221	100	102	107	120	101	107	114	100	112	152	180	128	56	85
1967	68	109	65	71	104	71	89	94	70	119	69	98	109	94	65
1968	203	136	108	116	110	201	155	165	197	195	104	76	114	169	127
1969	32	30	105	114	81	70	92	98	68	100	55	90	84	85	101
1970	95	111	120	128	58	104	125	134	101	58	0	106	62	85	102
1971	32	21	65	70	42	52	76	79	50	98	26	64	45	57	88

Stn	G101	G102	G103	G104	G105	G106	G107	G108	G109	G110	G111	G112	G113	G114	G115
LAT (S)	26.47	25.80	26.18	26.23	25.87	25.77	25.80	25.95	25.67	25.73	26.15	26.4	26.1	26.5	26.05
LONG (E)	29.45	28.73	28.55	28.78	29.23	29.47	28.85	28.80	29.62	29.82	29.72	29.77	29.32	29.18	29.07
1972	56	229	116	126	133	92	162	174	90	95	135	75	137	90	167
1973	141	115	131	144	90	57	80	86	57	110	129	133	94	131	126
1974	137	126	89	98	103	200	104	109	197	152	161	143	106	80	116
1975	167	107	89	98	172	78	81	85	77	102	128	113	180	167	40
1976	51	63	87	94	44	127	64	68	123	129	30	52	47	103	14
1977	47	16	60	65	26	48	34	35	48	84	24	66	28	58	35
1978	96	40	67	73	72	51	50	52	51	117	27	53	80	60	62
1979	83	107	66	70	53	113	67	68	111	160	175	67	54	129	107
1980	118	83	96	104	61	111	58	61	109	109	84	95	64	108	82
1981	94	106	103	112	53	39	88	92	39	94	74	36	55	124	86
1982	61	91	105	114	107	95	102	107	94	176	71	95	110	85	113
1983	147	34	92	99	70	39	62	65	38	96	123	79	73	93	79
1984	142	153	82	87	132	211	108	113	207	88	144	133	136	118	101
1985	145	228	106	113	103	120	142	151	116	149	44	170	109	123	207
1986	125	85	84	90	69	113	142	151	110	195	141	56	73	79	86
1987	112	66	55	60	92	96	112	118	94	187	105	119	96	124	94
1988	79	129	120	130	77	129	174	182	126	108	97	128	81	108	127
1989	97	55	101	109	142	199	144	153	195	92	103	78	148	170	165
1990	150	102	100	109	109	132	153	161	129	138	40	122	113	106	104
1991	105	117	71	75	106	179	143	153	173	167	257	177	109	117	156
1992	183	49	73	78	69	121	122	127	118	148	106	115	70	105	98
1993	35	91	92	101	111	94	90	96	93	108	104	96	117	50	70
1994	195	167	99	108	95	193	231	243	188	113	186	200	99	87	232
1995	132	60	82	88	107	95	45	48	95	50	113	90	110	97	105
1996	56	39	47	51	106	107	49	53	106	70	83	128	113	94	85

Appendices

Stn	G101	G102	G103	G104	G105	G106	G107	G108	G109	G110	G111	G112	G113	G114	G115
LAT (S)	26.47	25.80	26.18	26.23	25.87	25.77	25.80	25.95	25.67	25.73	26.15	26.4	26.1	26.5	26.05
LONG (E)	29.45	28.73	28.55	28.78	29.23	29.47	28.85	28.80	29.62	29.82	29.72	29.77	29.32	29.18	29.07
1997	85	139	156	170	114	145	121	129	143	141	142	183	120	118	156
1998	125	192	0	0	133	0	121	130	0	-999	244	120	141	104	69
1999	126	84	83	41	258	8	11	22	89	-999	91	161	141	102	193
2000	137	116	108	89	355	30	112	144	90	-999	116	181	194	144	211
2001	80	117	64	112	82	208	93	64	172	-999	166	107	46	104	107
2002	155	95	53	118	190	97	154	127	104	-999	152	159	118	154	143

3.2 JFM rainfall in the upper Olifants catchment (mm)

Stn	G101	G102	G103	G104	G105	G106	G107	G108	G109	G110	G111	G112	G113	G114	G115
LAT (S)	26.47	25.80	26.18	26.23	25.87	25.77	25.80	25.95	25.67	25.73	26.15	26.4	26.1	26.5	26.05
LONG (E)	29.45	28.73	28.55	28.78	29.23	29.47	28.85	28.80	29.62	29.82	29.72	29.77	29.32	29.18	29.07
1950	171	284	394	392	206	308	233	236	316	278	202	254	205	255	223
1951	168	318	288	293	253	199	252	254	203	224	172	218	248	210	239
1952	241	321	286	280	249	227	275	278	236	235	384	218	246	257	258
1953	306	420	315	319	279	551	350	352	559	332	307	357	275	360	357
1954	568	435	576	570	512	499	461	468	510	504	408	276	508	610	381
1955	201	265	232	225	216	262	347	349	265	349	266	197	212	175	181
1956	130	220	397	395	334	459	288	291	475	294	307	208	329	218	260
1957	232	426	284	284	301	235	360	367	236	276	236	307	297	218	237
1958	207	289	258	254	365	356	257	260	364	296	267	232	360	231	299
1959	200	211	145	141	244	201	155	157	206	261	230	202	240	262	172
1960	272	161	475	469	191	256	213	212	266	215	255	251	189	254	307
1961	262	341	275	274	225	244	332	332	247	217	258	396	220	275	278
1962	245	193	222	222	205	299	211	213	299	176	91	131	203	149	248
1963	434	290	245	242	306	317	273	280	323	289	317	396	306	316	270
1964	218	125	270	267	261	133	159	162	132	259	228	170	258	289	189
1965	220	218	223	218	128	155	135	136	156	148	67	213	126	201	138
1966	447	431	403	396	304	244	433	439	253	268	229	275	303	361	357
1967	325	315	236	237	206	204	246	250	210	322	180	188	205	250	221
1968	210	216	235	238	315	386	294	297	388	339	261	285	314	432	261
1969	464	394	310	311	324	368	309	310	374	238	249	327	318	326	411
1970	237	241	302	296	245	239	280	286	242	231	152	239	244	276	284
1971	225	226	449	451	269	342	283	291	347	420	172	221	267	225	309
1972	289	239	220	223	231	276	317	324	278	390	265	269	227	342	367

Stn	G101	G102	G103	G104	G105	G106	G107	G108	G109	G110	G111	G112	G113	G114	G115
LAT (S)	26.47	25.80	26.18	26.23	25.87	25.77	25.80	25.95	25.67	25.73	26.15	26.4	26.1	26.5	26.05
LONG (E)	29.45	28.73	28.55	28.78	29.23	29.47	28.85	28.80	29.62	29.82	29.72	29.77	29.32	29.18	29.07
1973	205	164	255	252	309	339	276	282	348	319	266	247	306	266	166
1974	313	433	558	547	515	479	526	543	489	406	366	296	509	462	353
1975	179	339	311	308	234	238	336	338	243	351	259	178	232	259	237
1976	371	281	244	246	212	193	242	244	192	257	128	295	211	322	155
1977	308	608	437	433	343	481	544	559	490	311	261	305	339	339	417
1978	137	281	199	197	146	173	199	202	176	139	103	112	144	109	129
1979	341	413	369	363	364	374	449	457	383	452	290	377	360	409	370
1980	240	256	267	262	359	244	322	328	248	258	152	304	355	287	330
1981	231	359	265	267	195	273	285	287	277	330	214	199	192	238	213
1982	214	230	195	192	223	275	243	248	276	251	253	129	222	164	278
1983	199	204	186	182	211	239	200	202	240	348	212	294	209	168	222
1984	307	376	295	292	257	366	337	337	371	320	341	407	254	260	357
1985	260	228	215	211	201	234	273	277	241	354	210	303	199	283	249
1986	316	143	187	183	213	149	178	182	152	352	332	287	211	242	253
1987	285	469	305	322	319	388	505	517	383	432	379	281	320	401	420
1988	255	644	277	271	277	246	382	381	254	276	201	266	277	220	262
1989	283	201	174	169	248	115	240	241	118	230	228	154	245	161	169
1990	367	454	373	376	301	285	479	480	293	482	301	373	298	416	325
1991	311	585	348	348	427	185	447	450	188	354	278	346	422	248	438
1992	240	233	219	215	292	276	288	291	286	163	260	249	291	130	264
1993	175	438	374	371	340	428	462	468	438	338	349	357	337	231	277
1994	124	252	265	261	228	185	178	186	185	238	287	215	225	198	116
1995	508	701	743	728	384	402	989	1000	414	410	429	501	380	385	512
1996	309	179	164	163	153	254	204	208	258	144	246	247	150	114	144
1997	342	382	474	487	360	291	386	391	292	260	356	275	354	378	310

Appendices

Stn	G101	G102	G103	G104	G105	G106	G107	G108	G109	G110	G111	G112	G113	G114	G115
LAT (S)	26.47	25.80	26.18	26.23	25.87	25.77	25.80	25.95	25.67	25.73	26.15	26.4	26.1	26.5	26.05
LONG (E)	29.45	28.73	28.55	28.78	29.23	29.47	28.85	28.80	29.62	29.82	29.72	29.77	29.32	29.18	29.07
1998	125	238	288	284	135	272	138	140	276	86	143	137	133	205	128
1999	376	377	563	571	472	0	428	628	402	406	416	361	417	394	433
2000	381	262	520	331	284	8	221	466	297	127	227	153	232	258	277
2001	226	137	272	324	251	224	111	204	265	-999	264	190	196	293	203
2002	290	217	277	294	364	290	215	169	174	-999	201	193	352	481	138

Appendix 4: Data Patching Methods Used for Rainfall Data in the Upper Olifants Catchment

Inverse Distance

The inverse distance method is used to estimate missing data because of its simplicity (Moeletsi, 2004).

$$y_t = \frac{\sum_{i=1}^{m} x_t^i / D_i^b}{\sum_{i=1}^{m} 1 / D_i^b}$$

Where y_t is the estimated value of the missing data, x_t^i is the value of the ith nearest weather station, and D_i is the distance between the station of missing dataset and the ith nearest weather station.

The closest station method

This is a simple method. Firstly, the closest station is identified, and then the data at a specific site would be replaced with data from the closest station for that specific day. The observations from this station are adjusted by the ratio of the long-term means between the two stations (Moeletsi, 2004).

All the stations were patched mostly with the inverse distance method with the power 2. Two to four nearest stations were used in an estimating equation. In the case where there were no more than two stations having concurrent data, the closest station method modified by the long-term means were used. The data patched were from 1990 to April 2004 for almost all the stations.

4.1 Station list

Station	Lat (S)	Long (E)	Altitude (m)
Bethal	-26.47	29.45	1640
Bronkhospruit Rotsvas	-25.78	28.77	1458
Sundra POL	-26.18	28.55	1680
Vlakplaas	-26.23	28.78	1615
Witbank - MUN	-25.87	29.23	1600
Middleburg	-25.77	29.47	1447
Wilgerivier	-25.80	28.85	1432
Blesbokfontein	-25.95	28.80	1495
Bankfontein	-25.67	29.62	1525
Roodepoort	-25.73	29.82	1737
Hendrina MUN	-26.15	29.72	1615
Tweefontein	-26.40	29.77	1756
Vandyksdrift	-26.10	29.32	1521
Secunda	-26.50	29.18	1628
Ogies POL	-26.05	29.07	1585

4.2 Neighbouring stations used for patching rainfall

3.2.1 Bethal

Station	Lat (S)	Long (E)	Altitude (m)	Dis. from target station (km)
Davel	-26.45	29.67	1700	21.7
Badplaas	-26.45	29.48	1648	23.8
Maizefield	-26.65	29.55	1650	22.7
Blinkpan	-26.10	29.45	1645	40.8
Charlcelliers	-26.65	29.18	1646	33.5
Kriel	-26.27	29.23	1555	31.0
Langsloot	-26.37	29.17	1555	30.4
Secunda	-26.50	29.18	1628	26.9
Nooitgedatch	-26.52	29.97	1694	50.8
Kinkroos	-26.42	29.10	1650	35.3
Ermelo	-26.52	29.95	1698	50.1

4.2.2 Bronkhospruit Rotsvas

Station	Lat (S)	Long (E)	Altitude (m)	Dis. from target station (km)
Bronkhospruit	-25.80	28.73	1460	3.8
Bronkhospruit MUN	-25.80	28.73	1427	3.8
Klippkopies	-25.90	28.50	1540	29.7
Kleinwater	-25.81	29.05	1463	28.6
Kleinzonderhoot	-25.86	28.56	1484	22.1
Donkerhoek	-25.78	28.46	1393	30.1
Wilgerivier	-25.80	28.85	1432	8.6
Englefield	-25.63	28.53	1375	28.8
Blesbokfontein	-25.95	28.80	1495	18.9

4.2.3 Sundra POL

Station	Lat (S)	Long (E)	Altitude (m)	Dis. from target station (km)
Delmas	-26.15	28.68	1571	13.8
Delmas Witklip	-26.15	28.68	1571	13.8
Delmas Pannar	-26.13	28.71	1571	17.6
Eloff	-26.18	28.50	1633	5.0
Endicott	-26.30	28.58	1620	13.4
Geduld	-26.20	28.43	1645	11.8
Petit	-26.16	28.67	1565	11.8
Springs	-26.20	28.45	1588	10.2
Springs Olympia	-26.26	28.43	1628	14.9

4.2.4 Vlakplaas

Station	Lat (S)	Long (E)	Altitude (m)	Dis. from target station (km)
Devon	-26.35	28.78	1600	13.0
Devon POL	-26.35	28.78	1670	13.0
Dryden	-26.11	28.75	1590	15.4
Hawerklys	-26.26	28.81	1600	5.0
Strehla	-26.20	28.93	1585	15.4
Delmas Pannar	-26.13	28.72	1571	13.0

4.2.5 Witbank MUN

Station	Lat (S)	Long (E)	Altitude (m)	Dis. from target station (km)
Witbank	-25.83	29.18	1549	6.2
Goedehoop colliery	-26.10	29.41	1570	31.8
Kleinkopje colliery	-26.01	29.23	1524	16.7
Kleinwater	-25.81	29.05	1463	19.2
Landau	-25.93	29.21	1555	7.6
Middleburg-TNK	-25.76	29.46	1447	25.9
Ogies - POL	-26.05	29.06	1585	26.4
Bronkhospruit Rotsvas	-25.78	28.76	1458	47.7

4.2.6 Middleburg TNK

Station	Lat (S)	Long (E)	Altitude (m)	Dis. from target station (km)
Witbank MUN	-25.86	29.23	1600	25.9
Bankfontein	-25.66	29.61	1525	18.7
Pan	-25.76	29.66	1660	20.1
Witbank	-25.84	29.18	1549	29.3
Ede farms	-25.86	29.68	1606	20.4
Middleburg	-25.78	29.46	1542	1.8
Blinkpan	-26.10	29.45	1645	37.1

4.2.7 Wilgerivier

Station	Lat (S)	Long (E)	Altitude (m)	Dis. from target station (km)
Bronkhorspruit Rotvas	-25.78	28.77	1458	8.6
Bronkhorspruit-MUN	-25.80	28.73	1427	11.7
Bronkhorspruit	-25.80	28.73	1460	11.7
Blesbokfontein	-25.95	28.80	1495	17.4
Kleinwater	-25.82	29.05	1463	20.1

4.2.8 Blesbokfontein

Station	Lat (S)	Long (E)	Altitude (m)	Dis. from target station (km)
Bronkhorspruit Rotvas	-25.78	28.76	1458	18.9
Dryden	-26.11	28.75	1590	19.2
Delmas	-26.15	28.68	1571	25.1
Kendal	-26.06	28.95	1600	19.8
Ogies - POL	-26.05	29.06	1585	28.9

4.2.9 Bankfontein

Station	Lat (S)	Long (E)	Altitude (m)	Dis. from target station (km)
Middleburg - TNK	-25.76	29.47	1447	18.7
Middleburg	-25.78	29.46	1542	19.9
Pan	-25.76	29.67	1660	12.2
Ede farms	-25.86	29.64	1606	21.9
Arnot	-25.78	29.78	1700	21.2
Bospoort	-25.68	29.90	1675	28.5
Rooderpoort	-25.73	29.81	1737	21.4

4.2.10 Rooderpoort

Station	Lat (S)	Long (E)	Altitude (m)	Dis. from target station (km)
Bankfontein	-25.66	29.61	1525	21.4
Ede	-25.85	29.66	1585	23.9
Pan	-25.76	29.66	1660	15.5
Ede farms	-25.86	29.64	1606	22.8
Arnot	-25.78	29.78	1700	6.5
Bospoort	-25.68	29.90	1675	10.0
Wonderfontein	-25.80	29.90	1798	11.2

4.2.11 Hendrina

Station	Lat (S)	Long (E)	Altitude (m)	Dis. from target station (km)
Carolina	-26.06	30.13	1690	42.7
Carolina_mun	-26.06	30.11	1689	41.0
Carolina	-26.06	30.11	1696	41.0
Driefontein	-26.10	29.55	1650	17.6
Ede	-25.85	29.61	1585	34.9
Ede farms	-25.86	29.64	1606	32.9
Morgerster	-26.20	29.81	1737	11.4
Wilderbeesfontein	-26.16	29.51	1635	20.1

4.2.12 Tweefontein

Station	Lat (S)	Long (E)	Altitude (m)	Dis. from target station (km)
Estacia	-26.4	29.86	1829	10.0
Davel	-26.45	29.66	1700	11.4
Douglas dam	-26.46	29.93	1675	18.2
Nooitgedacht	-26.51	29.96	1694	23.8
Bethal	-26.46	29.45	1640	32.4
Ermelo	-26.51	29.95	1698	22.4

3.2.13 Vandyksdrift

Station	Lat (S)	Long (E)	Altitude (m)	Dis. from target station (km)
Goedehoop	-26.10	29.42	1570	10.0
Klienkopje	-26.02	29.23	1524	12.5
Kriel	-26.27	29.23	1555	20.3
Blinkpan	-26.10	29.45	1645	13.3

4.2.14 Secunda

Station	Lat (S)	Long (E)	Altitude (m)	Dis. from target station (km)
Trichardt	-26.50	29.22	1650	3.3
Kinkross	-26.42	29.10	1650	12.4
Bethal	-26.47	29.45	1640	26.8
Kriel	-26.27	29.23	1555	26.4

4.2.15 Ogies POL

Station	Lat (S)	Long (E)	Altitude (m)	Dis. from target station (km)
Ogies	-26.05	29.07	1550	<1.0
Kendal	-26.07	28.95	1600	11.8
Kleinkopje	-26.02	29.23	1524	17.1
Witbank	-25.83	29.18	1549	26.8
Witbank MUN	-25.87	29.23	1600	26.4
Vandyksdrift	-26.10	29.32	1521	25.6
Cologne	-26.13	29.02	1585	10.5

Appendix 5:   Model Skill at Different Lead-Times during OND Season

5.1 Cross-validated correlations between the OND sum of monthly stream flow and Global SSTs for 1990-1997 during the ten lead times at eight stream flow stations in the Groot Olifants and Wilger sub-catchments

Pearson's correlation (OND)							
Lead (months)	Groot Olifants Sub-catchment				Wilger Sub-catchment			
	B1H012	B1H017	B1H020	B1H021	B2H007	B2H006	B2H014	B2H004
0	-0.0152	-0.0105	0.2460	0.0403	0.4126	0.5719	0.2969	0.3471
1	0.0740	-0.4106	0.0470	0.2325	0.1651	0.1691	-0.3193	-0.0511
2	0.6460	0.7549	0.8790	0.5858	0.1257	0.2554	0.1326	-0.0367
3	0.1550	0.1580	0.3412	0.4110	-0.0539	-0.1110	0.3236	0.2919
4	0.1420	0.1058	-0.1703	0.1652	0.5104	0.4220	-0.0511	0.3262
5	-0.0377	0.7271	0.3088	0.1195	0.4589	0.4638	0.3742	0.0778
6	-0.4466	0.8019	0.8063	0.5452	0.3883	0.4066	0.3325	0.1966
7	0.6021	0.8806	0.7786	0.5156	-0.4504	-0.9105	0.1631	0.0869
8	0.3407	0.5080	0.4490	0.3619	0.5732	0.5989	0.5971	0.3251
9	-0.1115	0.2352	0.2545	0.3635	0.1241	0.0937	0.1095	0.3386

Appendix 6:   Model Skill at Different Lead-Times during JFM Season

6.1 Cross-validated correlations between the JFM sum of monthly stream flow and SSTs for 1990-1997 during the ten lead times at eight stream flow stations in the Groot Olifants and Wilger sub-catchments

Pearson's correlation (JFM)							
Lead (months)	Groot Olifants Sub-catchment				Wilger Sub-catchment			
	B1H012	B1H017	B1H020	B1H021	B2H007	B2H006	B2H014	B2H004
0	0.1120	0.5434	0.7131	0.5180	0.3450	0.4450	0.5020	0.4780
1	0.8170	-0.2000	0.0800	-0.0500	0.9600	0.2080	0.2620	0.4670
2	0.3120	0.1550	0.1630	0.3780	0.2080	0.7870	0.5330	0.6480
3	0.3000	0.3680	0.1590	0.0850	-0.1360	0.2400	0.2070	-0.3300
4	0.6550	0.0707	0.1801	0.0094	-0.1305	0.1203	0.0201	0.6469
5	-0.1745	0.5128	-0.0033	0.0462	-0.0785	0.8008	0.7917	-0.3858
6	0.0010	0.2710	-0.5048	-0.2655	0.2432	0.3345	-0.0831	0.2799
7	-0.2871	-0.2297	-0.1283	-0.3264	-0.3391	0.1275	0.1030	-0.1935
8	0.0877	0.5985	0.4582	0.3933	0.1495	0.3752	0.2762	-0.0055
9	0.1103	-0.3442	0.5096	0.1241	-0.2935	0.1661	0.1589	-0.3007

Appendix 7:   SSTs and Stream Flow Correlations at the Selected Domains during the OND Season

7.1 Equatorial Atlantic Ocean's SSTs cross-validated correlation with the OND stream flow sum for 1990-1997 during the ten lead-times at eight stream flow stations in the Groot Olifants and Wilger sub-catchments

Pearson's correlation (OND) Atlantic Ocean							
Lead (months)	**Groot Olifants Sub-catchment**				**Wilger Sub-catchment**		
	B1H012	**B1H017**	**B1H020**	**B1H021**	**B2H007**	**B2H006**	**B2H014**	**B2H004**
0	0.6108	-0.1917	-0.0982	-0.6433	0.8531	0.7311	0.8377	0.1642
1	-0.4312	-0.2091	-0.3589	0.3042	0.2218	0.2505	0.3345	-0.1983
2	-0.5677	0.0552	0.1425	0.1101	-0.0555	-0.1585	0.0202	0.6544
3	0.0802	0.7210	0.7165	0.2565	-0.0691	0.0854	-0.0781	0.0362
4	0.3528	0.2033	-0.0496	-0.5829	0.7946	0.7139	0.8481	0.2650
5	-0.5041	0.8254	0.8157	0.5456	0.3684	0.5346	0.2656	0.0031
6	-0.3171	0.1828	0.6061	0.7834	-0.2010	-0.0900	0.2410	-0.0790
7	0.6771	0.7291	0.7450	0.5111	0.3495	0.5043	0.3283	0.1295
8	0.3772	0.0732	0.1217	-0.2077	-0.2244	-0.2195	-0.0965	0.2637
9	-0.4465	-0.0648	0.0906	0.7049	0.6526	0.5935	0.8634	-0.3654

7.2 Southern Atlantic Ocean's SSTs cross-validated correlation with the OND stream flow sum for 1990-1997 during the ten lead-times at eight stream flow stations in the Groot Olifants and Wilger sub-catchments

Pearson's correlation (OND) Southern Atlantic Ocean							
Lead (months)	**Groot Olifants Sub-catchment**				**Wilger Sub-catchment**		
	B1H012	**B1H017**	**B1H020**	**B1H021**	**B2H007**	**B2H006**	**B2H014**	**B2H004**
0	0.4430	0.0170	0.0466	-0.0047	0.1560	0.1528	-0.0572	0.1072
1	-0.7399	0.6610	0.7089	0.4409	0.2377	0.1818	0.3307	0.6340
2	0.1690	0.2335	0.2418	0.3814	0.5667	0.5578	0.3275	0.2645
3	0.3032	0.4766	-0.0139	-0.5802	0.8840	0.7315	0.8667	0.3313
4	-0.2493	0.3412	0.1270	0.1746	0.3277	0.3341	0.2486	0.3676
5	-0.1558	-0.3995	0.0901	0.2120	0.2483	0.2886	0.1473	0.1320
6	-0.4099	0.1846	0.2896	0.2711	0.2512	0.2979	0.3768	-0.1852
7	0.0945	0.7896	0.9052	0.3646	-0.0084	0.0528	-0.0880	0.2930
8	-0.4385	0.0322	-0.3641	-0.4121	0.4980	0.4993	0.4332	0.0299
9	0.5319	0.4007	0.9138	0.6761	-0.4859	-0.3065	0.0672	0.1734

7.3 Equatorial Indian Ocean's SSTs cross-validated correlation with the OND stream flow sum for 1990-1997 during the ten lead-times at eight stream flow stations in the Groot Olifants and Wilger sub-catchments

Pearson's correlation's (OND) Indian Ocean							
Lead (months)	Groot Olifants Sub-catchment				Wilger Sub-catchment		
	B1H012	B1H017	B1H020	B1H021	B2H007	B2H006	B2H014	B2H004
0	0.4449	0.7531	0.8653	0.2018	-0.0986	-0.0578	-0.0955	0.1905
1	-0.2999	-0.0107	0.3797	0.4601	0.1138	0.2185	0.5912	0.0845
2	0.6624	0.3953	0.2866	-0.4602	0.0024	0.1601	-0.3169	0.5380
3	0.0482	0.2215	0.3636	0.3272	0.2483	0.4165	0.0940	0.2912
4	0.4105	0.4129	0.5655	0.3657	0.1455	0.2545	0.0850	0.0745
5	-0.2872	0.4499	0.6310	0.4571	0.1044	0.0666	0.1483	-0.2675
6	0.1010	0.3906	0.4840	0.4652	0.3692	0.3543	0.4000	-0.2508
7	-0.4696	-0.3942	-0.0940	0.0341	0.3062	0.3625	0.3855	0.2618
8	0.3674	0.1203	0.3169	0.2367	0.3227	0.4703	0.2609	-0.3226
9	-0.4754	0.8357	0.8011	0.5286	0.1885	0.3023	0.2765	-0.1201

7.4 Equatorial Pacific Ocean's SSTs cross-validated correlation with the OND stream flow sum for 1990-1997 during the ten lead-times at eight stream flow stations in the Groot Olifants and Wilger sub-catchments

Pearson's correlation (OND) Pacific Ocean							
Lead (months)	Groot Olifants Sub-catchment				Wilger Sub-catchment		
	B1H012	B1H017	B1H020	B1H021	B2H007	B2H006	B2H014	B2H004
0	0.6693	0.9224	0.7249	0.4759	-0.3838	-0.3753	0.1011	0.1045
1	0.1467	0.5745	0.7181	0.4175	-0.0304	-0.0461	-0.0339	-0.2333
2	0.5140	0.7923	0.8272	0.5219	-0.3465	-0.5297	0.2586	0.0631
3	0.2197	0.7472	0.7918	0.5643	0.2705	0.2846	0.0936	-0.8070
4	0.4032	-0.8795	-0.3581	-0.8168	0.7994	0.6505	0.5590	0.3496
5	0.3567	0.0024	0.0331	-0.0054	0.2034	0.1865	-0.0300	-0.0491
6	-0.5094	0.8416	0.8157	0.5406	0.3351	0.5107	0.2743	-0.0775
7	0.4142	0.0357	0.2688	-0.3219	-0.1285	0.0992	-0.2504	0.0692
8	0.1261	-0.3548	-0.0168	-0.6140	0.8516	0.7293	0.7055	0.3519
9	-0.4936	-0.3796	-0.4205	-0.2965	0.8183	0.6739	0.6448	-0.3546

Appendix 8: Contingency Table and Forecast Frequency in Percentages Table for Forecast Verification in the Upper Olifants Catchment during OND and JFM Seasons

Note: A and a refer to above normal; N and n refer to near-normal; B and b refer to below-normal, lower case (simulated) and upper case actual stream flow for the upper Olifants during OND and JFM seasons.

Appendix 8.1 Contingency Table (Jolliffe and Stephenson, 2003)

		Forecast			
		1	**2**	**3**	**Total**
Observed	**1**	a	b	c	J
	2	d	e	f	K
	3	g	h	i	L
	Total	M	N	O	T

1. Percent Correct (PC) = $\dfrac{a+e+i}{T}*100$

2. Bias = $\dfrac{M}{J}, \dfrac{N}{K}, \dfrac{O}{L}$ **for the three categories (Normal, Near-normal and Above normal)**

3. Heidke Skill Score = $\left\{ \dfrac{(a+e+I) - \dfrac{JM + KN + LO}{T}}{T - \dfrac{JM + KN + LO}{T}} \right\}$

Appendix 8.2: Equatorial Atlantic Ocean contingency table of OND two months lead-time for the upper Olifants catchment

Observed Olifants		A	N	B	Total	Observed Wilger		A	N	B	Total
Forecast	**a**	1	1	1	3	**a**	9	6	6	21
	n	3	14	8	25	**n**	2	7	1	10
	b	0	0	0	0	**b**	0	1	0	1
	Total	4	15	9	28	**Total**	11	14	7	32

Appendix 8.3: OND two months lead-time forecast frequency in percentages table for the upper Olifants catchment

		Observed Olifants					Observed Wilger			
		A	N	B	Total		A	N	B	Total
	a	3.571	3.571	3.571	10.714	a	28.125	18.750	18.750	65.625
Forecast	n	10.714	50.00	28.571	89.286	n	6.250	21.875	3.125	31.250
	b	0.000	0.000	0.000	0.000	b	0.000	3.125	0.000	3.125
	Total	14.286	53.571	32.143	100	Total	34.375	43.750	21.875	100

Appendix 14.4: Equatorial Atlantic Ocean contingency table of JFM two months lead-time for the upper Olifants catchment

		Observed Olifants					Observed Wilger			
		A	N	B	Total		A	N	B	Total
	a	9	7	3	19	a	5	5	1	11
Forecast	n	0	2	6	8	n	2	14	2	18
	b	0	0	1	1	b	1	1	1	3
	Total	9	9	10	28	Total	8	20	4	32

Appendix 8.5: JFM two months lead-time forecast frequency in percentages table for the upper Olifants catchment

		Observed Olifants					Observed Wilger			
		A	N	B	Total		A	N	B	Total
	a	32.143	25.000	10.714	67.857	a	15.625	15.625	3.125	34.375
Forecast	n	0.000	1.143	21.429	28.571	n	6.250	43.750	6.250	56.250
	b	0.000	0.000	3.571	3.571	b	3.125	3.125	3.125	9.375
	Total	32.143	32.143	35.714	100	Total	25.000	62.500	12.500	100

Appendix 8.6: Southern Atlantic Ocean contingency table of OND two months lead-time for the upper Olifants catchment

		Observed Olifants					Observed Wilger			
		A	N	B	Total		A	N	B	Total
	a	2	3	1	6	a	11	1	6	18
Forecast	n	2	11	9	22	n	2	5	2	9
	b	0	0	0	0	b	1	4	0	5
	Total	4	14	10	28	Total	14	10	8	32

Appendix 8.7: OND two months lead-time forecast frequency in percentages table for the upper Olifants catchment

		Observed Olifants					Observed Wilger			
		A	N	B	Total		A	N	B	Total
	a	7.143	10.714	3.571	21.429	a	34.375	3.125	18.750	56.250
Forecast	n	7.143	39.286	32.143	78.571	n	6.250	15.625	6.250	28.125
	b	0.000	0.000	0.000	0.000	b	3.125	12.500	0.000	15.625
	Total	14.286	50.000	35.714	100	Total	43.750	31.250	25.000	100

Appendices

Appendix 8.8: Southern Atlantic Ocean contingency table of JFM two months lead-time for the upper Olifants catchment

		Observed Olifants					Observed Wilger			
		A	N	B	Total		A	N	B	Total
Forecast	a	6	3	1	10	a	3	3	0	6
	n	4	4	6	14	n	6	15	2	23
	b	1	1	2	4	b	0	2	1	3
		11	8	9	28		9	20	3	32

Appendix 8.9: JFM two months lead-time forecast frequency in percentages table for the upper Olifants catchment

		Observed Olifants					Observed Wilger			
		A	N	B	Total		A	N	B	Total
Forecast	a	21.429	10.714	3.571	35.714	a	9.375	9.375	0.000	18.750
	n	14.286	14.286	21.429	50.000	n	18.750	46.875	6.250	71.875
	b	3.571	3.571	7.143	14.286	b	0.000	6.250	3.125	9.375
	Total	39.286	28.571	32.143	100	Total	28.125	62.500	9.375	100

Appendix 8.10:.Indian Ocean contingency table of OND two months lead-time for the upper Olifants catchment

		Observed Olifants					Observed Wilger			
		A	N	B	Total		A	N	B	Total
Forecast	a	4	2	0	6	a	7	6	7	20
	n	1	11	10	22	n	2	7	1	10
	b	0	0	0	0	b	0	1	1	2
	Total	5	13	10	28	Total	9	14	9	32

Appendix 8.11: OND two months lead-time forecast frequency in percentages table for the upper Olifants catchment

		Observed Olifants					Observed Wilger			
		A	N	B	Total		A	N	B	Total
Forecast	a	14.286	7.143	0.000	21.429	a	21.875	18.750	21.875	62.500
	n	3.571	39.286	35.714	78.571	n	6.250	21.875	3.125	31.250
	b	0.000	0.000	0.000	0.000	b	0.000	3.125	3.125	6.250
	Total	17.857	46.429	35.714	100	Total	28.125	43.750	28.125	100

Appendix 8.12: Indian Ocean contingency table of JFM two months lead-time for the upper Olifants catchment

		Observed Olifants					Observed Wilger			
		A	N	B	Total		A	N	B	Total
Forecast	a	7	3	2	12	a	6	3	1	10
	n	2	4	6	12	n	4	13	2	19
	b	0	2	2	4	b	1	2	0	3
	Total	9	9	10	28	Total	11	18	3	32

Appendix 8.13: JFM two months lead-time forecast frequency in percentages table for the upper Olifants catchment

		Observed Olifants					Observed Wilger			
		A	N	B	Total		A	N	B	Total
	a	25	10.714	7.143	42.857	a	18.75	9.375	3.125	31.25
Forecast	n	7.143	14.286	21.429	42.858	n	12.5	40.625	6.250	59.375
	b	0	7.143	7.143	14.286	b	3.125	6.250	0.00	9.375
	Total	32.143	32.143	35.715	100	Total	34.375	56.250	9.375	100

Appendix 8.14: Pacific Ocean contingency table of OND two months lead-time for the upper Olifants catchment

		Observed Olifants					Observed Wilger			
		A	N	B	Total		A	N	B	Total
	a	2	3	0	5	a	6	2	6	14
Forecast	n	2	11	9	22	n	2	9	2	13
	b	0	1	0	1	b	3	1	1	5
	Total	4	15	9	28	Total	11	12	9	32

Appendix 8.15: OND two months lead-time forecast frequency in percentages table for the upper Olifants catchment

		Observed Olifants					Observed Wilger			
		A	N	B	Total		A	N	B	Total
	a	7.143	10.714	0.000	17.857	a	18.750	6.250	18.750	43.750
Forecast	n	7.143	39.286	32.143	78.571	n	6.250	28.125	6.250	40.625
	b	0.000	3.571	0.000	3.571	b	9.375	3.125	3.125	15.625
	Total	14.286	53.571	32.143	100	Total	34.375	37.500	28.125	100

Appendix 8.16: Pacific Ocean contingency table of JFM two months lead-time for the upper Olifants catchment

		Observed Olifants					Observed Wilger			
		A	N	B	Total		A	N	B	Total
	a	9	5	7	21	a	6	6	2	14
Forecast	n	0	2	4	6	n	2	15	1	18
	b	0	1	0	1	b	0	0	0	0
	Total	9	8	11	28	Total	8	21	3	32

Appendix 8.17: JFM two months lead-time forecast frequency in percentages table for the upper Olifants catchment

		Observed Olifants					Observed Wilger			
		A	N	B	Total		A	N	B	Total
	a	32.143	17.857	25.000	75.000	a	18.750	18.750	6.250	43.750
Forecast	n	0.000	7.143	14.286	21.429	n	6.250	46.875	3.125	56.250
	b	0.000	3.571	0.000	3.571	b	0.000	0.000	0.000	0.000
	Total	32.143	28.571	39.286	100	Total	25.000	65.625	9.375	100

Appendix 9:   SSTs and Stream Flow Correlations at the Selected Domains during the JFM Season

9.1 Equatorial Atlantic Ocean's SSTs cross-validated correlation against the JFM stream flow sum for 1990-1997 during the ten lead-times at eight stream flow stations in the Groot Olifants and Wilger sub-catchments

	Pearson's correlation (JFM) Equatorial Atlantic Ocean							
Lead (months)	**Groot Olifants Sub-catchment**				**Wilger Sub-catchment**			
	B1H012	**B1H017**	**B1H020**	**B1H021**	**B2H007**	**B2H006**	**B2H014**	**B2H004**
0	0.3070	-0.4301	0.4840	0.2854	0.2299	-0.0810	0.1507	0.2386
1	0.2972	-0.1577	0.3758	0.1660	0.1376	0.3652	0.3214	0.1278
2	-0.2778	0.5501	0.4259	0.2021	0.2142	0.4106	0.3971	-0.1840
3	-0.3120	0.2680	-0.0941	0.1715	0.3382	0.2886	0.4382	-0.1052
4	-0.2810	0.3440	0.2205	0.2099	0.2078	0.2825	0.2900	-0.3128
5	0.0862	0.1828	0.5034	0.2382	0.3750	-0.2214	-0.1010	0.4934
6	0.0155	0.4211	0.4101	0.0384	0.1126	0.7974	0.7844	0.1591
7	-0.0437	0.6206	0.7150	0.3687	0.2657	0.4974	0.4881	0.3454
8	-0.7186	0.6706	0.7600	0.7128	0.3435	0.8013	0.8242	-0.4817
9	0.1505	-0.0024	0.0099	0.2398	0.2292	-0.1100	-0.0330	0.3332

9.2 Southern Atlantic Ocean's SSTs cross-validated correlation against the JFM stream flow sum for 1990-1997 during the ten lead-times at eight stream flow stations in the Groot Olifants and Wilger sub-catchments

	Pearson's correlation (JFM) Southern Atlantic Ocean							
Lead (months)	**Groot Olifants Sub-catchment**				**Wilger Sub-catchment**			
	B1H012	**B1H017**	**B1H020**	**B1H021**	**B2H007**	**B2H006**	**B2H014**	**B2H004**
0	0.4280	0.3209	0.3622	0.1925	0.1353	0.1975	0.1931	0.7816
1	-0.6260	0.4819	0.7205	0.5834	0.2988	0.1260	0.2185	-0.3528
2	0.1672	0.1128	0.7082	0.4463	0.2421	-0.4792	-0.4410	0.5543
3	0.0829	-0.2737	0.1482	0.3138	0.3628	-0.2291	-0.1043	0.2253
4	0.1112	0.4624	0.3943	0.2859	0.1897	0.2637	0.2238	0.0418
5	0.2322	0.0204	0.1312	0.2813	-0.0453	0.2447	0.1827	-0.2576
6	0.4591	-0.7112	0.7020	0.2525	0.0215	0.4135	-0.4453	0.3128
7	0.6913	0.2851	0.0419	0.1921	0.0471	0.2604	0.2735	0.4616
8	-0.2230	0.5297	0.3018	0.2426	0.3185	0.4019	0.4023	-0.0082
9	0.2154	0.4091	0.3928	0.0744	-0.0585	0.3865	0.3719	0.3442

Appendices

9.3 Equatorial Indian Ocean's SSTs cross-validated correlation with the JFM stream flow sum for 1990-1997 during the ten lead-times at eight stream flow stations in the Groot Olifants and Wilger sub-catchments

Pearson's correlation (JFM) Indian Ocean							
Lead (months)	**Groot Olifants Sub-catchment**				**Wilger Sub-catchment**		
	B1H012	**B1H017**	**B1H020**	**B1H021**	**B2H007**	**B2H006**	**B2H014**	**B2H004**
0	-0.3290	0.6692	-0.3196	0.0889	-0.1242	0.7946	0.7509	-0.5346
1	0.0653	0.6146	-0.6061	-0.3161	0.2234	0.5182	0.4235	0.4649
2	0.2312	-0.0173	0.1683	0.2686	0.1975	-0.1011	0.0397	0.2815
3	0.4856	-0.3375	0.3639	0.2193	0.1595	0.2931	0.3350	0.4585
4	0.0132	0.3502	-0.2605	-0.2269	0.3012	0.2473	-0.1152	0.3188
5	0.3014	0.0091	-0.5379	-0.2714	0.2528	0.3618	0.2077	0.7224
6	-0.3203	0.4723	0.1455	0.2234	0.2108	0.2791	0.2640	-0.1630
7	-0.1606	0.1255	0.1099	0.0852	0.1982	0.2681	0.2811	0.4362
8	-0.4256	0.2284	0.2987	0.0945	0.0064	0.3548	0.3730	0.1000
9	-0.2029	0.3661	0.2908	0.0407	0.2055	-0.0616	-0.0857	0.3156

9.4 Equatorial Pacific Ocean's SSTs cross-validated correlation against the JFM stream flow sum for 1990-1997 during the ten lead-times at eight stream flow stations in the Groot Olifants and Wilger sub-catchments

Pearson's correlation (JFM) Pacific Ocean							
Lead (months)	**Groot Olifants Sub-catchment**				**Wilger Sub-catchment**		
	B1H012	**B1H017**	**B1H020**	**B1H021**	**B2H007**	**B2H006**	**B2H014**	**B2H004**
0	-0.2653	0.7504	-0.7909	-0.8371	0.4678	0.8994	0.8974	-0.2782
1	-0.4918	0.5086	0.2863	-0.1548	-0.0593	0.4961	0.3749	-0.2761
2	-0.4154	0.3006	0.1773	-0.2767	-0.2029	0.2473	0.1189	0.3389
3	0.7301	0.2285	-0.1288	0.0941	-0.0935	0.0804	0.0745	0.7683
4	0.2558	-0.3391	0.2347	0.2202	0.2337	0.0033	0.1480	0.4226
5	0.0390	0.4076	0.4982	0.2659	0.2259	0.2822	0.2817	0.3026
6	0.0149	0.4399	-0.4632	-0.2547	0.2369	0.3801	0.0110	0.2893
7	0.4597	-0.1909	-0.2945	-0.0845	-0.2268	0.3872	0.3485	0.5969
8	0.9744	-0.2429	-0.2024	0.1159	0.1300	-0.2239	-0.1888	0.7592
9	-0.3793	0.6233	-0.2491	-0.3251	-0.1491	0.6683	0.4231	-0.0351

Appendix 10: OND and JFM Retro-Active Stream Flow Hindcasts using Global SSTs

Note: A and a refer to above normal; N and n refer to near-normal; B and b refer to below-normal, lower case (simulated) and upper case actual stream flow for the upper Olifants during OND and JFM seasons.

10. 1 Sub-catchment annual hit scores at lead-time of two months during the OND season using the global SSTs as the predictors

Year	Groot Olifants Sub-catchment				Wilger Sub-catchment				Hits
	B1H012	B1H017	B1H020	B1H021	B2H007	B2H006	B2H014	B2H004	
1998	**Aa**	Na	**Aa**	Na	**Aa**	**Aa**	**Aa**	**Aa**	6
1999	**Aa**	**Nn**	**Aa**	Bn	**Aa**	Ba	**Nn**	**Aa**	6
2000	Na	**Nn**	An	**Nn**	**Aa**	An	An	Ba	3
2001	An	**Nn**	**Nn**	Bn	**Nn**	An	**Nn**	**Aa**	5
2002	**Nn**	**Nn**	Bn	Nb	Nb	Nb	Bn	**Aa**	4
2003	Ba	**Nn**	-999	**Bb**	Ab	Ba	**Nn**	Ba	3
2004	-999	Bn	-999	Bn	**Aa**	**Nn**	**Nn**	Ba	3
2005	Na	Bn	-999	Ba	**Aa**	Na	Na	Na	1
Hits	3	5	3	2	6	2	5	4	31

10. 2 Sub-catchment annual hit scores at a lead-time of two months during the JFM season using global SSTs as predictors

Year	Groot Olifants Sub-catchment				Wilger sub-catchment				Hits
	B1H012	B1H017	B1H020	B1H021	B2H007	B2H006	B2H014	B2H004	
1998	Na	Bn	**Nn**	**Aa**	Na	Na	Na	**Nn**	3
1999	Na	**An**	An	**Aa**	**Aa**	**Aa**	**Aa**	**Nn**	6
2000	**Aa**	Bn	Bn	Na	Na	Na	Ba	An	1
2001	Ba	Bn	Bn	Na	Na	**Nn**	**Nn**	Na	2
2002	Ba	**Nn**	**Nn**	**Aa**	Na	**Nn**	Bn	**Nn**	5
2003	Ba	**Nn**	-999	**Aa**	**Aa**	**Nn**	**Nn**	**Nn**	6
2004	Na	**Nn**	-999	**Aa**	Na	**Nn**	**Nn**	**Nn**	5
2005	**Aa**	-999	-999	**Aa**	**Aa**	**Aa**	**Aa**	**Nn**	6
Hits	2	4	2	6	3	6	5	6	34

Appendix 11: Stream Flow Hindcast Using Equatorial Atlantic SSTs

11.1 Sub-catchment annual hit scores at lead-time of seven months during the OND season using Equatorial Atlantic Ocean SSTs as the predictors

Year	Groot Olifants Sub-catchment				Wilger Sub-catchment				Hits
	B1H012	**B1H017**	**B1H020**	**B1H021**	**B2H007**	**B2H006**	**B2H014**	**B2H004**	
1998	**Aa**	**Nn**	**Aa**	Na	**Aa**	**Aa**	**Aa**	**Aa**	7
1999	Na	**Nn**	An	Bn	**Aa**	Na	**Nn**	**Aa**	4
2000	**Nn**	**Nn**	**Aa**	**Nn**	**Aa**	**Aa**	**Aa**	Bn	7
2001	An	**Nn**	**Nn**	Bn	**Nn**	**Nn**	**Nn**	**Aa**	6
2002	**Nn**	Na	Bn	Ba	Bn	**Nn**	Ba	An	2
2003	Ba	**Nn**	-999	Bn	Ba	Ba	Ba	Ba	1
2004	-999	Bn	-999	Bn	**Nn**	**Nn**	**Nn**	Ba	3
2005	Na	Bn	-999	Ba	**Aa**	Ba	Na	Na	1
Hits	3	5	3	1	6	5	5	3	31

11.2 Sub-catchment annual hit scores at lead-time of seven months during the JFM season using Equatorial Atlantic Ocean SSTs as the predictors

Year	Groot Olifants Sub-catchment				Wilger Sub-catchment				Hits
	B1H012	**B1H017**	**B1H020**	**B1H021**	**B2H007**	**B2H006**	**B2H014**	**B2H004**	
1998	Na	Bn	Ba	**Aa**	Na	Na	Na	**Nn**	2
1999	Na	**Aa**	**Aa**	**Aa**	**Aa**	**Aa**	**Aa**	Bn	6
2000	**Aa**	Bn	Ba	Na	Na	Na	Bn	An	1
2001	Ba	Bn	Bn	Na	Na	**Nn**	**Nn**	**Nn**	3
2002	Ba	**Nn**	Bn	**Aa**	Na	**Nn**	Bn	**Nn**	4
2003	Ba	**Nn**	-999	**Aa**	Aa	**Nn**	**Nn**	**Nn**	5
2004	**Nn**	**Nn**	-999	An	Na	**Nn**	**Nn**	**Nn**	5
2005	**Aa**	-999	-999	**Aa**	**Aa**	**Nn**	An	**Nn**	5
Hits	3	4	1	5	2	6	4	6	31

11.3 Sub-catchment annual hit scores at lead-time of eight months during the OND season using Equatorial Atlantic Ocean SSTs as the predictors

Year	Groot Olifants Sub-catchment				Wilger Sub-catchment				Hits
	B1H012	**B1H017**	**B1H020**	**B1H021**	**B2H007**	**B2H006**	**B2H014**	**B2H004**	
1998	**Aa**	**Nn**	**Aa**	**Nn**	**Aa**	**Aa**	**Aa**	**Aa**	8
1999	Na	**Nn**	An	Bn	**Aa**	Na	Na	**Aa**	3
2000	**Nn**	**Nn**	**Aa**	**Nn**	An	**Aa**	An	Bn	5
2001	An	**Nn**	**Nn**	Bn	Na	**Nn**	**Nn**	**Aa**	5
2002	**Nn**	**Nn**	Ba	Ba	Bn	**Nn**	Ba	An	3
2003	**Nn**	**Nn**	-999	Bn	Ba	Ba	Ba	Ba	2
2004	-999	Bn	-999	Bn	Na	**Nn**	**Na**	Ba	2
2005	Na	Bn	-999	Bn	**Aa**	Ba	Na	Na	1
Hits	4	6	3	2	3	5	3	3	29

11.4 Sub-catchment annual hit scores at lead-time of eight months during the JFM season using Equatorial Atlantic Ocean SSTs as the predictors

Year	Groot Olifants Sub-catchment				Wilger Sub-catchment				Hits
	B1H012	**B1H017**	**B1H020**	**B1H021**	**B2H007**	**B2H006**	**B2H014**	**B2H004**	
1998	Na	Bn	Ba	**Aa**	Na	**Aa**	**Nn**	**Nn**	4
1999	Na	**Aa**	**Aa**	**Aa**	**Aa**	**Aa**	**Aa**	Bn	6
2000	Na	Bn	Bn	Na	Na	Na	Bn	An	0
2001	**Aa**	Bn	Bn	Na	Ba	**Nn**	**Nn**	**Nn**	4
2002	Ba	**Nn**	Bn	An	Na	**Nn**	Bn	**Nn**	3
2003	Ba	**Nn**	-999	**Aa**	**Aa**	**Nn**	**Nn**	**Nn**	6
2004	Ba	**Nn**	-999	Ab	Na	**Nn**	**Nn**	**Nn**	4
2005	**Nn**	-999	-999	An	**Aa**	**Nn**	An	**Nn**	4
Hits	2	4	1	3	3	7	5	6	31

Appendix 12: Stream Flow Hindcast Using Southern Atlantic Ocean SSTs

12.1 Sub-catchment annual hit scores at lead-time of seven months during the OND season using Southern Atlantic Ocean SSTs as the predictors

Year	Groot Olifants Sub-catchment				Wilger Sub-catchment				Hits
	B1H012	B1H017	B1H020	B1H021	B2H007	B2H006	B2H014	B2H004	
1998	**Aa**	**Nn**	**Aa**	**Nn**	An	An	**Aa**	**Aa**	6
1999	**Nn**	**Nb**	An	**Bb**	**Bb**	Bn	Bn	**Aa**	5
2000	Na	Na	**Aa**	**Nn**	**Bb**	**Aa**	**Aa**	Bn	5
2001	An	**Nn**	**Nn**	Ba	Na	Nb	**Nn**	**Aa**	4
2002	Na	**Nn**	Ba	Bn	**Aa**	Bn	**Nn**	**Aa**	4
2003	**Bb**	**Nn**	-999	Bn	**Nn**	**Bb**	**Bb**	Ba	5
2004	-999	Ba	-999	Bn	Na	**Nn**	**Nn**	Bn	2
2005	**Nn**	Bn	-999	Ba	An	An	Ba	**Nn**	2
	4	5	3	3	4	3	6	5	33

12.2 Sub-catchment annual hit scores at lead-time of seven months during the JFM season using Southern Atlantic Ocean SSTs as the predictors

Year	Groot Olifants Sub-catchment				Wilger Sub-catchment				Hits
	B1H012	B1H017	B1H020	B1H021	B2H007	B2H006	B2H014	B2H004	
1998	**Nn**	Bn	Ba	**Aa**	Na	Na	**Nn**	**Nn**	4
1999	**Nn**	An	An	An	**Aa**	An	An	Bn	2
2000	**Aa**	Ba	Ba	Na	Na	Na	Ba	**Aa**	2
2001	Bn	Bn	Bn	**Nn**	Na	**Nn**	**Nn**	**Nn**	4
2002	**Bb**	**Nn**	Bn	Ab	**Nn**	**Nn**	**Nn**	**Bb**	6
2003	**Bb**	**Nn**	-999	Ab	An	**Nn**	**Nn**	Nb	4
2004	Na	**Nn**	-999	**Aa**	Na	**Nn**	**Nn**	**Nn**	5
2005	An	-999	-999	**Aa**	**Aa**	**Nn**	An	**Nn**	4
	5	3	0	4	3	5	5	6	31

Appendix 13: Stream Flow Hindcast Using Equatorial Indian Ocean SSTs

13.1 Sub-catchment annual hit scores at lead-time of two months during the OND season using the equatorial Indian Ocean SSTs as the main stream flow predictors

Year	Groot Olifants Sub-catchment				Wilger Sub-catchment				Hits
	B1H012	B1H017	B1H020	B1H021	B2H007	B2H006	B2H014	B2H004	
1998	**Aa**	**Nn**	**Aa**	**Nn**	**Aa**	**Aa**	**Aa**	**Aa**	8
1999	**Nn**	**Nn**	**Aa**	Bn	**Aa**	Bn	**Nn**	An	5
2000	**Nn**	**Nn**	An	**Nn**	**Aa**	**Aa**	**Aa**	**Nn**	7
2001	**Aa**	**Nn**	Na	Bn	Na	Na	Na	**Aa**	3
2002	**Nn**	**Nn**	Bn	Bn	Ba	Na	Ba	An	2
2003	Bn	**Nn**	-999	Bn	Ba	Ba	Na	**Nn**	2
2004	-999	Bn	-999	Bn	**Nn**	**Nn**	**Nn**	Ba	3
2005	**Nn**	Bn	-999	Bn	Nn	Ba	Ba	Na	1
Hits	6	6	2	2	4	3	4	4	31

13.2 Sub-catchment annual hit scores at lead-time of two months during the JFM season using the equatorial Indian Ocean SSTs as the main stream flow predictors

Year	Groot Olifants Sub-catchment				Wilger Sub-catchment				Hits
	B1H012	B1H017	B1H020	B1H021	B2H007	B2H006	B2H014	B2H004	
1998	**Na**	Bn	Bn	**Aa**	Na	**Nn**	**Nn**	Na	4
1999	**Na**	An	An	An	**Aa**	An	An	Bn	2
2000	**Aa**	Bn	Bn	**Nn**	Na	**Nn**	**Nn**	**Aa**	5
2001	Ba	Bn	Bn	**Nn**	Na	**Nn**	**Nn**	An	3
2002	Ba	**Nn**	Ba	Ab	Na	**Nn**	**Nn**	**Nn**	4
2003	Ba	**Nn**	-999	An	**Aa**	**Nn**	**Nn**	Na	4
2004	Na	**Nn**	-999	**Aa**	Na	**Nn**	**Nn**	**Nn**	5
2005	**Aa**	-999	-999	**Aa**	**Aa**	**Nn**	**Nn**	**Nn**	6
Hits	4	3	0	5	3	7	7	4	33

Appendix 14: Stream Flow Hindcast Using Equatorial Pacific Ocean SSTs

14.1 Sub-catchment annual hit scores at lead-time of two months during the OND season using the equatorial Pacific Ocean as the main stream flow predictors

Year	Groot Olifants Sub-catchment				Wilger Sub-catchment				Hits
	B1H012	B1H017	B1H020	B1H021	B2H007	B2H006	B2H014	B2H004	
1998	**Aa**	Na	Na	**Nn**	**Aa**	**Aa**	**Aa**	**Aa**	6
1999	Na	**Nn**	**Aa**	Bn	**Aa**	Ba	Na	**Aa**	4
2000	**Nn**	**Nn**	An	**Nn**	Ab	An	An	**Nn**	4
2001	An	**Nn**	**Nn**	Bn	**Nn**	**Nn**	**Nn**	Ab	5
2002	**Nn**	**Nn**	Bn	Bn	Bn	Nn	Bn	Ab	2
2003	Ba	**Nn**	-999	Bn	Ba	Ba	Ba	Ba	1
2004	-999	Bn	-999	Bn	**Nn**	**Nn**	**Nn**	**Bb**	4
2005	**Nn**	Bn	-999	Bn	Na	**Nn**	Ba	**Nn**	3
Hits	4	5	2	2	4	4	3	5	29

14.2 Sub-catchment annual hit scores at lead-times of two months during the JFM season using the equatorial Pacific Ocean as the main stream flow predictors

Year	Groot Olifants Sub-catchment				Wilger Sub-catchment				Hits
	B1H012	B1H017	B1H020	B1H021	B2H007	B2H006	B2H014	B2H004	
1998	**Nn**	Bn	Bn	**Aa**	Na	**Nn**	**Nn**	**Nn**	5
1999	Na	**Aa**	**Aa**	**Aa**	**Aa**	**Aa**	**Aa**	Ba	6
2000	**Aa**	Ba	Ba	Na	Na	Na	Ba	**Aa**	2
2001	Ba	Ba	Bn	Na	Na	**Nn**	**Nn**	**Nn**	3
2002	Ba	Na	Bn	Na	Na	**Nn**	Bn	**Nn**	2
2003	Ba	**Nn**	-999	**Aa**	**Aa**	**Nn**	**Nn**	**Nn**	6
2004	Ba	Na	-999	**Aa**	Na	**Nn**	**Nn**	**Nn**	4
2005	**Aa**	-999	-999	**Aa**	**Aa**	An	An	**Nn**	4
Hits	3	2	1	5	3	6	5	7	32

Appendices

14.3 Sub-catchment annual hit scores at lead-times of nine months during the OND season using the equatorial Pacific Ocean as the main stream flow predictors

Year	Groot Olifants Sub-catchment				Wilger Sub-catchment				Hits
	B1H012	B1H017	B1H020	B1H021	B2H007	B2H006	B2H014	B2H004	
1998	An	**Nn**	An	**Nn**	**Aa**	An	An	**Aa**	4
1999	**Nn**	**Nn**	**Aa**	Bn	An	Ba	Na	An	3
2000	**Nn**	**Nn**	**Aa**	**Nn**	An	**Aa**	**Aa**	Bn	7
2001	An	**Nn**	Na	Bn	Na	Na	Na	An	2
2002	**Nn**	**Nn**	Bn	Bn	Ba	**Aa**	Ba	Bn	2
2003	Bn	**Nn**	-999	Bn	Ba	Bn	Ba	Ba	2
2004	-999	Bn	-999	Bn	Na	**Nn**	**Nn**	Ba	2
2005	**Nn**	Bn	-999	Bn	**Aa**	**Nn**	Bn	Na	3
Hits	4	6	2	2	4	4	2	1	25

14.4 Sub-catchment annual hit scores at lead-times of nine months during the JFM season using the equatorial Pacific Ocean as the main stream flow predictors

Year	Groot Olifants Sub-catchment				Wilger Sub-catchment				Hits
	B1H012	B1H017	B1H020	B1H021	B2H007	B2H006	B2H014	B2H004	
1999	**Aa**	**Aa**	**Aa**	**Aa**	**Aa**	**Aa**	An	Ba	6
2000	**Aa**	Bn	**Nn**	**Nn**	Na	**Nn**	Bn	**Aa**	5
2001	Ba	Bn	Ba	Na	**Nn**	Na	**Nn**	**Nn**	3
2002	**Aa**	**Nn**	Bn	Ab	**Nn**	**Nn**	Bn	**Nn**	5
2003	Bn	**Nn**	-999	**Aa**	**Aa**	**Nn**	**Nn**	**Nn**	6
2004	**Aa**	**Nn**	-999	**Aa**	Na	Na	**Nn**	**Nn**	5
2005	An	-999	-999	**Aa**	**Aa**	**Nn**	An	**Nn**	4
Hits	5	4	2	5	6	6	4	6	34